On hyperbolic 3-orbifolds of small volume

by

Tyler Gaona

B.S. in Mathematics, Duquesne University, 2017

Submitted to the Graduate Faculty of

the Dietrich School of Arts and Sciences in partial fulfillment

of the requirements for the degree of

Doctor of Philosophy

University of Pittsburgh

2022

UNIVERSITY OF PITTSBURGH

DIETRICH SCHOOL OF ARTS AND SCIENCES

This dissertation was presented

by

Tyler Gaona

It was defended on

July 13th 2022

and approved by

Jason DeBlois, Associate Professor, Mathematics - University of Pittsburgh

Thomas Hales, Andrew Mellon Professor of Mathematics - University of Pittsburgh

Neil Hoffman, Assistant Professor, Mathematics - Oklahoma State University

Armin Schikorra, Associate Professor, Mathematics - University of Pittsburgh

On hyperbolic 3-orbifolds of small volume

Tyler Gaona, PhD

University of Pittsburgh, 2022

This thesis is concerned with hyperbolic 3-orbifolds of small volume. An n-orbifold is a space which locally, i.e. in a neighborhood of any point, looks like a quotient of Euclidean space $\mathbb{R}^n$. We are interested in those spaces which may be equipped with hyperbolic geometry, i.e. are locally modeled on the quotient $\mathbb{H}^n$ by a discrete subgroup of its isometries.

Following the work of Meyerhoff and Adams we classify minimal volume orbifolds with one rigid and one nonrigid cusp.

We then discuss joint work with J. DeBlois, A. H. Ekanayake, M. Fincher, A. Gharagozlou, and P. Mondal on establishing a census of orbifolds commensurable with the figure eight knot complement.

Table of Contents

Preface . . . x

1.0 Introduction . . . 1

2.0 Background in Hyperbolic Geometry . . . 5

2.1 Hyperbolic Geometry . . . 5

2.2 Orbifolds . . . 10

2.3 Volume . . . 16

3.0 Minimal orbifolds with one rigid and one nonrigid cusp . . . 26

3.1 The minimal volume orbifolds . . . 27

3.2 Geometric Lemmas . . . 33

3.3 Classification . . . 40

3.4 Proof of Theorem 3.2 . . . 45

3.4.1 Simultaneously maximized cusps . . . 46

3.4.1.1 H_r is not centered at any singularity . . . 46

3.4.1.2 H_r is centered at the order 2 singularity . . . 46

3.4.1.3 H_r is centered at the order 3 singularity . . . 46

3.4.1.4 H_r is centered at the order 6 singularity . . . 47

3.4.2 Rigid cusp is not self-tangent . . . 48

3.4.3 Disjoint cusps . . . 50

3.4.3.1 H_r is not centered at any singularity . . . 50

3.4.3.2 H_r is centered at the order 2 singularity . . . 51

3.4.3.3 H_r is centered at the order 3 singularity . . . 52

3.4.3.4 H_r is centered at the order 6 singularity . . . 53

3.5 Proof of Theorem 3.3 . . . 62

3.5.1 Cusps are simultaneously maximized . . . 62

3.5.2 Rigid cusp is not self tangent . . . 62

3.5.3 Disjoint cusps . . . 69

4.0 Orbifolds commensurable with the figure eight knot complement . . . 76
4.1 Outline of the program . . . 76
4.2 Constructing covers of $\mathbb{H}^3/PGL_2(O_3)$ . . . 78
4.3 Cusps and singular loci of elements of $\mathcal{C}_{\text{main}}$ . . . 86
4.3.1 Cusps . . . 87
4.3.2 Singular Locus . . . 89
4.4 Enumerating Q_π and $\widetilde{Q}_\pi$ with small volume . . . 94
Appendix. Data about $\mathcal{C}_{\text{main}}$ . . . 99
Bibliography . . . 102

List of Tables

1 Number $s(n)$ of elements of $\mathcal{C}_{\text{main}}$ triangulated by n tetrahedra 99

2 Destination sequences and cusp types for elements of $\mathcal{C}_{\text{main}}$ triangulated by at most 10 tetrahedra 100

3 Minimal elements of $\mathcal{C}_3 - \mathcal{C}_{\text{main}}$ 101

List of Figures

1 (a) 2222 (b) 333 13
2 (a) 442 (b) 632 13
3 An ideal tetrahedron with dihedral angles labeled $\alpha = \alpha', \beta = \beta', \gamma = \gamma'$. 17
4 Projection onto the plane of the decomposition of $T_{\alpha,\beta,\gamma}$ into six orthoschemes . 20
5 Singular loci diagrams for $O_{(4,4,2)}$ (left) and $O_{(6,3,2)}$ (right) 27
6 $\mathcal{P}_{(6,3,2)}$ with labels at an edge indicating its dihedral angle. 29
7 (632 rigid cusp) Diagrams of C_N and C_R, with fundamental domain for Γ_∞ in yellow. 30
8 (442 rigid cusp) Diagrams of C_N and C_R, with a fundamental domain for Γ_∞ in yellow. 32
9 Red and blue horoballs are inverse to each other with respect to the dashed hemisphere 35
10 The setting of Proposition 3.2.1. The fixed point of $\rho_C\rho_A\rho_B$ is the final vertex of the parallelogram with vertices A, B, C. 38
11 Combinatorics of $V(C_N)$ and $V(C_R)$ with rigid (6,3,2) cusp. 41
12 Combinatorics of $V(C_N)$ and $V(C_R)$ with rigid (4,4,2) cusp. 42
13 (333 rigid cusp) Diagrams of C_N and C_R, with fundamental domain for Γ_∞ in yellow. 43
14 The maximum distance between H and H_n 49
15 A plot of the lower bound for $\mathrm{vol}(O)$ versus v_0 50
16 The purple horoball is the image under g of a full-sized red horoball 51
17 For $\sqrt{3} < d \leq 2$, $\theta_u(d) < \theta_l(d)$ is a contradiction 53
18 View of model $V_h(C_R)$ with our eye at ∞ 55
19 The setting of Lemma 3.4.2 57
20 The setting of Lemma 3.4.3 58
21 Plotting $\mathrm{vol}\, V_{h_*(d)}$ vs. $v_0/3$ 60

22 Least volume rigid cusp diagrams when (a) cusps are simultaneously maximized (b) rigid cusp is not self tangent 63
23 Computing the distance between H' and $\rho_4^2(g(H'))$. 64
24 (a) the maximum value of e (b) if $\beta \geq \pi/4$, the maximum distance from P to the center of H_n. 66
25 The maximum distance between H and H_n 68
26 Plot of v_0 versus the lower bound on vol(O) 69
27 The setting of Lemma 3.5.3 72
28 The lower bound for vol(O) vs. v_1 74
29 $t(d, \theta_{\min}) \leq$ visible height of $\mathcal{P}(H) \leq \sqrt{2r_1(d)}$ is not satisfied for $1/\sqrt{2} < d < .74$ 75
30 The tetrahedron T 80
31 Cusp cross section determined by $\{t_0, t_1, t_3\}$ 89
32 Cusp cross section determined by $\{t_2, t_4, t_5\}$ 90
33 (a) 1-skeleton of the triangulation (b) after removing non-singular edges 91
34 (a) the singular locus (b) output of the algorithm 92
35 Tetrahedral decomposition of the figure eight knot complement 93
36 Singular locus of O_0^{10} 93

Preface

It is a great pleasure at this point in my journey to thank those who have helped me along the way. This dissertation would not have been possible without the guidance of my advisor, Jason DeBlois. I will be forever grateful for his kind and patient assistance. I thank my committee members for their careful reading and commentary which greatly improved the quality of this thesis. I am thankful for the friends I have made in the department here at Pitt and am excited to see where they will go next.

I would not have made it this far without the constant love and support of my family, especially my mom, my dad, and my sister Lauren. I thank my fiancée Alexis for her immense love and devotion. I'm also grateful to her for putting up with my long and late hours of study and to the Hernandez family for adopting me as one of their own.

I give all glory and praise to my Redeemer and my Comforter, the Lord Jesus Christ.

Thou hast turned for me my mourning into dancing; thou hast put off my sackcloth, and girded me with gladness,
To the end that my glory may sing praise to thee, and not be silent.
O Lord, my God, I will give thanks unto thee forever

Psalm 30 v. 11-12

1.0 Introduction

By Mostow Rigidity, each homeomorphism class of 3-orbifolds supports a unique hyperbolic metric. In this setting, geometric invariants of a hyperbolic 3-orbifold are also topological invariants. The Thurston-Jørgenson theory (extended to the orbifold case by Dunbar & Meyerhoff in [17]) may be summarized by the statement that the set of volumes of complete hyperbolic 3-manifolds is well ordered of type ω^ω. In this thesis, we present results on the classification of hyperbolic 3-orbifolds in terms of increasing volume. Thurston remarked in chapter 6 of [34] that "one gets a feeling that volume is a very good measure of the complexity of a link complement". We take this informal statement as the unifying theme of this thesis.

Chapter two recalls the background necessary for the remainder of the work. We give a brief account of hyperbolic space and its group of isometries. We give Thurston's definition of an orbifold in terms of an atlas of charts, and state a result about the structure of a 3-orbifold's singular locus. We then move on to the setting of complete hyperbolic 3-orbifolds, which are realized as quotients of hyperbolic space by a discrete group of isometries (a *Kleinian group*). We state a structure theorem for complete hyperbolic 3-orbifolds of finite volume - the orbifold is the union of a compact part and a finite number of cusps. We then discuss results relevant to the volumes of hyperbolic 3-orbifolds. In particular, we describe Meyerhoff's work [30] which uses a sphere packing result of Böröczky to obtain a lower bound on the volume of a cusped hyperbolic 3-orbifold in terms of the volumes of its cusps. An immediate corollary of this result is the classification of $\mathbb{H}^3/PGL_2(O_3)$ as the minimal volume cusped orientable hyperbolic 3-orbifold, where O_3 denotes the ring of integers in the number field $\mathbb{Q}(\sqrt{-3})$.

Chapter three is devoted to the classification of the minimal volume orientable hyperbolic 3-orbifolds with one rigid cusp and one nonrigid cusp. We prove two results that fit into a tradition in three dimensional hyperbolic geometry of classifying the least volume element of some family of spaces. As we mentioned earlier, Meyerhoff proved $\mathbb{H}^3/PGL_2(O_3)$ to be the minimal volume orientable cusped hyperbolic 3-orbifold in [29]. Our work here continues a

trail of thought investigated by Colin Adams, over a series of papers, which we now describe.

The cusp neighborhoods (see Definition 2.2.6) of an orbifold lift to $\mathbb{H}^3$ as a collection of horoballs. By studying the horoball packing in $\mathbb{H}^3$, one can obtain information about the volume of the cusp, hence about the volume of the orbifold. In [1], Adams uses an argument about the density of circle packings in the plane to prove that the volume of a cusp in a finite volume hyperbolic 3-manifold is at least $\sqrt{3}/2$. He uses this to prove that the Gieseking manifold, which is double covered by the figure eight knot complement, has minimum volume among all (orientable or not) cusped hyperbolic 3-manifolds. In [3], Adams makes a detailed analysis of the horoball diagrams which correspond to a rigid cusp in an orbifold and classifies the six noncompact orbifolds of least volume. In [4], Adams extends his results to the setting of multiple cusps. He proves that an orbifold with more than one cusp, at least one of which is nonrigid, has volume at least $7v_0/12$. Here, $v_0 \approx 1.01494146$ is the volume of a regular ideal tetrahedron in $\mathbb{H}^3$.

In section 3.1, we construct examples $O_{(6,3,2)}$ and $O_{(4,4,2)}$ of orbifolds with one nonrigid cusp and one rigid cusp of type $(6,3,2)$ and $(4,4,2)$ respectively. The corresponding Kleinian groups are generated by rotations in the edges of polyhedra in $\mathbb{H}^3$. We also prove

Theorem 3.1. *Let O be a complete, orientable, finite-volume hyperbolic 3-orbifold with one nonrigid cusp and one rigid cusp of type $(3,3,3)$. Then $\mathrm{vol}(\mathcal{O}) > v_0$.*

We make a conjecture about the minimal orbifold with one nonrigid and one $(3,3,3)$-cusp. We expect this conjecture can be proven using the tools developed in sections 3.2 - 3.5

We have the following improvements on Adams' bound of $7v_0/12$.

Theorem 3.2. *Let O be a complete, orientable, finite-volume hyperbolic 3-orbifold with one nonrigid cusp and one rigid cusp of type $(6,3,2)$. Then either $O = O_{(6,3,2)}$ or $\mathrm{vol}(O) > 5v_0/6$.*

Theorem 3.3. *Let O be a complete, orientable, finite-volume hyperbolic 3-orbifold with one nonrigid cusp and one rigid cusp of type $(4,4,2)$. Then either $O = O_{(4,4,2)}$ or $\mathrm{vol}(O) > v_1$, where $v_1 \approx 0.91596544\ldots$ is the volume of an ideal tetrahedron with dihedral angles $\pi/4, \pi/4$, and $\pi/2$.*

Section 3.2 collects a variety of results which are used repeatedly in the proofs of the above

theorems. Section 3.3 gives a general overview of the classification argument, independent of the type of the rigid cusp. The remainder of the chapter is devoted to the proofs of Theorems 3.2 and 3.3.

Chapter four focuses on mapping out the category $\mathcal{C}_3$ of orbifolds commensurable (that share a common finite degree covering space) with $\mathbb{H}^3/PGL_2(O_3)$, by enumerating such orbifolds and determining the covering relations between them. The practice of enumerating objects in 3-dimensional topology has a long history. For those interested in hyperbolic geometry or knot diagrams, the most famous example is probably the SnapPea census [9] of cusped hyperbolic 3-manifolds with a geometric ideal triangulation with at most 9 tetrahedra. This project's most direct inspiration comes from the work of Fominkyh, Garoufalidis, Goerner, Tarkaev, and Vesnin [19], in which they construct a census of hyperbolic 3-manifolds which can be decomposed into regular ideal tetrahedra.

The figure eight knot complement (see example 4.3.3), along with its "sister", is the minimal volume orientable cusped hyperbolic 3-manifold [12]. Thurston showed how it may be obtained by face pairing on two regular ideal tetrahedra in $\mathbb{H}^3$. It is a 24-fold cover of $\mathbb{H}^3/PGL_2(O_3)$ (since this orbifold is the quotient of a regular ideal tetrahedron by its orientation preserving symmetry group). Since commensurability is an equivalence relation, this links up our census with that of [19].

Chapter four begins with a broad overview of the steps involved in describing the category $\mathcal{C}_3$. We focus on those elements whose volume is at most $4v_0$, where $v_0 \approx 1.01494146$ is the volume of a regular ideal tetrahedron. A key step is describing the subcategory $\mathcal{C}_{\text{main}}$ whose objects are the orbifolds which cover $\mathbb{H}^3/PGL_2(O_3)$. Any orbifold which covers $\mathbb{H}^3/PGL_2(O_3)$ is triangulated by copies of a certain tetrahedron which is a fundamental domain for the action of $PGL_2(O_3)$ on $\mathbb{H}^3$. In section 4.2 we adapt an algorithm of [19] to enumerate these triangulations. In section 4.3 we describe algorithms for computing geometric data, namely the cusps and singular locus, of such an orbifold from its triangulation.

Some of the interesting structure of $\mathcal{C}_3$ arises from the fact that $\mathbb{H}^3/PGL_2(O_3)$ is arithmetic. Margulis' arithmeticity criterion implies that there are infinitely many minimal elements, in the sense that they cover no other orientable orbifold, in $\mathcal{C}_3$. We close this chapter by describing how one may find the other minimal elements in $\mathcal{C}_3$, as well as how to identify

their canonical covers in $\mathcal{C}_{\text{main}}$.

The background material in chapter two is either well known or a relatively easy exercise. General references are given at the end of each section. The results of section 3.2, with the exception of Proposition 3.2.1, are either stated in Adams' work or would have been no surprise to him. The remainder of this chapter is original, with the caveat that some details are fairly direct applications of Adams' tools. Estimating the volume of a cusp's Voronoi cell is novel to the best of our knowledge. The project of chapter four is a joint work with my advisor Jason DeBlois, my fellow students Anuradha Ekanayake, Arshia Gharagozlou, Mark Fincher, and recently minted Ph.D. Priyadip Mondal. The enumeration algorithm 1 is adapted from [19]. In section 4.2, we describe the nontrivial aspects of porting the algorithm to our setting. Using ideas and code of Mathias Goerner [22], we wrote a concurrent implementation of the algorithm to improve its performance. The remaining algorithms in this section are original. The theorems of section 4.4 are due to my advisor's reading of [26] and [6].

2.0 Background in Hyperbolic Geometry

In this chapter we give a brief summary of hyperbolic space and its isometries. We recall some general theory of orbifolds, before focusing on complete hyperbolic 3-orbifolds and their cusps. Finally we discuss some results relevant to the volumes of cusped hyperbolic 3-orbifolds.

2.1 Hyperbolic Geometry

The origins of hyperbolic geometry lie in attempts to prove Euclid's parallel postulate from his first four postulates. Many great mathematicians since antiquity have failed at this task, and it wasn't until the 19th century that J. Bolyai and N. I. Lobachevsky examined the consequences of an alternative parallel postulate and found the resulting geometry to be consistent. The modern point of view erects hyperbolic geometry upon the foundations laid by Riemann. In this thesis, we adopt this point of view, if only for reasons of economy. The reader who is interested in investigating hyperbolic geometry from the axiomatic perspective is encouraged to consult [32] or [15]

Let $\mathbb{H}^n$ be a complete, simply connected Riemannian n-manifold with constant sectional curvature equal to -1. It is a theorem of Killing and Hopf that such a manifold is unique up to isometry (see Theorem 12.4 of [25]). One representative of this isometry class is Poincaré's upper half space model

$$\mathbb{H}^n = \{(x_1, \ldots, x_{n-1}, t) \in \mathbb{R}^n \mid t > 0\}$$

with Riemannian metric given in global coordinates by

$$ds^2 = \frac{dx_1^2 + \ldots + dx_{n-1}^2 + dt^2}{t^2}$$

There are other useful models of hyperbolic space and one may consult [11] for a nice account of them, but in this thesis we work exclusively in upper half space, and when we refer to $\mathbb{H}^n$

we mean this model. A nice feature of this model is that is conformal, i.e. the metric is a pointwise rescaling of the Euclidean metric. Therefore angles between vectors in $\mathbb{H}^n$ are just Euclidean angles.

We will mostly concern ourselves with $\mathbb{H}^3$. The geodesics of $\mathbb{H}^3$ are Euclidean lines and semicircles orthogonal to $\mathbb{R}^2 \times \{0\}$. Hyperbolic space has an intrinsic notion of a *boundary*, or *sphere at infinity*. Define an equivalence relation on (oriented, parametrized by arclength s) geodesics by declaring two geodesics to be equivalent if they remain within bounded distance of each other as $s \to \infty$. Such an equivalence class is called an *asymptotic pencil* of geodesics, and each asymptotic pencil determines an *ideal point* on $\partial\mathbb{H}^3$. In the upper half space model, we can just think of $\partial\mathbb{H}^3$ as the set of "endpoints" of geodesics, namely $\mathbb{C} \cup \{\infty\}$. Here $\mathbb{C}$ is $\mathbb{R}^2 \times \{0\}$ and visually we think of ∞ as being the "endpoint" of the vertical geodesics which is not contained in $\mathbb{C}$.

The totally geodesic subspaces of $\mathbb{H}^3$ are Euclidean planes and hemispheres orthogonal to $\mathbb{C}$. We refer to these as *planes* in $\mathbb{H}^3$, as they are isometric to $\mathbb{H}^2$.

By analogy with Euclidean geometry, one might expect that the isometries of hyperbolic space can be generated by "reflections" in its planes. This is true if we take reflection in a plane to mean reflection in vertical half planes and *inversion* in Euclidean hemispheres. For a fixed Euclidean sphere of radius r centered at C, the *inverse* of a point $P \neq C$ is defined to be the point P' on the ray $\overrightarrow{CP}$ which satisfies

$$|CP||CP'| = r^2.$$

From this definition, one sees that inversion in the unit hemisphere is given by the map

$$x \mapsto \frac{x}{|x|^2}.$$

For the general sphere $S(a, r)$ centered at $a \in \mathbb{R}^n$ of radius r, conjugating inversion in the unit hemisphere by the composition of translation and dilation which sends $S(a, r)$ onto $S(0, 1)$, we see that inversion in $S(a, r)$ is given by

$$x \mapsto a + r^2 \frac{x - a}{|x - a|^2}.$$

Since reflection in a vertical half plane is a Euclidean isometry which preserves the t-coordinate of $(x,t) \in \mathbb{H}^n$, it preserves the hyperbolic metric and hence is a hyperbolic isometry.

Lemma 2.1.1. *Inversion in the sphere $S(a,r)$ is an isometry of $\mathbb{H}^n$*

Proof. Let σ denote inversion in $S(a,r)$ and let $x, y \in \mathbb{H}^n$. Here $|y-x|$ is the Euclidean distance between x and y. Using the identity $|x|^2 = \langle x, x\rangle$, we have

$$|y-x|^2 = |(y-a)+(a-x)|^2 = |y-a|^2 - 2\langle y-a, x-a\rangle + |x-a|^2$$

and

$$|\sigma(y)-\sigma(x)|^2 = r^4\left(\frac{1}{|y-a|^2} - 2\frac{\langle y-a, x-a\rangle}{|x-a|^2|y-a|^2} + \frac{1}{|x-a|^2}\right)$$

Therefore

$$|\sigma(y)-\sigma(x)|^2 = r^4\frac{|y-x|^2}{|x-a|^2|y-a|^2}$$

Since $a_{n+1} = 0$, we have

$$\sigma(x)_{n+1} = a_{n+1} + r^2\frac{(x-a)_{n+1}}{|x-a|^2} = r^2\frac{x_{n+1}}{|x-a|^2}$$

and we compute

$$\frac{|\sigma(y)-\sigma(x)|^2}{\sigma(x)_{n+1}\sigma(y)_{n+1}} = \frac{\frac{r^4|x-y|^2}{|x-a|^2|y-a|^2}}{\frac{r^2x_{n+1}\cdot r^2y_{n+1}}{|x-a|^2|y-a|^2}} = \frac{|x-y|^2}{x_{n+1}y_{n+1}}$$

It follows that σ preserves the metric on $\mathbb{H}^n$. □

Define the group of Möbius transformations on $\mathbb{R}^n$ as the group $M(\mathbb{R}^n)$ generated by reflections in planes or spheres. The restriction of any $\sigma \in M(\mathbb{R}^n)$ maps $\mathbb{H}^n$ to itself, and we have just proven that $M(\mathbb{R}^n) \subset \mathrm{Isom}(\mathbb{H}^n)$. Let $M^+(\mathbb{R}^n) \leq M(\mathbb{R}^n)$ denote the subgroup of Möbius transformations which can be written as the product of an even number of reflections. Then $M^+(\mathbb{R}^n)$ acts on $\mathbb{H}^n$ by orientation preserving isometries. Conversely, any orientation preserving isometry of $\mathbb{H}^n$ is in $M^+(\mathbb{R}^n)$ (compare pg. 10 of [27] or 7.4 of [5]).

Example 2.1.1. We may recognize some familiar transformations as Möbius transformations and hence as isometries of hyperbolic space.

- For a vector $v \in \mathbb{R}^{n-1} \times \{0\}$, the translation $x \mapsto x + v$ is a product of reflections in two vertical half planes.
- Inversion in the sphere $S(a, 1)$ followed by inversion in $S(a, r)$ is the dilation $x \mapsto r^2 x$.
- The product of reflections in two vertical half planes which intersect with a dihedral angle of θ is a rotation about the axis defined by the intersection of the planes through an angle of 2θ.

The orientation preserving Möbius transformations on $\mathbb{R}^3$ which preserve $\mathbb{H}^3$ may be identified with the group of *fractional linear transformations* acting on $\mathbb{C} \cup \infty$. This is the set of all maps of the form

$$z \mapsto \frac{az + b}{cz + d} \text{ where } a, b, c, d \in \mathbb{C} \text{ and } ad - bc \neq 0$$

The *Poincaré extension* for $\phi \in M(\mathbb{R}^2)$ is defined as follows. It relies on the embedding $\iota \colon \mathbb{R}^2 \to \mathbb{R}^3$ defined by $\iota(x, y) = (x, y, 0)$. Reflection in a line l in $\mathbb{R}^2$ extends to reflection in the vertical half plane above the line $\iota(l)$. Inversion in a circle centered at C of radius r extends to inversion in the hemisphere centered at $\iota(C)$ of radius r. The extension of ϕ is the product of the extensions of its constituent reflections. Any orientation preserving Möbius transformation which preserves $\mathbb{H}^3$ is the Poincaré extension of some $\phi \in M(\mathbb{R}^2)$.

Some fractional linear transformations are dilations $z \mapsto az$ for $a \in \mathbb{R}$, translations $z \mapsto z + b$, and rotations $z \mapsto e^{i\theta} z$. Moreover, reflection in the real axis is given by $z \mapsto \overline{z}$ and inversion in the unit circle is given by $z \mapsto 1/\overline{z}$. After conjugating by an appropriate composition of the maps above, we may represent reflection in any line or inversion in any circle by a map of the form

$$z \mapsto \frac{a\overline{z} + b}{c\overline{z} + d}$$

and any product of an even number of such maps is a fractional linear transformation.

We have proven that any $\phi \in M^+(\mathbb{R}^2))$ is a fractional linear transformation. Conversely, one may prove that any fractional linear transformation is a composition of dilations, rotations, translations and the map $z \mapsto 1/z$ (compare II.7 of [20]). Therefore any fractional linear transformation is a Möbius transformation.

The mapping $GL_2(\mathbb{C}) \to M^+(\mathbb{R}^2)$ defined by

$$\begin{pmatrix} a & b \\ c & d \end{pmatrix} \to z \mapsto \frac{az+b}{cz+d}$$

is a surjective group homomorphism. We say the matrix represents the transformation. Its kernel is $K = \{aI \mid a \neq 0\}$, so we have

$$\mathrm{Isom}^+(\mathbb{H}^3) \approxeq M^+(\mathbb{R}^2) \approxeq PGL_2(\mathbb{C}) = GL_2(\mathbb{C})/K$$

For $A \in GL_2(\mathbb{C})$, the function $\mathrm{tr}(A)^2/\det(A)$ is constant on the coset AK, so induces a well defined function on $PGL_2(\mathbb{C})$. Moreover, this function is invariant under conjugation. For a fractional linear transformation g, define $\mathrm{tr}(g)^2$ to be $\mathrm{tr}(A)^2/\det(A)$ for any matrix $A \in GL_2(\mathbb{C})$ which represents g.

The isometries of $\mathbb{H}^3$ may be classified up to conjugacy by their trace and by their fixed points. We summarize the results below.

Proposition 2.1.1. *Let $g \neq I$ be an isometry of $\mathbb{H}^3$. Then g satisfies exactly one of the following three lists of equivalent properties*

(i) *g is parabolic*
- *g is conjugate to $z \mapsto z+1$*
- *g has exactly one fixed point on $\mathbb{C} \cup \infty$*
- $\mathrm{tr}^2(g) = 4$

(ii) *g is loxodromic*
- *g is conjugate $z \mapsto kz$ for some $k \in \mathbb{C}, |k| \neq 1$*
- *g has exactly two fixed points on $\mathbb{C} \cup \infty$*
- $\mathrm{tr}^2(g) \notin [0,4]$

(iii) *g is elliptic*
- *g is conjugate to $z \mapsto e^{i\theta}z$ for some $\theta \in (0, 2\pi)$*
- *g has infinitely many fixed points in $\mathbb{H}^3$*
- $\mathrm{tr}^2(g) \in [0,4)$

An elliptic transformation has an invariant axis in $\mathbb{H}^3$, fixed pointwise. A loxodromic transformation also has an invariant axis in $\mathbb{H}^3$, but it only fixes the endpoints of the axis. A parabolic transformation has no axis, but a family of invariant surfaces which we now describe.

Given an asymptotic pencil of oriented geodesics, terminating in an ideal point $p \in \mathbb{C} \cup \{\infty\}$, a surface orthogonal to every geodesic in the pencil is called a *horosphere* centered at p. If $p \in \mathbb{C}$, then a horosphere centered at p is a Euclidean sphere tangent to p. A horosphere centered at ∞ has the form $\{(z,t) \mid t = \text{const.}\}$. We call this a horosphere at height t. For $p \in \mathbb{C}$, a *horoball* centered at p is the solid region bounded by a horosphere centered at p. The *horoballs* centered at ∞ have the form $\{(z,t) \mid t \geq \text{const.}\}$.

A parabolic transformation with fixed point $p \in \mathbb{C} \cup \{\infty\}$ leaves any horosphere centered at p invariant.

Notes: The information in this section can be found in many books on hyperbolic geometry. For instance, consult chapter 1 of [27] or chapters 3 and 4 of [5].

2.2 Orbifolds

An orbifold is a space locally modeled on $\mathbb{R}^n$ modulo a finite group action.

Definition 2.2.1. A *local model* is a pair $(\widetilde{U}, G)$ where $\widetilde{U} \subset \mathbb{R}^n$ is open and G is a finite group of diffeomorphisms of $\widetilde{U}$.

An *orbifold map* between local models $(\widetilde{U}, G), (\widetilde{U}', G')$ is a pair $(\widetilde{\psi}, \gamma)$ where $\widetilde{\psi} \colon \widetilde{U} \to \widetilde{U}'$ is smooth, $\gamma \colon G \to G'$ is a homomorphism, and $\widetilde{\psi}$ is equivariant in the sense that $\widetilde{\psi}(g \cdot x) = \gamma(g) \cdot \widetilde{\psi}(x)$. The equivariance requirement implies that $\widetilde{\psi}$ induces a smooth map $\psi \colon \widetilde{U}/G \to \widetilde{U}'/G'$. When $\gamma, \widetilde{\psi}$ and ψ are injective, we say the orbifold map is a *local orbifold isomorphism*.

A (smooth) orbifold O is an underlying Hausdorff, paracompact space X_O covered by open sets U_i with diffeomorphisms $\phi_i \colon U_i \to \widetilde{U}_i/G_i$ satisfying the property that when $U_i \subset U_j$, the inclusion induces a local orbifold isomorphism between the local models $\widetilde{U}_i/G_i$ and $\widetilde{U_j}/G_j$.

Definition 2.2.2. A *orbifold covering* $O \to O'$ is a continuous map $p\colon X_O \to X_{O'}$ such that each $x \in X_{O'}$ has a neighborhood $U \cong \widetilde{U}/G$ such that each component of $p^{-1}(U)$ is isomorphic to $\widetilde{U}/G_i$ for a subgroup $G_i \leq G$. Moreover, the restriction of p to each component of $p^{-1}(U)$ corresponds to the projection $\widetilde{U}/G_i \to \widetilde{U}/G$.

Definition 2.2.3. For an orbifold O and a point $x \in O$ in a local model $\widetilde{U}_i/G_i$, its *local group* G_x is the stabilizer of a point $\widetilde{x} \in \widetilde{U}_i$ which projects to x. The *singular locus* of O is the set of points with non-trivial local group.

When the singular locus is empty, O is a manifold. One can prove that the local models may be taken to be $\mathbb{R}^n/G$ where G is a finite subgroup of the orthogonal group $O(n)$ (compare Theorem 2.3 of [14]). A point in the local model has a neighborhood which is a cone on the orbifold S^{n-1}/G. Combining this with the identification of finite subgroups of $SO(3)$ as the spherical triangle groups, we obtain the following result on the structure of the singular locus

Theorem 2.1 (Theorem 2.5 of [14])**.** *For an orientable 3-orbifold O, its singular locus consists of edges of order $k \geq 2$ and trivalent vertices. The three edges at a vertex have orders $(2,2,k)$ for $k \geq 2$, $(2,3,3), (2,3,4)$, or $(2,3,5)$.*

We will not concern ourselves with the general theory of orbifolds, other than to make use of the above result. We are primarily interested in complete hyperbolic 3-orbifolds.

Definition 2.2.4. When $X = \mathbb{H}^n, \mathbb{R}^n$, or S^n and $G = \mathrm{Isom}(X)$, a (G,X)-orbifold is locally modeled on X modulo finite subgroups of G. Such orbifolds are called, respectively, *hyperbolic*, *Euclidean*, and *spherical*.

The main result is

Theorem 2.2 (Theorem 2.26 of [14])**.** *Any complete (G,X)-orbifold is isometric to X/Γ, where Γ is a discrete subgroup of $G = \mathrm{Isom}(X)$ that acts properly discontinuously on X*

A discrete subgroup of $PGL_2(\mathbb{C}) \cong \mathrm{Isom}^+(\mathbb{H}^3)$ is called a *Kleinian group*. When a discrete $\Gamma \leq PGL_2(\mathbb{C})$ acts on $\mathbb{H}^3$ without fixed points (in other words, Γ contains no elliptics), $\mathbb{H}^3/\Gamma$ is a hyperbolic manifold. A fundamental structure theorem for hyperbolic 3-orbifolds is the *thick-thin decomposition*. For $\Gamma \leq PGL_2(\mathbb{C})$ and $\epsilon > 0$, the ϵ-thin part of

$O = \mathbb{H}^3/\Gamma$ is

$$O_{\text{thin}}(\epsilon) = \{x \in O \mid d(\widetilde{x}, \gamma\widetilde{x}) \leq \epsilon \text{ for some lift } \widetilde{x} \text{ of } x \text{ to } \mathbb{H}^3 \text{ and some } \gamma \text{ of infinite order in } \Gamma\}$$

The ϵ-thick part is

$$O_{\text{thick}}(\epsilon) = \{x \in O \mid d(\widetilde{x}, \gamma\widetilde{x}) \geq \epsilon \text{ for all lifts } \widetilde{x} \text{ of } x \text{ to } \mathbb{H}^3 \text{ and all } \gamma \text{ of infinite order in } \Gamma\}$$

In general, the structure of the thin part is a consequence of the Margulis lemma:

Proposition 2.2.1 (Corollary 2.2 of [17]). *There is a constant $\epsilon' > 0$, such that for any complete oriented hyperbolic 3-orbifold $O = \mathbb{H}^3/\Gamma$ and any $0 < \epsilon < \epsilon'$, each component of $O_{thin}(\epsilon)$ is isometric to either*

(1) a cusp neighborhood, the quotient of a horoball by an orientation-preserving frieze group or wallpaper group.

(2) a solid tube, the quotient of a tubular neighborhood of a geodesic by a cocompact orientation-preserving group of isometries.

In this thesis we only consider finite volume orbifolds, for which we have the following:

Proposition 2.2.2 (Proposition 3.2 of [17]). *A complete oriented hyperbolic 3-orbifold with finite volume is the union of a compact sub-orbifold, bounded by Euclidean 2-suborbifolds, and a finite collection of horoballs modulo wallpaper group actions.*

Notice that solid tubes belong to the compact part, while the quotient of a horoball modulo a frieze group has infinite volume.

Convention: For the remainder of this thesis, when we say a hyperbolic 3-orbifold we mean a complete, orientable, finite volume hyperbolic 3-orbifold.

Next, we survey the five orientation preserving wallpaper groups.

Definition 2.2.5. A *wallpaper group* is a discrete group of isometries of the Euclidean plane which contains two independent translations.

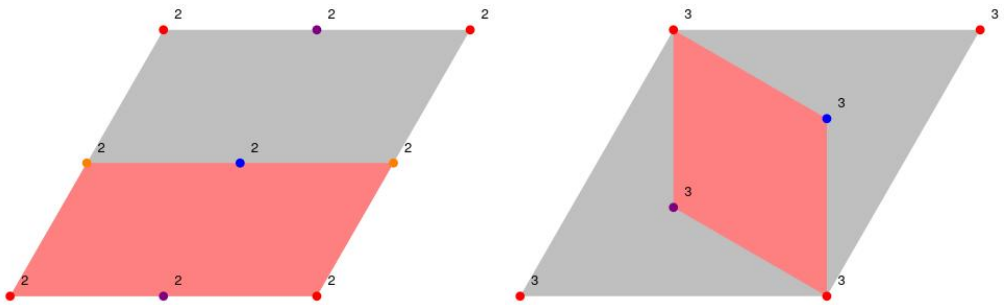

Figure 1: (a) 2222 (b) 333

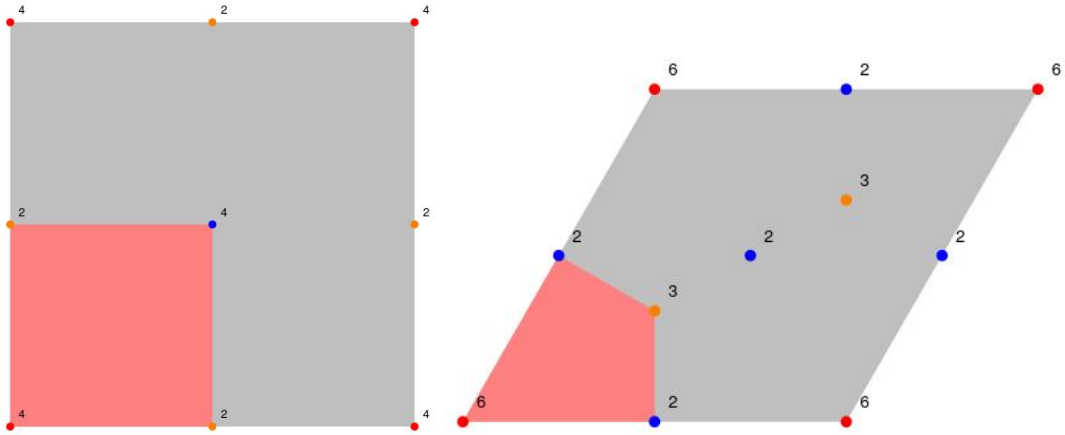

Figure 2: (a) 442 (b) 632

There are seventeen wallpaper groups, the following five of which contain only orientation preserving isometries. In figures 1 and 2, a circle labeled k indicates the center of a $2\pi/k$-rotation. Circles of the same color indicate rotations which are equivalent in the sense that one may obtained from the other by pre or post composition with another rotation in the group. The pink region is a fundamental domain for the action of the group on the plane.

We list the five orientation preserving wallpaper groups in Conway's orbifold notation [13].

- The group o generated by two independent translations. The corresponding orbifold (the

quotient of the plane by o) is a Euclidean torus.

- The group 2222 containing four rotations of order two. Once three of these rotations are specified, the remaining one is determined. The corresponding orbifold is a *pillowcase* and is double covered by a torus. The lattice of rotation centers may be any parallelogram, which is contrasted with the following three groups whose lattices are fixed (rigid).
- The group 333 containing three rotations of order 3.
- The group 442 containing two rotations of order 4 and one of order 2.
- The group 632 containing one rotation each of orders 2, 3, and 6.

We reserve H_∞ for the "standard" horoball $\{(z,t) \mid t \geq 1\}$ centered at ∞.

Definition 2.2.6. An *embedded cusp neighborhood* in O is a connected open subset of O which lifts to a collection $\mathcal{B}$ of disjoint horoball interiors.

Given a collection of horoballs projecting to a cusp neighborhood, one may equivariantly expand or contract the horoballs to obtain a new cusp neighborhood which still projects to the same topological end of the orbifold. See Example 3.1.1 for a concrete application of this idea. We want to think of such neighborhoods as equivalent since they project to the same cusp. We make this precise as follows.

Definition 2.2.7. Define a relation on the set of all embedded cusp neighborhoods in O in the following manner. Given horoball collections $\mathcal{B}_1$ and $\mathcal{B}_2$ which project to cusp neighborhoods C_1 and C_2, we say C_1 and C_2 are equivalent if every horoball in $\mathcal{B}_1$ is contained in a horoball in $\mathcal{B}_2$ (in which case we abuse notation and write $\mathcal{B}_1 \subset \mathcal{B}_2$), or vice versa every horoball in $\mathcal{B}_2$ is contained in $\mathcal{B}_1$.

Lemma 2.2.1. *The relation defined above on the set of embedded cusp neighborhoods in O is an equivalence relation.*

Proof. The only condition which requires some thought is transitivity. Let $\mathcal{B}_1, \mathcal{B}_2$, and $\mathcal{B}_3$ be horoball collections projecting to cusp neighborhoods C_1, C_2, and C_3. Suppose $\mathcal{B}_1 \sim \mathcal{B}_2$ and $\mathcal{B}_2 \sim \mathcal{B}_3$. If $\mathcal{B}_1 \subset \mathcal{B}_2$ and $\mathcal{B}_2 \subset \mathcal{B}_3$ then $\mathcal{B}_1 \sim \mathcal{B}_3$ follows directly. Suppose instead $\mathcal{B}_1 \subset \mathcal{B}_2$ and $\mathcal{B}_3 \subset \mathcal{B}_2$.

If $\mathcal{B}_1 = \mathcal{B}_3$ then there is nothing to prove. We claim that if a horoball $H_1 \in \mathcal{B}_1$ is properly contained in a horoball $H_3 \in \mathcal{B}_3$, then every horoball of $\mathcal{B}_1$ is contained in a horoball of $\mathcal{B}_3$.

For sake of contradiction, suppose there are $H_1' \in \mathcal{B}_1$ and $H_3' \in \mathcal{B}_3$ such that $H_3' \subset H_1'$. Let $\Gamma \leq \mathrm{Isom}^+ \mathbb{H}^3$ be such that $O = \mathbb{H}^3/\Gamma$. Then Γ is the group of deck transformations of the cover $\mathbb{H}^3 \to \mathbb{H}^3/\Gamma$. Since isometries of $\mathbb{H}^3$ send horoballs to horoballs and every horoball in $\mathcal{B}_i$ projects to the same subset of O, Γ acts transitively on each collection $\mathcal{B}_i$.

There is $\gamma \in \Gamma$ satisfying $\gamma(H_1) = H_1'$. But then $H_3' \subset H_1' \subset \gamma(H_3)$, which contradicts the assumption that H_3' and $\gamma(H_3)$ have disjoint interiors. □

Definition 2.2.8. A *cusp* is an equivalence class of embedded cusp neighborhoods. When we say "choose a neighborhood of a cusp", we mean choose a representative of the equivalence class. We will often elide the distinction between a cusp and one of its representative neighborhoods.

By the homogeneity of hyperbolic space, all points on the sphere at infinity are equivalent in the sense that an isometry carries one to another (in fact, as we remarked earlier, the group of isometries acts simply transitively on triples in $\mathbb{C} \cup \{\infty\}$). From the point of view of the upper half space model however, the point ∞ is convenient to work with. Hence, we often want to assume that H_∞ covers a chosen cusp. This is no loss of generality for the following reason.

Let $O = \mathbb{H}^3/\Gamma$ and fix a cusp $C \subset O$. Let H denote a horoball covering C. There is an isometry $g \in \mathrm{Isom}^+ \mathbb{H}^3$ such that $g(H) = H_\infty$. For $x \in \mathbb{H}^3$, one observes directly that g sends the Γ orbit of $x \in \mathbb{H}^3$ to the $g\Gamma g^{-1}$ orbit of $g(x)$, so in fact g induces an isometry $\mathbb{H}^3/\Gamma \cong \mathbb{H}^3/g\Gamma g^{-1}$. Thus after applying g to $\mathbb{H}^3$ and quotienting by $g\Gamma g^{-1}$, we have H_∞ covering C.

Definition 2.2.9. For a fixed cusp C and an embedded cusp neighborhood of C, if H_∞ covers C, the projection of the horoballs in $\mathcal{B} - \{H_\infty\}$ onto $\mathbb{C}$ is called a *cusp diagram* or *horoball diagram* of C.

Definition 2.2.10. An embedded cusp neighborhood is *maximal* if there is a pair of horoballs in $\mathcal{B}$ which are tangent.

A pair of embedded cusp neighborhoods C, C' are *tangent* if there is a horoball covering C which is tangent to a horoball covering C'.

Definition 2.2.11. A cusp is *nonrigid* if it is the quotient of a horoball by either o or 2222. Otherwise, it is *rigid*.

Notes: References for this section are chapter 13 of [34], [14], and [17].

2.3 Volume

In this section we compute the volumes of certain regions in $\mathbb{H}^3$, including ideal tetrahedra. We define the Voronoi cell of a cusp in a hyperbolic 3-orbifold, and discuss Böröczky's theorem which yields a lower bound on the volume of an orbifold in terms of the volumes of its cusps.

In some cases, we can find the volume of a region in $\mathbb{H}^3$ by directly integrating the volume form of the metric on $\mathbb{H}^3$.

Example 2.3.1. let C be a cusp in a hyperbolic 3-orbifold. Then C is the quotient of a horoball H by one of the five wallpaper groups discussed above. Since all horoballs are isometric, we may assume that $H = \{(z,t) \mid t \geq 1\}$. Let F denote a fundamental domain for the action of C's wallpaper group on the horosphere $\{(z,1) \mid z \in \mathbb{C}\}$. Then

$$\text{vol}(C) = \iint_F \int_{t\geq 1} \frac{dt}{t^3} dA = \iint_F \frac{-1}{2t^2}\Big|_1^\infty dA = \frac{1}{2}\iint_F dA = \frac{\text{area}(F)}{2}$$

By an ideal tetrahedron, we mean a tetrahedra in $\mathbb{H}^3$ with all of its vertices on the sphere at infinity.

Fact 2.3.1. *Opposite dihedral angles of an ideal tetrahedron are equal.*

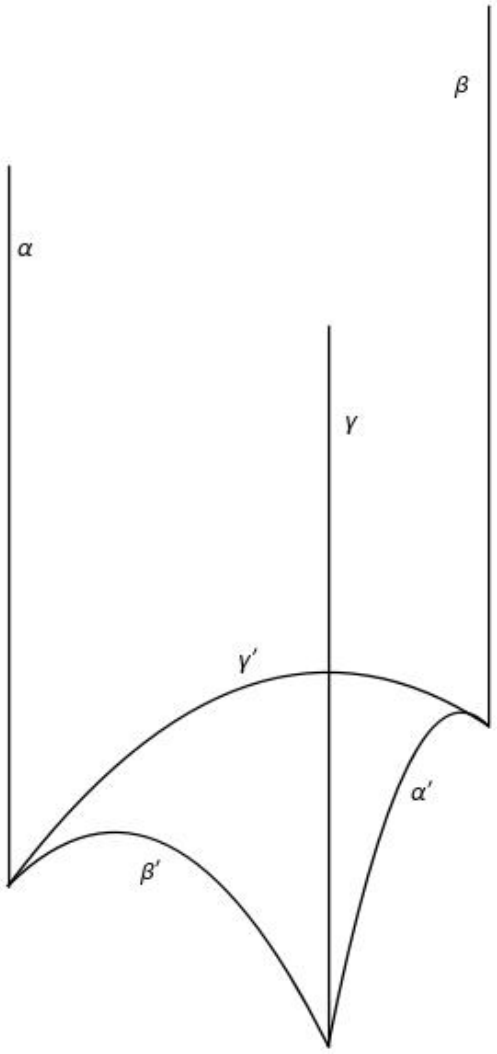

Figure 3: An ideal tetrahedron with dihedral angles labeled $\alpha = \alpha', \beta = \beta', \gamma = \gamma'$.

Proof. Label the dihedral angles α, β, γ and their opposites α', β', γ' as in Figure 3. Since the link of each ideal vertex is an Euclidean triangle, we obtain four equations

$$\alpha + \beta + \gamma = \pi$$
$$\alpha + \beta' + \gamma' = \pi$$
$$\alpha' + \beta' + \gamma = \pi$$
$$\alpha' + \beta + \gamma' = \pi$$

Subtracting the second equation from the first, and the fourth from the third yields

$$\beta + \gamma = \beta' + \gamma'$$
$$\beta' + \gamma = \beta + \gamma'$$

Subtracting these two equations yields

$$\beta - \beta' = \beta' - \beta \iff \beta = \beta'$$

Back substitution yields $\gamma = \gamma'$ and $\alpha = \alpha'$. □

In fact, an ideal tetrahedron is determined up to isometry by its dihedral angles.

The volumes of tetrahedra in $\mathbb{H}^3$ are closely related to *Lobachevsky's function* $\Lambda(\theta)$, defined by

$$\Lambda(\theta) = -\int_0^\theta \log|2\sin u|du.$$

Fact 2.3.2. *Lobachevsky's function* $\Lambda(\theta)$ *is odd and* π*-periodic. For* $n \in \mathbb{Z}$

$$\Lambda(n\theta) = n\sum_{j=0}^{|n-1|} \Lambda(\theta + j\pi/n).$$

The Lobachevsky function has a series representation

$$\Lambda(\theta) = \theta\left(1 - \log|2\theta| + \sum_{n=1}^{\infty} \frac{B_{2n}}{2n}\frac{(2\theta)^{2n}}{(2n+1)!}\right)$$

where the B_{2n} are Bernoulli numbers. This is what we use when we compute $\Lambda(\theta)$ numerically.

Definition 2.3.1. For our purposes, an *orthoscheme* is a hyperbolic tetrahedron (whose vertices may be ideal or not) with a sequence x_0x_1, x_1x_2, x_2x_3 of three mutually perpendicular edges. The orthoscheme $S_{\alpha,\beta,\gamma}$ has three right dihedral angles and is determined by its remaining dihedral angles α, β and γ.

In our applications, we will frequently encounter orthoschemes with an ideal vertex. The link of an ideal vertex is a Euclidean triangle with angles $\alpha, \beta, \pi/2$, so we obtain $\beta = \pi/2 - \alpha$.

The following computation of the volume of such an orthoscheme is due to Lobachevsky.

Fact 2.3.3 (Lemma 7.2.2 of [34])**.**

$$\mathrm{vol}(S_{\alpha,\pi/2-\alpha,\gamma}) = 1/4[\text{Л}(\alpha+\gamma) + \text{Л}(\alpha-\gamma) + 2\text{Л}(\pi/2-\alpha)].$$

In the special case where $\alpha = \gamma$, this reduces to

$$\mathrm{vol}(S_{\alpha,\pi/2-\alpha,\alpha}) = (1/2)\text{Л}(\alpha)$$

We record a basic observation that allows us to compute γ.

Lemma 2.3.1. *Consider an Euclidean hemisphere of radius R and a vertical half plane that is perpendicular to a diameter of the sphere and is a distance $0 \leq l \leq R$ away from the sphere's center. The dihedral angle γ of the sphere and the plane satisfies*

$$\cos\gamma = \frac{l}{R}$$

Proof. Without loss of generality, center the sphere at the origin and let the half plane by determined by $x = l$. The dihedral angle is constant, so we may compute it at the point (l, y, z) on the sphere and the half plane. Then a normal to the sphere is $n_1 = (l, y, z)$ with $|n_1| = R$ and a normal to the plane is $n_2 = (1, 0, 0)$. Therefore

$$\cos\gamma = \cos\angle n_1, n_2 = \frac{n_1 \cdot n_2}{|n_1||n_2|} = \frac{l}{R}$$

□

The volume of an ideal tetrahedron $T_{\alpha,\beta,\gamma}$ with dihedral angles α, β, γ follows easily from the formula for the volume of an orthoscheme. Assume one of the vertices of the tetrahedron is ∞, and drop a perpendicular from ∞ to the plane containing its opposite face: let O denote the base of the perpendicular. Connect O to the other vertices of $T_{\alpha,\beta,\gamma}$ by geodesics, and drop perpendiculars from O to the vertical faces of $T_{\alpha,\beta,\gamma}$.

When the perpendicular from ∞ is in the interior of the opposite face, the result is illustrated in figure 4 with our eye looking down from ∞. We see that $T_{\alpha,\beta,\gamma}$ decomposes as the union of two copies each of $S_{\alpha,\pi/2-\alpha,\alpha}$, $S_{\beta,\pi/2-\beta,\beta}$, and $S_{\gamma,\pi/2-\gamma,\gamma}$, so

$$\mathrm{vol}(T_{\alpha,\beta,\gamma}) = \text{Л}(\alpha) + \text{Л}(\beta) + \text{Л}(\gamma)$$

This also holds in the case that Figure 4 is not accurate (the perpendicular from ∞ is not in the interior of the opposite face).

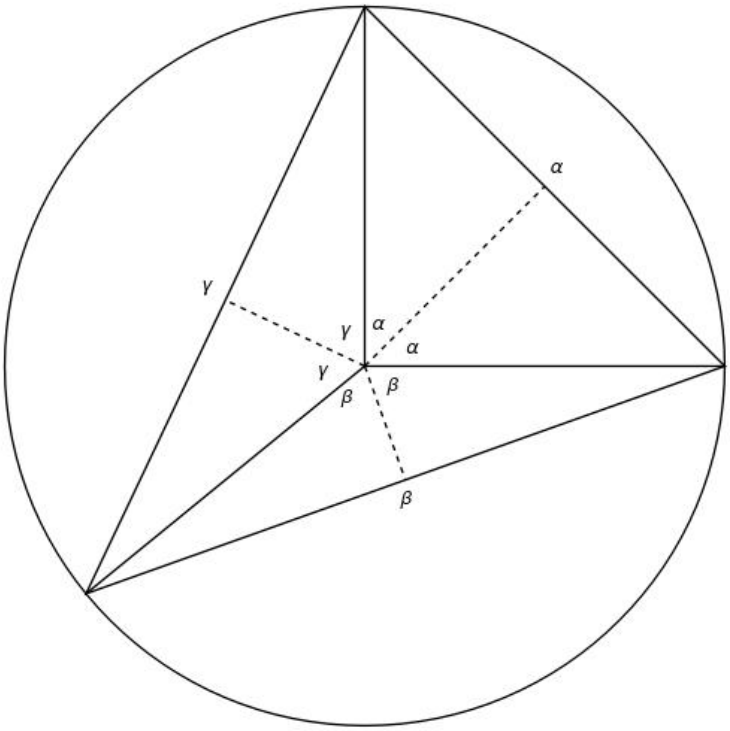

Figure 4: Projection onto the plane of the decomposition of $T_{\alpha,\beta,\gamma}$ into six orthoschemes

Definition 2.3.2. We define $v_0 = 3\Lambda(\pi/3) \approx 1.01494\ldots$ to be the volume of a regular ideal tetrahedron, and $v_1 = 2\Lambda(\pi/4) \approx 0.915966\ldots$ to be the volume of a $(\pi/2, \pi/4, \pi/4)$ ideal tetrahedron.

We record the volumes of a few different orthoschemes in terms of v_0 and v_1.

Fact 2.3.4.

(α, γ)	$\mathrm{vol}(S_{\alpha,\pi/2-\alpha,\gamma})$
$\pi/3, \pi/3$	$v_0/6$
$\pi/6, \pi/6$	$v_0/4$
$\pi/6, \pi/3$	$v_0/24$
$\pi/4, \pi/4$	$v_1/4$
$\pi/4, \pi/3$	$v_1/12$

Proof. The first and fourth claims are apparent from the formula $\mathrm{vol}(S_{\alpha,\pi/2-\alpha,\alpha}) = 1/2\Lambda(\alpha)$.

For the second claim, observe

$$Л(\pi/3) = Л(2 \cdot \pi/6) = 2(Л(\pi/6) + Л(2\pi/3)) = 2(Л(\pi/6) - Л(\pi/3))$$

which implies

$$\mathrm{vol}(S_{\pi/6,\pi/3,\pi/6}) = \frac{1}{2}Л(\pi/6) = \frac{3}{4}Л(\pi/3) = \frac{v_0}{4}$$

The relation $Л(\pi/6) = \frac{3}{2}Л(\pi/3)$ implies

$$\begin{aligned}\mathrm{vol}(S_{\pi/6,pi/3,pi/3}) &= \frac{1}{4}(Л(\pi/2) + Л(-\pi/6) + 2Л(\pi/3)) \\ &= \frac{1}{4}(2Л(\pi/3) - \frac{3}{2}Л(\pi/3)) \\ &= \frac{1}{8}Л(\pi/3) \\ &= \frac{v_0}{24}\end{aligned}$$

For the final claim, begin by observing

$$Л(\pi/4) = Л(3 \cdot \pi/12) = 3(Л(\pi/12) + Л(5\pi/12) + Л(3\pi/4))$$

Since $Л(3\pi/4) = -Л(\pi/4)$, we have

$$Л(\pi/4) = \frac{3}{4}(Л(\pi/12) + Л(5\pi/12)) = -\frac{3}{4}(Л(-\pi/12) + Л(7\pi/12))$$

Then

$$\begin{aligned}\mathrm{vol}(S_{\pi/4,\pi/4,\pi/3}) &= \frac{1}{4}(Л(7\pi/12) + Л(-\pi/12) + 2Л(\pi/4)) \\ &= \frac{1}{4} \cdot \frac{2}{3}Л(\pi/4) \\ &= \frac{v_1}{12}\end{aligned}$$

□

We end this discussion of volume with two simple formulas which will be useful in chapter 3. Given a subset A of $\mathbb{C}$ whose area is well defined, the *flat chimney* $\Pi_f(A,h)$ with base A and height $h>0$ is $A\times[h,\infty)$. We define a *spherical chimney* $\Pi_s(r,h)$ of radius $0<r$ and height $0<h<r$ in $\mathbb{H}^3$ as follows. Consider a Euclidean hemisphere in $\mathbb{H}^3$ centered at $p\in\mathbb{C}$ with radius r and a Euclidean cylinder concentric with the hemisphere and intersecting the hemisphere at height h. The spherical chimney is the intersection of the (solid) cylinder with the complement of the (solid) hemisphere.

Fact 2.3.5.

$$\mathrm{vol}(\Pi_f(A,h))=\frac{\mathrm{area}(A)}{2h^2}$$

and

$$\mathrm{vol}(\Pi_s(r,h))=\pi\log(r/h)$$

Proof. The first computation was already given in Example 2.3.1.

For the spherical chimney, with $p\in\mathbb{C}$ the center of the hemisphere, let $D=\{\omega\in\mathbb{C}||\omega-p|\leq\sqrt{r^2-h^2}\}$. Notice $D\times(0,\infty)$ is the cylinder intersecting the hemisphere at height h. Then the volume of the spherical chimney is given by

$$\iint_D\int_{z\geq\sqrt{r^2-|\omega|^2}}\frac{dz}{z^3}dA=\iint_D\frac{-1}{2z^2}\Big|_{\sqrt{R^2-|\omega|^2}}^{\infty}dA=\frac{1}{2}\iint_D\frac{1}{R^2-|\omega|^2}dA$$

Convert to polar coordinates $\rho=|\omega|,\theta=\arg\omega$, then make the substitution $u=r^2-\rho^2$:

$$\frac{1}{2}\int_0^{2\pi}\int_0^{\sqrt{r^2-h^2}}\frac{\rho}{r^2-\rho^2}d\rho d\theta=\frac{-\pi}{2}\int_{r^2}^{h^2}\frac{du}{u}=\frac{\pi}{2}\log|u|\Big|_{h^2}^{r^2}=\pi\log(r/h)$$

□

Next we discuss how a horosphere-packing result of Böröczky yields a lower bound on the volume of a cusped orbifold $O=\mathbb{H}^3/\Gamma$ in terms of the volumes of its cusps.

Choose an embedded cusp neighborhood for each cusp C_i in O and lift each neighborhood to a collection of horoballs $\mathcal{B}_i$ such that the horoball collections are pairwise disjoint. Let $\mathcal{B}=\bigcup_i\mathcal{B}_i$.

Definition 2.3.3. For a horoball H, we define the distance $d(x,H)$ from a point $x\in\mathbb{H}^3-H$ to H by the length of the perpendicular segment from x to ∂H.

For any horoball $H \in \mathcal{B}$, define the region

$$D(H, \mathcal{B}) = \{x \in \mathbb{H}^3 \mid d(x, H) \leq d(x, H') \text{ for any } H' \in \mathcal{B}\}$$

Let F_0 be a fundamental domain for the action of Γ_∞ on H_∞ where Γ_∞ is the stabilizer of ∞ in Γ. Let $F = F_0 \times (0, \infty)$.

Definition 2.3.4. With notation as above, the *Voronoi cell* $V(C)$ of the cusp C covered by H_∞ is

$$V(C) = D(H_\infty, \mathcal{B}) \cap F$$

Another useful characterization of $V(C)$ is as follows. For each horoball $H \in \mathcal{B}$ centered in the plane, the bisecting plane between H and H_∞ is

$$\mathcal{P}(H) = \{x \in \mathbb{H}^3 \mid d(x, H) = d(x, H_\infty)\}$$

If H is centered at $z \in \mathbb{C}$ and has Euclidean radius $r \leq 1/2$, then $\mathcal{P}(H)$ is a Euclidean hemisphere centered at z of radius $\sqrt{2r}$. By the *exterior* $\operatorname{ext} \mathcal{P}(H)$ of the bisecting plane, we mean the unbounded component of $\mathbb{H}^3 - \mathcal{P}(H)$. Then

$$D(H_\infty, \mathcal{B}) = \bigcap_{H \in \mathcal{B} - \{H_\infty\}} \operatorname{ext} \mathcal{P}(H)$$

and

$$V(C) = \left(\bigcap_{H \in \mathcal{B} - \{H_\infty\}} \operatorname{ext} \mathcal{P}(H) \right) \cap F$$

In fact, we need not take the intersection over the entire collection $\mathcal{B} - \{H_\infty\}$. It is sufficient to take the intersection over the *visible planes*. For $H \in \mathcal{B} - \{H_\infty\}$, we say $\mathcal{P}(H)$ is *visible* if there is $x \in \mathcal{P}(H)$ so the vertical geodesic connecting x to H_∞ does not meet any other $\mathcal{P}(H')$. We say $\mathcal{P}(H)$ is *visible above height* h, if we can choose x so its t-coordinate is h. The terminology is meant to reflect that, if we are looking out from the cusp centered at ∞, the visible planes are the only faces of $V(C_r)$ we would see.

Definition 2.3.5. For a cusped orbifold O with cusps $C_1, \ldots, C_n$, its *Voronoi cell* $V(O)$ is the union of the Voronoi cells for each of its cusps. $V(O)$ depends on the choice of neighborhood for each cusp and the choice of fundamental domain F_0 for the action of Γ_∞ on H_∞ for each cusp neighborhood.

Independent of these choices we have the following (compare Theorem 3.6.1, Lemma 3.5.2, and Theorem 3.5.1 of [27])

Proposition 2.3.1. *For a finite volume cusped orbifold $O = \mathbb{H}^3/\Gamma$, a Voronoi cell for O is a fundamental domain for the action of Γ on $\mathbb{H}^3$. If each fundamental domain F_0 is a finite sided polygon, then $V(O)$ is a polyhedron with finitely many faces, and O is the quotient of $V(O)$ by face pairing isometries.*

Let H_∞ cover the cusp C. The *density* of H_∞ with respect to $V(C)$ is

$$\frac{\mathrm{vol}(H_\infty \cap V(C))}{\mathrm{vol}\, V(C)} = \frac{\mathrm{vol}(C)}{\mathrm{vol}(V(C))}$$

The following theorem is a restatement of Böröczky's theorem on the density of horoball packings found in [7]

Theorem 2.3. *The density of H_∞ with respect to $V(C)$ is no greater than the density of 4 mutually tangent horoballs with respect to the ideal tetrahedron spanned by the centers of the horoballs. This bound is sharp when the ideal tetrahedron is regular.*

Here, the density of the collection of horoballs S with respect to the ideal tetrahedron T is $\mathrm{vol}(S \cap T)/\mathrm{vol}(T)$. We compute this directly when T is regular. For an ideal regular tetrahedron T, the horoballs of Euclidean radius $1/2$ centered at its vertices in $\mathbb{C}$ and H_∞ are all mutually tangent. The region $T \cap H_\infty$ is a chimney above an equilateral triangle of side length 1, hence $\mathrm{vol}(T \cap H_\infty) = \sqrt{3}/8$. Since T has a symmetry exchanging any pair of its vertices, $\mathrm{vol}(T \cap H) = \sqrt{3}/8$ for any of the other three horoballs. Thus the density of these horoballs with respect to T is $\sqrt{3}/2v_0$.

From Böröczky's theorem we obtain the following lower bound on the volume of a cusped orbifold

Proposition 2.3.2. *For an orbifold O with pairwise disjoint embedded cusp neighborhoods $C_1, \ldots, C_n$,*

$$\mathrm{vol}(O) \geq \frac{2v_0}{\sqrt{3}} \sum_{i=1}^{n} \mathrm{vol}(C_i)$$

Proof. Böröczky's theorem implies that

$$\frac{\text{vol}(C_i)}{\text{vol}(V(C_i))} \leq \frac{\sqrt{3}}{2v_0} \iff \text{vol}(V(C_i)) \geq \frac{2v_0}{\sqrt{3}} \text{vol}(C_i)$$

Then

$$\text{vol}(O) = \text{vol}(V(O)) = \sum_{i=1}^{n} \text{vol}(V(C_i)) \geq \frac{2v_0}{\sqrt{3}} \sum_{i=1}^{n} \text{vol}(C_i)$$

□

We refer to this lower bound as *Meyerhoff's bound*.

In [29], Meyerhoff uses this to prove

Theorem 2.4. *$Q = \mathbb{H}^3/PGL_2(O_3)$ has minimum volume among all orientable cusped hyperbolic 3-orbifolds.*

Proof. Let O be any orbifold with at least one cusp C. We may choose an embedded cusp neighborhood of C to be *maximal*, one that intersects itself on its boundary. Lifting this neighborhood to $\mathbb{H}^3$, we see at least one *full-sized* horoball H in C's cusp diagram, i.e., H has Euclidean radius $1/2$ and is tangent to H_∞.

By considering the different cusp types and locations for the center of H, one sees that the least volume cusp is a $(2, 3, 6)$ cusp with H centered at the order 6 singularity. Then the volume of the cusp is at least $\sqrt{3}/24$, and the lower bound implies that

$$\text{vol}(O) \geq \frac{2v_0}{\sqrt{3}} \cdot \frac{\sqrt{3}}{24} = \frac{v_0}{12} = \text{vol}(\mathbb{H}^3/PGL_2(O_3))$$

where the last equality will be established in chapter 3 by constructing a fundamental domain for $\mathbb{H}^3/PGL_2(O_3)$. □

Notes: An excellent reference for the computation of volume in hyperbolic space is John W. Milnor's contribution of chapter 7 to [34]. Böröczky's result appears in a more general context in [7]. Meyerhoff applied this result to obtain bounds on the volume of cusp neighborhoods in [30] and [29].

3.0 Minimal orbifolds with one rigid and one nonrigid cusp

In this chapter we classify the minimal volume orbifolds with one rigid cusp of type $(6,3,2)$ or $(4,4,2)$ and one nonrigid cusp. We begin by constructing the minimal volume examples $O_{(6,3,2)}$ and $O_{(4,4,2)}$ and study their cusp diagrams for a particular choice of cusp neighborhoods. We prove that these cusp diagrams uniquely determine these orbifolds in section 3.3. Section 3.2 collects a number of basic geometric results that are essential for our classification arguments. Finally we prove the following theorems.

Theorem 3.1. *Let O be a complete, orientable, finite-volume hyperbolic 3-orbifold with one nonrigid cusp and one rigid cusp of type $(3,3,3)$. Then $\mathrm{vol}(\mathcal{O}) > v_0$.*

Theorem 3.2. *Let O be a complete, orientable, finite-volume hyperbolic 3-orbifold with one nonrigid cusp and one rigid cusp of type $(6,3,2)$. Then either $O = O_{(6,3,2)}$ or $\mathrm{vol}(O) > 5v_0/6$.*

Theorem 3.3. *Let O be a complete, orientable, finite-volume hyperbolic 3-orbifold with one nonrigid cusp and one rigid cusp of type $(4,4,2)$. Then either $O = O_{(4,4,2)}$ or $\mathrm{vol}(O) > v_1$, where $v_1 \approx 0.91596544\ldots$ is the volume of an ideal tetrahedron with dihedral angles $\pi/4, \pi/4$, and $\pi/2$.*

In this chapter, when proving statements about a non-rigid cusp, we only prove it for a $(2,2,2,2)$-cusp. The assumptions made in these statements will always yield a larger volume in a torus cusp than in a $(2,2,2,2)$-cusp. The reader may wish to review the definitions of cusp neighborhood, cusp diagram, and Voronoi cell of a cusp from section 2.3 before proceeding. For a cusp C in an orbifold $\mathbb{H}^3/\Gamma$, given as the quotient of a horoball centered at $p \in \partial\mathbb{H}^3$ by a wallpaper group action, the *cusp subgroup* $\Gamma(C)$ is the stabilizer of p in Γ. When we refer to a point in $\mathbb{C}$ as a *singularity*, we mean the vertical geodesic above this point is the axis of an elliptic element of $\Gamma(C)$ for the cusp C covered by H_∞.

For a horoball centered in $\mathbb{C}$, when we say its radius we mean its Euclidean radius. Such a horoball is *full-sized* if its radius is $1/2$ (it is tangent to H_∞). If we refer to the distance between a pair of horoballs, we mean the Euclidean distance between their centers, not the hyperbolic distance between their boundaries.

3.1 The minimal volume orbifolds

A polyhedron in $\mathbb{H}^3$ is a *Coxeter polyhedron* if the dihedral angle at each edge divides π. For a Coxeter polyhedron P, let Γ be the isometry group generated by reflections in the faces of P. Then Γ is a discrete group and P is a fundamental domain for Γ (compare Theorem 3.4.7 of [28]). In our examples, Γ will contain an index two subgroup $\Gamma' \leq \Gamma$ generated by rotations in the edges of P. Then $\mathbb{H}^3/\Gamma'$ will be an orientable orbifold with double the volume of $\mathbb{H}^3/\Gamma$.

Figure 5: Singular loci diagrams for $O_{(4,4,2)}$ (left) and $O_{(6,3,2)}$ (right)

Figure 5 contains diagrams for the singular loci of orbifolds with one rigid and one non-rigid cusp. An open circle denotes a cusp. The label k on an edge indicates that the local model for a point on the interior of the edge is the quotient of a ball by a $2\pi/k$ rotation about that edge. The labels on the edges running into a cusp determine the cusp's type. For example, the diagram on the right of Figure 5 contains a nonrigid (2,2,2,2) cusp and a rigid (6,3,2) cusp. The juncture of three edges represents a finite vertex, whose local group is the spherical triangle group determined by the labels on the three edges incident to the vertex (recall Theorem 2.1).

For each diagram, we explicitly describe Coxeter polyhedra in $\mathbb{H}^3$ whose 1-skeleta are isomorphic with the singular graphs by a mapping which sends an edge labeled k in the singular graph to an edge of dihedral angle π/k in the polyhedron.

Let $z_0 = \frac{1}{2} + i\frac{\sqrt{3}}{2}$. Consider an ideal polyhedron $\mathcal{P}_{(6,3,2)}$ in the upper half space model of $\mathbb{H}^3$ with two ideal vertices at ∞ and z_0, and finite vertices lying on the unit hemisphere directly above the ideal points $0, 1/2$, and $i\sqrt{3}/2$. Join the vertices by edges as indicated by Figure 6. One can verify the correspondence between edges in the graph at right of figure 5

with label α and edges in $\mathcal{P}_{(6,3,2)}$ with dihedral angle π/α.

Consider the group generated by reflections in the faces of $\mathcal{P}_{(6,3,2)}$. Let $\Gamma_{(6,3,2)}$ be the index two subgroup generated by rotations in the edges of $\mathcal{P}_{(6,3,2)}$, where an edge labeled π/k is the axis of a rotation of order k.

Definition 3.1.1. Define $O_{(6,3,2)}$ to be $\mathbb{H}^3/\Gamma_{(6,3,2)}$.

The union of $\mathcal{P}_{(6,3,2)}$ and its image under one of the π-rotations about a vertical edge constitutes a fundamental domain for $O_{(6,3,2)}$. The singular locus of $O_{(6,3,2)}$ is as specified by the right side of Figure 5.

We construct a fundamental domain for the orientable orbifold $O_{(4,4,2)}$ with a $(4,4,2)$ rigid cusp by repeating the above construction with $z_1 = \frac{1}{\sqrt{2}} + i\frac{1}{\sqrt{2}}$ in place of z_0.

Subdivide $\mathcal{P}_{(6,3,2)}$ along the vertical half plane containing the ideal points 0 and z_0, and observe that $\mathcal{P}_{(6,3,2)}$ is the union of $S_{\pi/3,\pi/6,\pi/3}$ and $S_{\pi/6,\pi/3,\pi/6}$ identified along the faces contained in this half plane. Therefore Fact 2.3.4 implies

$$\mathrm{vol}(O_{(6,3,2)}) = 2\,\mathrm{vol}(\mathcal{P}_{(6,3,2)}) = 2(\mathrm{vol}(S_{\pi/3,\pi/6,\pi/3}) + \mathrm{vol}(S_{\pi/6,\pi/3,\pi/6})) = 2(\frac{v_0}{6} + \frac{v_0}{4}) = \frac{5}{6}v_0$$

A similar construction applied to the polyhedron for $O_{(4,4,2)}$ shows that a fundamental domain can be constructed from four copies of $S_{\pi/4,\pi/4,\pi/4}$ so

$$\mathrm{vol}(O_{(4,4,2)}) = 4\,\mathrm{vol}(S_{\pi/4,\pi/4,\pi/4}) = v_1,$$

We now choose cusp neighborhoods in $O_{(6,3,2)}$, study their cusp diagrams, and compute the cusp volumes.

Notation: Let $[z,w]$ denote the geodesic in $\mathbb{H}^3$ with ideal endpoints z and w in $\mathbb{C}\cup\infty$, oriented from z to w.

We choose cusp neighborhoods explicitly by declaring which horoballs in $\mathbb{H}^3$ project to the corresponding cusp. Choose H_∞ to cover the nonrigid cusp C_N, and choose a full-sized horoball H_{z_0} centered at z_0 to cover the rigid cusp C_R. Letting $\Gamma_{(6,3,2)}$ act on these horoballs generates the cusp diagram in figure 7 (a). In particular, we obtain a full-sized nonrigid horoball centered at the origin by applying the π-rotation about the axis $[-1,1]$ to H_∞. The remaining full-sized horoballs are obtained by applying the π-rotations in the vertical

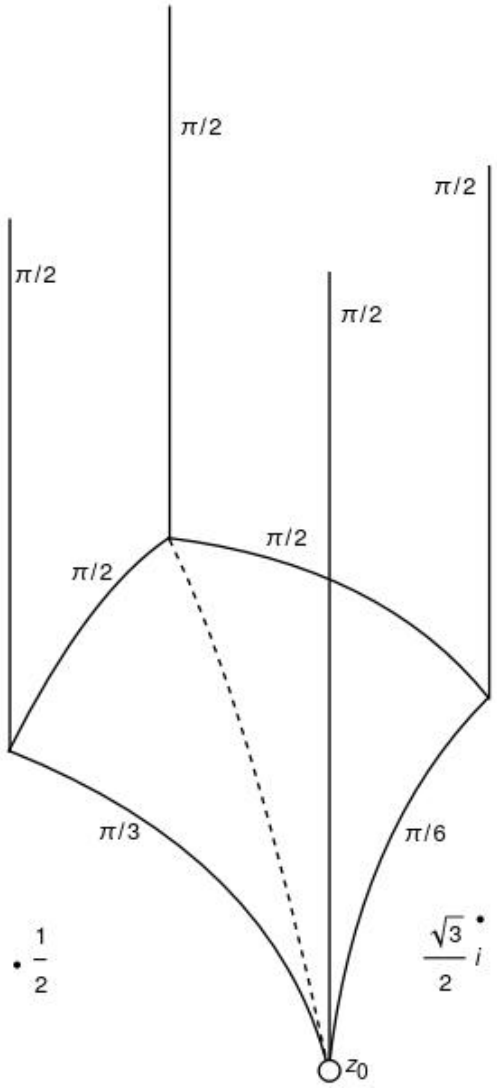

Figure 6: $\mathcal{P}_{(6,3,2)}$ with labels at an edge indicating its dihedral angle.

geodesics to the full-sized horoballs centered at 0 and z_0. In this diagram and the subsequent ones, we make the convention that blue horoballs cover the nonrigid cusp and red horoballs cover the rigid cusp. Notice that in this example both cusps are simultaneously maximized, i.e. are both self-tangent and tangent to each other.

The volume of the nonrigid cusp is half the area of a fundamental domain for the cusp subgroup. In this case, the fundamental domain consists of two copies of a rectangle with

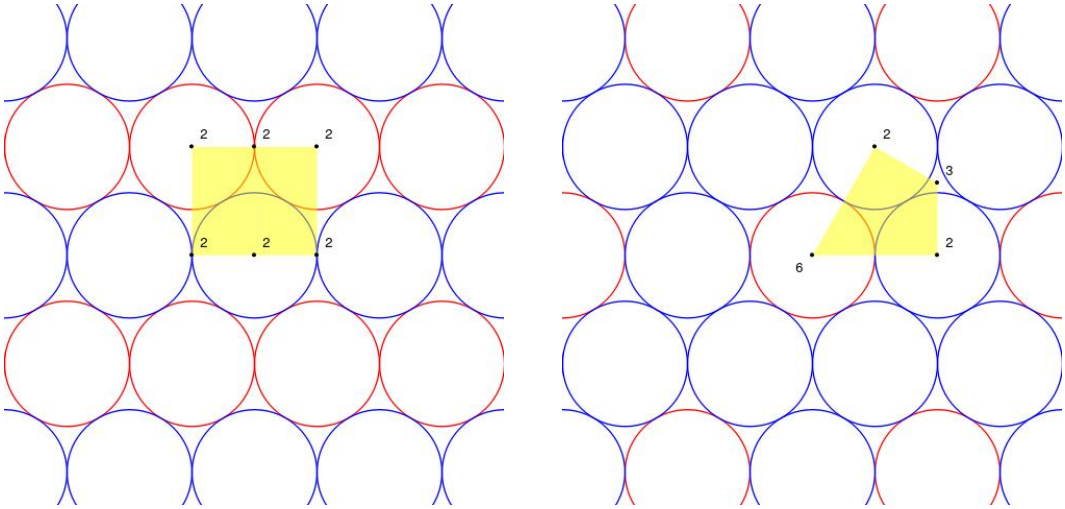

Figure 7: (632 rigid cusp) Diagrams of C_N and C_R, with fundamental domain for Γ_∞ in yellow.

side lengths $1/2$ and $\sqrt{3}/2$, giving a cusp volume of $\sqrt{3}/4$. In fact, Lemma 3.2 of [2] says this is the least possible cusp volume for a maximal nonrigid cusp in an orbifold with more than one cusp.

To determine the volume of the rigid cusp, we change perspective (apply an isometry) so that H_∞ covers C_R. One way to accomplish this is to translate the horoball H centered at z_0 to the origin and apply an elliptic isometry exchanging the origin with infinity. This is given by

$$\rho(z) = \frac{1}{z_0 - z}$$

The geodesics $[\infty, z_0], [-\overline{z_0}, z_0], [\overline{z_0}, z_0]$ all run into the rigid cusp. They pass through the vertices of the Euclidean triangle $\partial H_{z_0} \cap \mathcal{P}_{(6,3,2)}$. Their images under ρ will be vertical geodesics running to infinity which pass through the vertices of a Euclidean triangle giving (half of) the fundamental domain of the rigid cusp subgroup. We calculate the images of

these geodesics under ρ by the formula $\rho[z,w] = [\rho(z), \rho(w)]$.

$$\begin{aligned}
\rho(z_0) &= \frac{1}{-z_0 + z_0} = \infty \\
\rho(\infty) &= \lim_{z\to\infty} \frac{1}{-z + z_0} = 0 \\
\rho(-\overline{z_0}) &= \frac{1}{\overline{z_0} + z_0} = 1 \\
\rho(\overline{z_0}) &= \frac{1}{-\overline{z_0} + z_0} = \frac{1}{i\sqrt{3}} = \frac{-1}{\sqrt{3}}i
\end{aligned}$$

As an aside, these calculations give us rigid horoballs centered at 1 and $-\frac{1}{\sqrt{3}}i$ and a nonrigid horoball centered at the origin. Applying the isometries in the rigid cusp subgroup gives us figure 7(b).

We see that the geodesics running into H in the original picture are sent to:

$$\begin{aligned}
\rho([\infty, z_0]) &= [0, \infty] \\
\rho([-\overline{z_0}, z_0]) &= [1, \infty] \\
\rho([\overline{z_0}, z_0]) &= [-\frac{i}{\sqrt{3}}, \infty]
\end{aligned}$$

Then the fundamental domain is two copies of an Euclidean right triangle with side lengths 1 and $1/\sqrt{3}$. This gives a cusp volume of $\frac{1}{2\sqrt{3}} = \frac{\sqrt{3}}{6}$. According to Meyerhoff's bound, we have

$$\mathrm{vol}(O_{(6,3,2)}) \geq \frac{2v_0}{\sqrt{3}} \left(\frac{\sqrt{3}}{4} + \frac{\sqrt{3}}{6} \right) = \frac{5v_0}{6} = \mathrm{vol}(O_{(6,3,2)})$$

We could have deduced this without any calculation by noting that the horoball packings corresponding to the cusp diagrams are the densest possible, according to Böröczky's theorem. As an exercise, the reader may wish to choose cusp neighborhoods for $O_{(4,4,2)}$ and compute their volumes.

We summarize the results obtained from similar investigations for $O_{(4,4,2)}$. Again we start by considering the polyhedron we constructed for $O_{(4,4,2)}$ and choose H_∞ to cover the nonrigid cusp and the full-sized ball H_{z_1} centered at z_1 to cover the rigid cusp. The cusp

diagrams are illustrated in figure 8. We obtain a disjoint cusp volume $\beta = \frac{1}{2} + \frac{1}{4}$ and a Meyerhoff bound of

$$\text{vol}(O_{(4,4,2)}) \geq \frac{2v_0}{\sqrt{3}} \left(\frac{1}{2} + \frac{1}{4} \right) \approx 0.878965$$

whereas $\text{vol}(O_{(4,4,2)}) = v_1 \approx 0.915966$. Notice that C_N is maximal, and C_R is tangent to C_N but not itself.

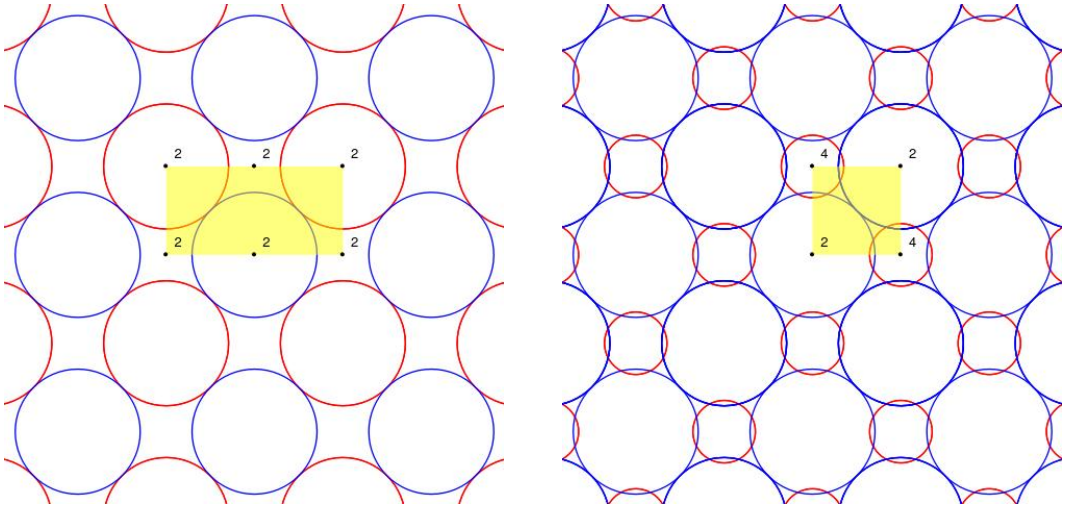

Figure 8: (442 rigid cusp) Diagrams of C_N and C_R, with a fundamental domain for Γ_∞ in yellow.

The following example indicates an extra factor of complexity that arises when analyzing multi-cusped orbifolds. An orbifold with a single cusp has a unique maximal cusp neighborhood. Our choice of cusp neighborhoods above is not unique. Could there be another choice of cusp neighborhoods with greater disjoint cusp volume?

Example 3.1.1. For $O_{(4,4,2)}$, we construct a one-parameter family of cusp neighborhoods, varying from the neighborhoods above to a choice of neighborhoods for which C_R is maximal.

Begin with the choice of cusp neighborhoods given above. From the point of view of the nonrigid cusp at ∞, we can simultaneously raise the height of the horoball centered at ∞ and increase the diameter of the horoball covering the rigid cusp at z_1. The rigid cusp will be maximized when the horoballs centered at z_1 and $-\overline{z_1}$ become tangent, i.e. when their Euclidean diameters are equal to $\sqrt{2}$. We can explicitly parametrize the disjoint cusp

volume in terms of the height h of the horoball $\{t \geq h\}$ centered at ∞ by $\beta[1, \sqrt{2}] \to (0, \infty)$,

$$\beta(h) = \frac{h^2}{4} + \frac{1}{2h^2}$$

To derive this formula, let $\{t \geq h\}$ be the horoball centered at ∞ covering the nonrigid cusp. Since a fundamental domain for the nonrigid cusp subgroup consists of two squares of side length $\frac{1}{\sqrt{2}}$, we have that the volume of the nonrigid cusp is $\frac{1}{2h^2}$. Next, apply the isometry

$$z \mapsto \frac{h^2}{z_1 - z},$$

which sends the horoball centered at z_1 to a horoball centered at ∞. Since this isometry preserves the plane $\{t = h\}$, and the horoballs centered at z_1 and ∞ are tangent at this plane, it maps the horoball centered at z_1 to the horoball centered at ∞ of height h. Moreover, it maps $\overline{z_1}$ and $-\overline{z_1}$ to $-\frac{h^2}{\sqrt{2}}i$ and $\frac{h^2}{\sqrt{2}}$ respectively. Then a fundamental domain for the rigid cusp subgroup is a square with area $h^4/2$, so the rigid cusp has volume $\frac{h^2}{4}$.

It's interesting to note that the maximum value of β is obtained by both endpoints of the one-parameter family of cusp neighborhoods.

The example above raises a natural question for further research (which we do not attempt to answer in this thesis), namely, given a cusped orbifold O, what choice of cusp neighborhoods maximizes the disjoint cusp volume?

3.2 Geometric Lemmas

In this section we record some useful facts which are used throughout our classification arguments. The first is a simple criterion that determines when two horoballs centered in the plane overlap (intersect in their interiors).

Lemma 3.2.1. *Tangent horoballs of Euclidean radii r_1 and r_2 have centers a distance $2\sqrt{r_1 r_2}$ apart.*

Proof. Project onto the plane spanned by the vector pointing from one center to the other and the z-direction, so we are looking at a pair of tangent circles with centers $(x_1, r_1), (x_2, r_2)$. Two circles are tangent exactly when the distance between their centers is equal to the sum of their radii:

$$\sqrt{(x_1 - x_2)^2 + (r_1 - r_2)^2} = r_1 + r_2$$

Equivalently,

$$|x_1 - x_2| = \sqrt{(r_1 + r_2)^2 - (r_1 - r_2)^2} = \sqrt{4r_1 r_2}.$$

□

The following result of Adams [3] allows us to deduce the existence of isometries in the orbifold group from points of tangency between horoballs.

Lemma 3.2.2 (Lemma 2.1 of [3])**.** *Fix a cusp C and let H_∞ cover C (recall that the remark following Definition 2.2.8 states there is no loss of generality in assuming this). If $\Gamma_\infty(C)$ identifies all of the full-sized horoballs which cover C, then every point of tangency between two such horoballs lies on the axis of an order two elliptic isometry in $\Gamma(O)$ such that the axis is tangent to both horoballs.*

Remark: Throughout we will assume the hypothesis of this theorem. If there are multiple equivalence classes of full-sized horoballs in a diagram, the cusp volume will be sufficiently large that we may ignore those cases.

We will be interested in how such order two elliptics act on other horoballs in the cusp diagram. We can understand such isometries geometrically as being inversion in a hemisphere centered in the plane followed by reflection in a vertical half plane.

Lemma 3.2.3. *Let g be an order two elliptic isometry whose axis is a Euclidean semicircle of radius R. If H is a horoball of radius r whose center is a distance c away from the center of g's axis, then $g(H)$ is a horoball of radius $\frac{R^2}{c^2} \cdot r$ whose center is a distance $\frac{R^2}{c}$ away from the center of g's axis.*

Proof. The action of g on $\mathbb{H}^3 \cup \partial\mathbb{H}^3$ is that of inversion σ in the hemisphere containing g's axis followed by reflection in the vertical half plane containing g's axis. Note g is a composition of two reflections in perpendicular hyperbolic planes.

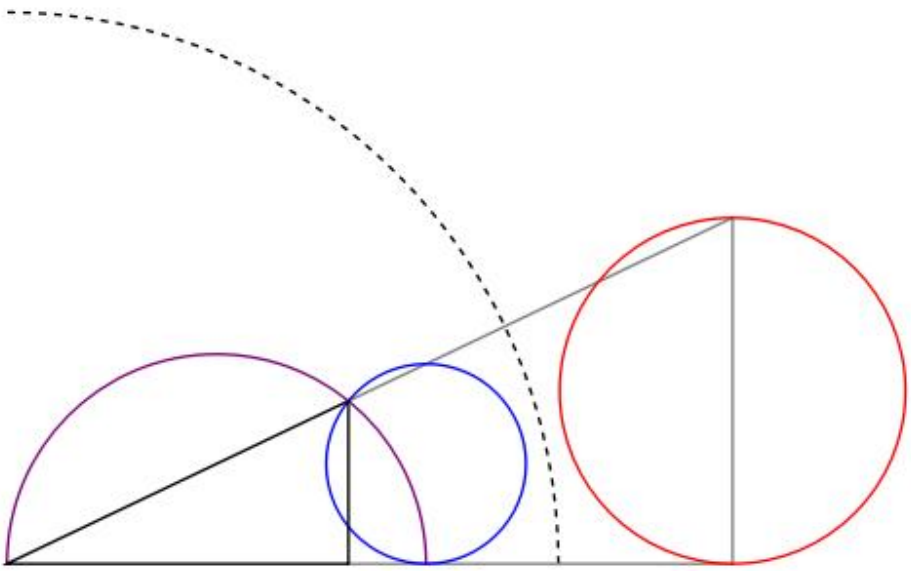

Figure 9: Red and blue horoballs are inverse to each other with respect to the dashed hemisphere

Reflection in the vertical half plane preserves both the distance from the center of $\sigma(H)$ to the center of g's axis and the radius of $\sigma(H)$, so it is enough to consider the effect of σ on H.

In Figure 9, let H denote the blue horoball. Connect the center of H to the center of g's axis by a geodesic l. Then $g(l)$ is a vertical geodesic through a point a distance R^2/c away from the center of g's axis. The point (x, y) at which l intersects ∂H may be found by solving the equations

$$(x - c/2)^2 + y^2 = c^2/4$$
$$(x - c)^2 + (y - r)^2 = r^2$$

Thus we obtain

$$x = \frac{c^3}{c^2 + 4r^2}, \quad y = \frac{2c^2 r}{c^2 + 4r^2}$$

By similarity of triangles, we have

$$\frac{2r(\sigma(H))}{y} = \frac{\frac{R^2}{c}}{x}$$

so

$$r(\sigma(H)) = \frac{y}{2x}\frac{R^2}{c} = \frac{2c^2 r}{2c^3}\frac{R^2}{c} = \frac{R^2}{c^2}r$$

□

Corollary 3.2.1. *Let H be a full-sized horoball, H' a horoball tangent to H with centers a distance c apart, and g an order 2 elliptic which exchanges H with H_∞. Then $g(H')$ is full-sized and its center is a distance $1/c$ away from the center of $g(H_\infty)$.*

Corollary 3.2.2. *Suppose that H_∞ and a full-sized horoball H cover the same cusp. The horoball of largest Euclidean radius among all non full-sized horoballs which cover a different cusp is either tangent to H or its center is a distance at least 1 from the center of H.*

Proof. By Lemma 3.2.2, there is an order 2 elliptic g whose axis goes through the point of tangency of H and H_∞. Let H' denote a horoball of largest Euclidean radius less than $1/2$ which covers a different cusp. If the center of H' has distance less than 1 to the center of H, then 3.2.3 implies that $g(H')$ has larger radius than H'. In order that we do not contradict the maximality of H''s radius, $g(H')$ must be a full-sized ball, which implies that H' is tangent to H. □

Next we give a lower bound for the volume of the nonrigid cusp in the presence of another cusp in terms of lower bounds on the distances between different classes of full-sized horoballs in the nonrigid cusp diagram. The following results are used in the case of the classification arguments in which the nonrigid cusp is tangent to the rigid cusp, but the rigid cusp does not meet itself.

Proposition 3.2.1. *Let C_N be a maximal nonrigid cusp and C another cusp which is tangent to C_N (recall from Definition 2.2.10 this means a pair of horoballs, one covering each cusp, are tangent). Then either* $\mathrm{vol}(C_N) \geq \sqrt{3}/2$ *or*

$$\mathrm{vol}(C_N) \geq v_n(a,b) := \begin{cases} \frac{ab}{2}\sqrt{1-\frac{b^2}{4a^2}} & \text{if } b < \sqrt{2}a \\ \frac{ab}{2\sqrt{2}} & \text{if } b \geq \sqrt{2}a \end{cases}$$

where $a \geq 1$ is a lower bound on the distance between two full-sized horoballs in C_N's diagram which cover different cusps, and $b \geq 1$ is a lower bound on the distance between two full-sized horoballs in C_N's diagram which both cover C_N.

Notice that when $a = b = 1$ we get the apriori bound $\text{vol}(C_N) \geq \frac{\sqrt{3}}{4}$ obtained by Adams, and when $a = 1, b = \sqrt{2}$ we obtain $\text{vol}(C_N) \geq 1/2$ as is seen in the case of $O_{(4,4,2)}$.

Proof. Our assumptions imply that we have full-sized horoballs covering C_N and C in the cusp diagram of C_N. If there is any full-sized horoball which is not centered at an order 2 singularity, the density argument that Adams uses to obtain the bound $\frac{\sqrt{3}}{4}$ (compare Lemma 3.1 and Lemma 3.2 of [2]) can be applied to obtain $\text{vol}(C_N) \geq \frac{\sqrt{3}}{2}$. Let us briefly recall this argument.

Looking down on the plane from ∞, the full-sized horoballs are disks of radius $1/2$ which do not overlap in their interiors. Consider the density of this collection of disks with respect to a parallelogram P which is a fundamental domain for $\Gamma_\infty(C_N)$. Each equivalence class of disks contributes an area of $\pi/4$. Supposing there are n equivalence classes of full-sized horoballs, comparing the density with the density of a hexagonal packing yields

$$\frac{n \cdot \frac{\pi}{4}}{\text{area}(P)} \leq \frac{\pi}{2\sqrt{3}} \iff \text{area}(P) \geq n \cdot \frac{\sqrt{3}}{2}.$$

In the case of a (2,2,2,2) cusp, in the worst case the area of the parallelogram is reduced by a factor of 2. Compare Figure 10 when there are order 2 rotations about the red vertices.

Thus when there is an additional full-sized horoball not centered at an order 2 singularity, we obtain

$$\text{vol}(C_N) = \frac{\text{area}(P)}{2} \geq 2\frac{\sqrt{3}}{4} = \frac{\sqrt{3}}{2}.$$

So we will assume that any full-sized horoball in the diagram is centered at an order 2 singularity. Let A denote the center of a full-sized horoball H_A covering C_N. Let B denote the center of a full-sized horoball H_B which covers C_N and is nearest to H_A. Finally, let C denote the center of a full-sized horoball H_C which covers the other cusp and is the nearest such center to A such that AC and AB are linearly independent vectors. Let ρ_A denote the order two rotation about A, and likewise for ρ_B and ρ_C.

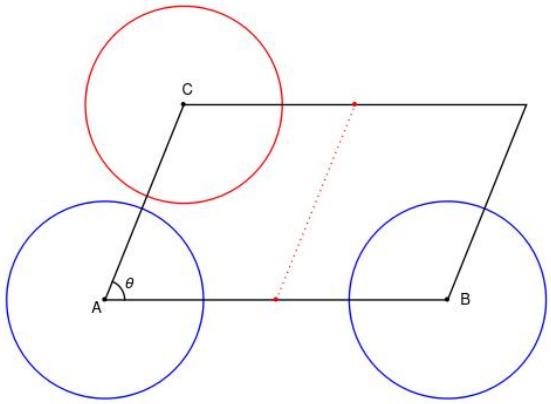

Figure 10: The setting of Proposition 3.2.1. The fixed point of $\rho_C\rho_A\rho_B$ is the final vertex of the parallelogram with vertices A, B, C.

We may obtain a fundamental domain F for $\Gamma(C_N)$ in the following manner. Choose a parallelogram P in the cusp diagram of minimal area which has order 2 singularities only at its vertices. Then we may take F to be the union of P with one of its images under translation along a side of P. It follows that the volume of C_N is the area of P.

Let $\theta = \angle CAB$, so without loss of generality $0 < \theta < \pi$ by the assumption that AC and AB are independent. Moreover, we may assume $0 < \theta \leq \pi/2$, for if $\theta > \pi/2$ replace H_B by its image under the order 2 rotation centered at A. Finally, we assume that $\theta \geq \theta' := \angle CBA$, for otherwise we just exchange the roles of H_B and H_A.

Let B' be the image of B under the order 2 rotation centered at C. By the assumption about H_B, we must have $|AB'| \geq |AB|$. Consider that the triangles ACB and ACB' have side AC in common, and CB, CB' are congruent. The greater side is opposite the greater included angle, so

$$|AB'| \geq |AB| \iff \angle ACB' \geq \angle ACB \iff \angle ACB \leq \pi/2$$

This latter condition is equivalent to $\theta + \theta' \geq \pi/2$. Therefore

$$2\theta \geq \theta + \theta' \geq \pi/2 \iff \theta \geq \pi/4$$

We claim there are no order singularities on the interior of the segment AC, for the horoballs H_A and H_C cover different cusps, thus cannot be exchanged by an isometry of the orbifold group. If there is any order 2 singularity not at the midpoint of AC, but on its interior, then the image of H_C under this rotation will be closer to H_A than H_C is. This contradicts the choice of H_C.

The same argument shows that the only possible location of an order 2 singularity on the interior of AB is at its midpoint. The order 2 singularities at A, C, and B or $(A+B)/2$ determine the parallelogram P described above. Then

$$\text{area}(P) \geq |AC|\frac{|AB|}{2}\sin\theta \geq \frac{ab}{2}\sin\theta$$

We now determine the minimal angle θ. We must have $|CB| \geq a$. If $b \geq \sqrt{2}a$, then the best that can be done is the apriori bound of $\theta \geq \pi/4$, resulting in $\text{area}(P) \geq \frac{ab}{2\sqrt{2}}$. If $b < \sqrt{2}a$, then θ must be greater than $\pi/4$, otherwise the law of cosines implies

$$|CB|^2 = a^2 + b^2 - 2ab\cos\pi/4 = a^2 + b^2 - \sqrt{2}ab = a^2 + b(b - \sqrt{2}a) < a^2$$

contradicting $|CB| \geq a$.

The law of cosines shows that the minimal value of θ for which $|CB| \geq a$ occurs when $\cos\theta = b/2a$. Equivalently, $\sin\theta = \sqrt{1 - b^2/4a^2}$, and this yields our result. □

To apply the previous result, we need some way of obtaining the lower bounds on distances between full-sized horoballs in the nonrigid cusp diagram. These may be obtained from the rigid cusp diagram thanks to the following lemma.

Lemma 3.2.4. *Let C_1, C_2 be cusps covered respectively by H_∞ and a full-sized horoball H. Let e denote the maximum distance between the center of H and the center of any horoball H' which is tangent to H and covers C_i, where $i \in \{1, 2\}$.*

Assuming that there is a single equivalence class of full-sized horoballs covering each cusp, $1/e$ is the minimum distance between the centers of full-sized horoballs in the diagram of C_2 which cover C_1 and C_i respectively.

Proof. An isometry g which exchanges H_∞ with H sends H' to a full-sized horoball whose center is a distance at least $1/e$ away from $g(H_\infty)$. Any full-sized ball closer to $g(H_\infty)$ is sent by g to a horoball tangent to H with centers a distance greater than e apart. □

The next result is a minor generalization of Adams' idea of a *disk of no tangency*. This is a (spherical) disk on the boundary of a horoball containing no points of tangency with other horoballs. Its radius is its Euclidean radius, measured with respect to the Euclidean metric on the horosphere.

Lemma 3.2.5. *Let H be a horoball of Euclidean radius $r < 1/2$. Suppose the largest Euclidean radius of any horoball tangent to H is r'. Then H has a disk of no tangency on its boundary of radius $\sqrt{r/r'}$.*

Proof. An order two elliptic g which exchanges H with H_∞ will have axis an Euclidean semicircle of radius $\sqrt{2r}$. A horoball H' of radius r' and tangent to H must have its center a distance $2\sqrt{rr'}$ away from the center of H. Then $g(H')$ is a full-sized horoball whose center is a distance

$$\frac{(\sqrt{2r})^2}{2\sqrt{rr'}} = \sqrt{\frac{r}{r'}}$$

away from the point directly above the center of H on $\partial g(H)$. Any full-sized horoball closer to this point correpsonds under g to a horoball tangent to H of radius larger than r', so there are no points of tangency within this disk. □

3.3 Classification

The cusp diagrams of $O_{(6,3,2)}$ and $O_{(4,4,2)}$ computed in section 3.1 contain enough information to recover the orbifolds themselves. Each cusp diagram determines the combinatorics of the cusp's Voronoi cell. We can also deduce enough information (see Lemma 3.2.2) to determine the face pairings of each cell, hence the orbifold is determined.

Theorem 3.4. *An orbifold O with a nonrigid cusp and a rigid cusp of type $(6,3,2)$ or $(4,4,2)$ with cusp diagrams as in Figures 7 or 8 is isometric to $O_{(6,3,2)}$ or $O_{(4,4,2)}$.*

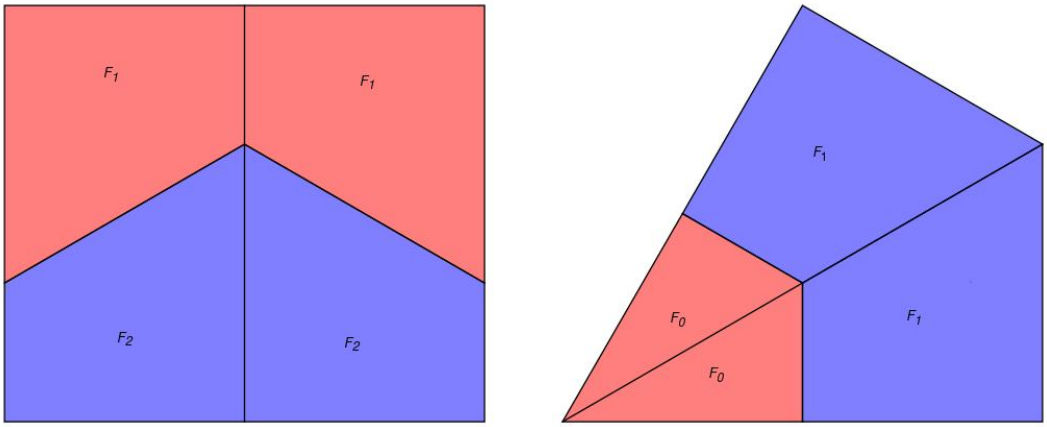

Figure 11: Combinatorics of $V(C_N)$ and $V(C_R)$ with rigid (6,3,2) cusp.

Proof. Suppose an orbifold O has a nonrigid cusp and rigid $(6, 3, 2)$ cusp with diagrams as in Figure 7. In Figure 11, we see $V(C_N)$ and $V(C_R)$ from the viewpoint of ∞. The faces of a Voronoi cell which are contained in vertical half planes have their pairings determined by the cusp subgroup. In $V(C_R)$, the faces denoted F_0 are identified by an order two elliptic isometry which exchanges the full-sized ball centered at the order 6 singularity and H_∞. The face pairing isometry exists by Lemma 3.2.2, and it makes an angle of $\pi/6$ with the horizontal, as it needs to act as a reflective symmetry on the union of the two faces F_0.

The faces labeled F_1 in the Voronoi diagram of C_R intersects the faces labeled F_1 in the Voronoi diagram of C_N. In the diagram of $V(C_N)$, the faces labeled F_2 are identified by an order two elliptic which exchanges the full-sized ball whose bisecting plane contains F_2 with H_∞.

If instead O has a rigid $(4, 4, 2)$ cusp, we see the Voronoi diagrams in 12. The faces labeled F_0 in $V(C_R)$ intersect $V(C_N)$ in the faces labeled F_0 there. In $V(C_N)$, consider the order 2 elliptics which exchange the full-sized ball whose plane contains F_1 with ∞. In principle, elliptics whose axes make an acute angle of $\pi/4$ with the horizontal are symmetries of the horoball packing. But then the rigid cusp would have distinct order two axes running into it, which is not possible. So there is an order 2 elliptic whose axis is perpendicular to the horizontal, and this isometry identifies the two faces labeled F_1, and the two faces labeled

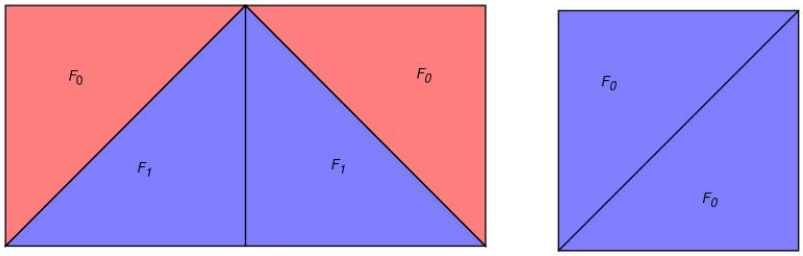

Figure 12: Combinatorics of $V(C_N)$ and $V(C_R)$ with rigid (4,4,2) cusp.

F_0.

□

We remark that the perspective of obtaining the orbifold via face pairings of its Voronoi cells gives another way to compute the orbifold's volume. By looking at the diagrams in Figure 11, for $O_{(6,3,2)}$, $V(C_R)$ can be decomposed into eight orthoschemes $S_{\pi/6,\pi/3,\pi/3}$ while $V(C_N)$ can be decomposed into twelve such orthoschemes, and we recover

$$\operatorname{vol}(O_{(6,3,2)}) = 20 \operatorname{vol}(S_{\pi/6,\pi/3,\pi/3}) = 20 \cdot \frac{v_0}{24} = \frac{5}{6} v_0.$$

Likewise, the Voronoi cells of $O_{(4,4,2)}$ decompose into twelve orthoschemes $S_{\pi/4,\pi/4,\pi/3}$ and we obtain

$$\operatorname{vol}(O_{(4,4,2)}) = 12 \operatorname{vol}(S_{\pi/4,\pi/4,\pi/3}) = 12 \cdot \frac{v_1}{12} = v_1.$$

Finally, we remark that this perspective led us to wonder what is the minimal volume orbifold with one nonrigid cusp and one rigid $(3,3,3)$ cusp?

Conjecture. *The minimal volume orbifold with one nonrigid cusp and one rigid* $(3,3,3)$ *cusp has volume* $5v_0/3$ *and cusp diagrams given in Figure 13.*

Now we aim to prove theorems 3.1, 3.2, and 3.3. Before proceeding with the details, we give a general outline of the argument without regard to the type of the rigid cusp.

Assume O is an orbifold with one non-rigid and one rigid cusp. Let C_N be a maximal non-rigid cusp, and choose the rigid cusp C_R to be maximal with respect to C_N. There are three qualitatively different ways in which the two cusps may interact.

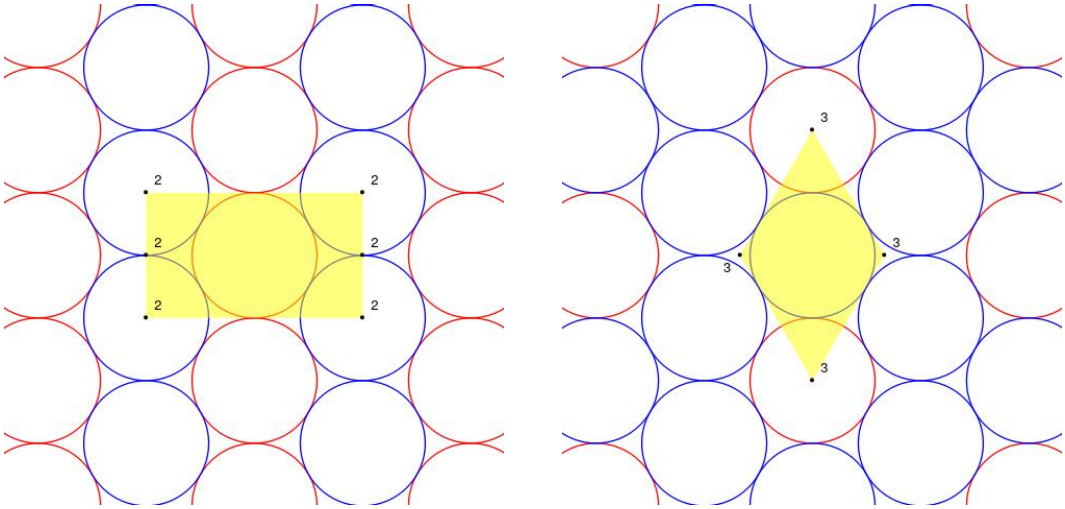

Figure 13: (333 rigid cusp) Diagrams of C_N and C_R, with fundamental domain for Γ_∞ in yellow.

(i) Both C_N and C_R may be "simultaneously maximized", i.e. they are tangent to each other as well as being self tangent.

(ii) C_N and C_R are tangent, but C_R is not tangent to itself.

(iii) C_N and C_R are disjoint, in which case C_R is tangent to itself.

In our examples, the cusp choices for $O_{(6,3,2)}$ and $O_{(4,4,2)}$ exhibit cases (i) and (ii) respectively.

Once the cusp interaction has been determined, we study horoball diagrams. We say a horoball is *rigid* (resp. *non-rigid*) if it covers C_R (resp. C_N). Our goal is to either prove that the horoball diagrams match those of our examples, or $\mathrm{vol}(O)$ is sufficiently large.. The tools for increasing volume we use are slightly different in each case.

Case (i) is typically the easiest to handle, since we may assume the presence of two different classes of full-sized horoballs in C_R's diagram. Lemma 2.3 of [2] implies that any non-rigid horoball may only be centered at a singularity if it's order is 2. Any full-sized rigid horoballs give rise to an order 2 elliptic isometry via Lemma 3.2.2. With the exception of highly symmetric diagrams, these elliptic isometries are used to show that $\mathrm{vol}(C_R)$ must be sufficiently large in order that different horoballs do not overlap.

In case (ii), we only have the presence of a full-sized nonrigid horoball H_n in C_R's diagram. Without the order 2 elliptics present in case (i), it is not clear how to force $\mathrm{vol}(C_R)$ to be larger. By asking what are the largest horoballs tangent to H_n, we are able to leverage Proposition 3.2.1 to improve the lower bound on $\mathrm{vol}(C_N)$ beyond the apriori bound $\mathrm{vol}(C_N) \geq \sqrt{3}/4$ from Lemma 3.2 of [2].

In case (iii), we see a dichotomy in C_R's diagram. If full-sized horoballs are far apart, then $\mathrm{vol}(C_R)$ is large. If full-sized horoballs are close together, then the remaining horoballs in the diagram must have small Euclidean radii. In the latter case, we directly estimate volume in the compact part of O by computing the volume of a model of the truncated Voronoi cell (see section 3.4.3.4 for definitions).

We hope this outline helps the reader follow the thread of the argument without being lost in the forest of technical details.

Real work is required when the rigid cusp has type $(6, 3, 2)$ or $(4, 4, 2)$. First we dispense with the case of a $(3, 3, 3)$ rigid cusp, which is simpler since this type of cusp has a larger fundamental domain for $\Gamma(C_R)$, namely a rhombus with order 3 singularities only at its vertices, with one pair of opposite vertices being equivalent (compare section 2.3). In coordinates, we may assume there are order 3 singularities $(0, 0), (\pm\sqrt{3}d/6, d/2), (0, d)$, with $(0, 0)$ and $(0, d)$ being identified by the other two order 3 rotations, then the rhombus has area $\sqrt{3}d^2/6$ and $\mathrm{vol}(C_R) = \sqrt{3}d^2/12$.

Theorem 3.1. *Let O be a complete, orientable, finite-volume hyperbolic 3-orbifold with one nonrigid cusp and one rigid cusp of type $(3, 3, 3)$. Then $\mathrm{vol}(\mathcal{O}) > v_0$.*

Proof. In cases (i) and (ii) described above, there is a full-sized nonrigid horoball H_n in C_R's diagram. H_n cannot be centered at any singularity. In order that it does not overlap with any of its translates, H_n must stay a distance at least $1/\sqrt{3}$ away from each order 3 singularity. Without loss of generality, assume that H_n is closer to $(0, 0)$ than it is to $(0, d)$. Then disks of radius $1/\sqrt{3}$ centered at $(0, 0)$ and $(\pm\sqrt{3}d/6, d/2)$ must not cover the bottom half of the rhombus.

We see that the circles centered at $(\pm\sqrt{3}d/6, d/2)$ intersect when $x = 0$ and

$$y = \frac{d}{2} \pm \sqrt{\frac{1}{3} - \frac{d^2}{12}}$$

Then the minimal value of d required for the disks to not cover the bottom half of the rhombus satisfies

$$\frac{d}{2} - \sqrt{\frac{1}{3} - \frac{d^2}{12}} = \frac{1}{\sqrt{3}}$$

Solving this equation yields $d = \sqrt{3}$. So $d \geq \sqrt{3}$ which implies $\mathrm{vol}(C_R) \geq \sqrt{3}/4$. Therefore,

$$\mathrm{vol}(O) \geq \frac{2v_0}{\sqrt{3}} \left(\frac{\sqrt{3}}{4} + \frac{\sqrt{3}}{4} \right) = v_0.$$

In case (iii), there is a full-sized rigid horoball H_r in C_R's diagram. There is also a nonrigid horoball H of largest Euclidean radius. By Corollary 3.2.2 the distance between the centers of H and H_r must be at least one. Since H cannot be centered at an order 3 singularity, this implies that $d/\sqrt{3} > 1$, i.e. $d > \sqrt{3}$. Applying Meyerhoff's bound as above, we obtain

$$\mathrm{vol}(O) \geq v_0$$

□

3.4 Proof of Theorem 3.2

Theorem 3.2. *Let O be a complete, orientable, finite-volume hyperbolic 3-orbifold with one nonrigid cusp and one rigid cusp of type $(6,3,2)$. Then either $O = O_{(6,3,2)}$ or $\mathrm{vol}(O) > 5v_0/6$.*

Throughout, let d denote the distance between two order 6 singularities in the rigid cusp diagram. A fundamental domain for the cusp subgroup is a flat chimney above a quadrilateral with vertices at order 6, 3, and 2 singularities (see Figure 2). Introduce coordinates so that the order 6 singularity is at $(0,0)$, there are order 2 singularities at $(d/2, 0)$ and $(d/4, \sqrt{3}d/4)$, and the order 3 singularity is at $(d/2, \sqrt{3}d/6)$. Let ρ_6 denote the $\pi/3$ rotation about $(0,0)$, ρ_2 denote the π rotation about $(d/2, 0)$, and ρ_3 denote the $2\pi/3$ rotation about $(d/2, \sqrt{3}d/6)$. We see that $\mathrm{vol}(C_R) = \frac{\sqrt{3}d^2}{24}$.

3.4.1 Simultaneously maximized cusps

The first case implies the existence of a full-sized rigid horoball H_r and a full-sized nonrigid horoball H_n in the rigid cusp's diagram. In what follows, we consider the least volume cusp diagram that occurs depending on where H_r is centered.

In order to obtain $\text{vol}(O) \geq 5v_0/6$, it is sufficient to prove $d \geq 2$.

(Aside: Figures of the cusp diagrams have been included for the more complex cases, but the reader is encouraged to sketch their own figures in each case. It will make the lower bounds obtained on d more apparent.)

3.4.1.1 H_r is not centered at any singularity

The least volume diagram has H_n centered at the order 2 singularity. Since H_n must be a distance at least one away from H_r, the center of H_r is a distance at least one away from the order 2 singularity. In order that H_r not overlap with $\rho_6(H_r)$, its center must be a distance at least one away from the order 6 singularity. Hence the equilateral triangle with vertices at the order 6 and order 2 singularities has distance from any vertex to its orthocenter at least 1. Therefore $d > 2\sqrt{3}$.

3.4.1.2 H_r is centered at the order 2 singularity

Then H_n is not centered at any singularity. By swapping the roles of H_r and H_n in the argument above, we have $d > 2\sqrt{3}$.

3.4.1.3 H_r is centered at the order 3 singularity

The least volume diagram has H_n centered at the order 2 singularity. Then the distance between the order 3 and order 2 singularities is at least 1, which implies $d \geq 6/\sqrt{3} = 2\sqrt{3}$.

3.4.1.4 H_r is centered at the order 6 singularity

The least volume diagram has H_n centered at the order 2 singularity, and $d \geq 2$. Observe that when $d = 2$ we have the rigid cusp diagram of $O_{(6,3,2)}$, and by changing perspective (apply an isometry sending a full-sized rigid horoball to H_∞) we also have its nonrigid cusp diagram, so Theorem 3.4 implies that $O = O_{(6,3,2)}$

Lemma 3.4.1. *If $d > 2$, then $d > 2\sqrt[4]{3}$*

Proof. Suppose $d > 2$. Let g_θ be the order two elliptic which exchanges H_r with H_∞, where θ denotes the angle between the projection of g_θ's axis and the x-axis. The point of tangency between H_r and H_∞ is a lift of a (6,2,2) finite vertex of the singular locus, so there is another order two elliptic whose axis makes an angle of $\pi/6$ with g_θ's axis, hence we may assume $0 \leq \theta < \pi/6$.

Then $g_\theta(H_n)$ is a horoball of radius $2/d^2$ whose center is a distance $2/d$ away from the center of H_r. Let $a(\theta)$ and $b(\theta)$ denote the distance from the center of $g_\theta(H_n)$ to the center of H_n and of $\rho_6(H_n)$ respectively. Then the law of cosines implies

$$a(\theta)^2 = \frac{d^2}{4} + \frac{4}{d^2} - 2\cos 2\theta$$
$$b(\theta)^2 = \frac{d^2}{4} + \frac{4}{d^2} - 2\cos(\pi/3 - 2\theta)$$

One calculates that $a(\theta) \leq b(\theta$ if and only if $\theta \leq \pi/12$. If $\theta > \pi/12$, the distance between the centers of $g_\theta(H_n)$ and $\rho_6(H_n)$ equals the distance between the centers of $g_{\pi/12-\theta}(H_n)$ and H_n, so without loss of generality we assume $\theta \leq \pi/12$. Observe that $b(\theta) \leq b(\pi/12)$ for all $\theta \in [0, \pi/12]$. In order that $g_\theta(H_n)$ and H_n do not overlap, we must have

$$2\sqrt{\frac{2}{d^2} \cdot \frac{1}{2}} \leq b(\theta) \leq b(\pi/12)$$

The left hand side reduces to $2/d$, so we have

$$\frac{4}{d^2} \leq b(\pi/12)^2 = \frac{d^2}{4} + \frac{4}{d^2} - \sqrt{3}.$$

It follows that $d \geq 2\sqrt[4]{3}$. □

We observe that either $O = O_{(6,3,2)}$ or $d > 2\sqrt[4]{3}$ which implies that

$$\text{vol}(O) \geq \frac{2v_0}{\sqrt{3}}\left(\frac{\sqrt{3}}{4} + \frac{1}{2}\right) = \left(\frac{2+\sqrt{3}}{2\sqrt{3}}\right) v_0 > v_0$$

3.4.2 Rigid cusp is not self-tangent

Consider the second case, in which C_N and C_R are tangent, but C_R does not touch itself. Then we only have a full-sized horoball H_n covering C_N in the rigid cusp's diagram. The least volume case occurs when H_n is centered at the order 2 singularity and is tangent to its translates by the order 3 rotation, so $d \geq 2$.

We obtain inputs to Proposition 3.2.1 by asking: what is the maximum distance between the centers of H_n and a horoball H which is tangent to H_n? If H covers C_N and $d = 2$, then clearly the maximum distance is 1. It is less than 1 if $d > 2$ or H covers C_R.

Suppose H is a rigid horoball. By assumption, H is not full-sized, so it cannot be centered at the order six singularity. Let c denote the distance between the center of H and the nearest full-sized nonrigid horoball. Let a denote the distance from the center of H to the nearest order 6 singularity. Note $a > 0$. We observe that c will be maximized when H is on the equidistant line between the points $(d/2, 0)$ and $(d/4, \sqrt{3}d/4)$.

The maximum c corresponds to the minimal a. In order that H not overlap with its translates by ρ_6, we must have $a \geq 2r(H)$. Since H is tangent to H_n, we must have $r = c^2/2$, so the maximum value of c occurs when $c^2 = a$.

The law of cosines implies that a and c are related by

$$\begin{aligned} c^2 &= a^2 + \frac{d^2}{4} - \frac{\sqrt{3}}{2}ad \\ &= c^4 + \frac{d^2}{4} - \frac{\sqrt{3}d}{2}c^2 \end{aligned}$$

equivalently,

$$c^4 - (\frac{\sqrt{3}d}{2} + 1)c^2 + \frac{d^2}{4} = 0$$

We obtain the following upper bound on c:

$$c \leq c(d) := \sqrt{\frac{\frac{\sqrt{3}d}{2} + 1 - \sqrt{(\frac{\sqrt{3}d}{2} + 1)^2 - d^2}}{2}}$$

According to Lemma 3.2.4, in C_N's diagram we have a minimum distance $1/c(d)$ between full-sized horoballs covering different cusps. The distance b between full-sized horoballs covering the same cusp is 1 when $d = 2$ or $1/c(d)$ if $d > 2$.

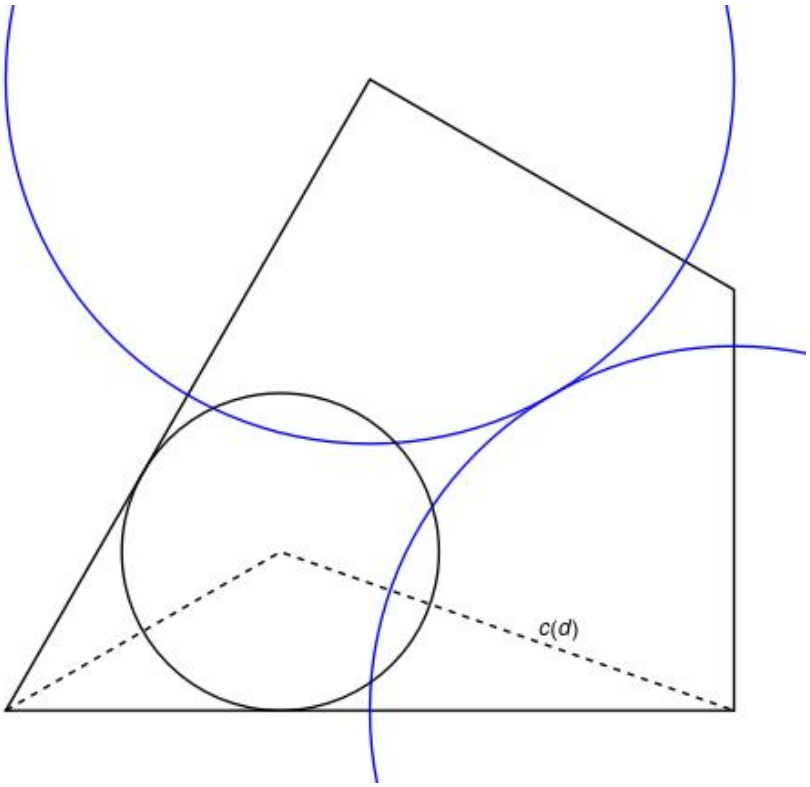

Figure 14: The maximum distance between H and H_n

By Proposition 3.2.1 we calculate, when $d = 2$,

$$\text{vol}(O) \geq \frac{2v_0}{\sqrt{3}} \left(v_n(1/c(d), 1) + \frac{\sqrt{3}}{6} \right) \approx 1.17662 > v_0$$

and for $2 < d \leq \sqrt{6}$ we have

$$\text{vol}(O) \geq \frac{2v_0}{\sqrt{3}} \left(v_n(1/c(d), 1/c(d)) + \frac{\sqrt{3}d^2}{24} \right) > v_0$$

as can be seen in figure 15

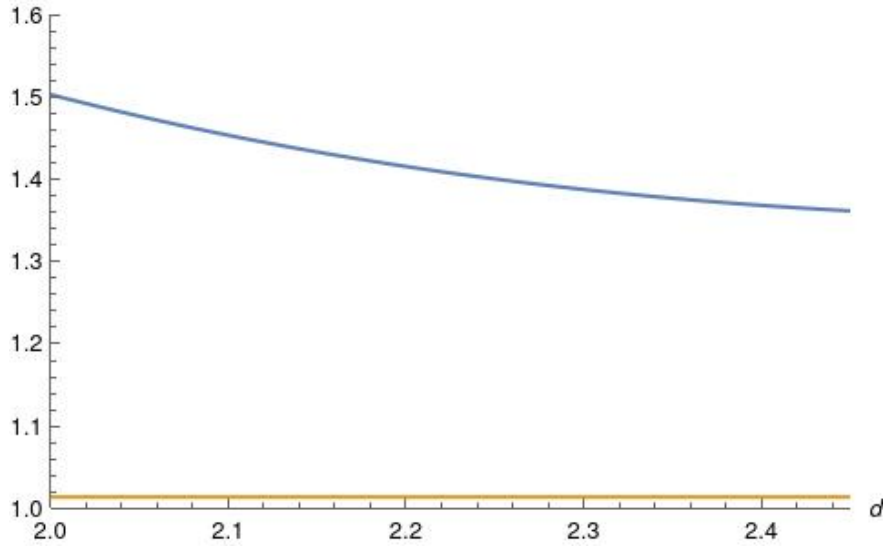

Figure 15: A plot of the lower bound for vol(O) versus v_0

3.4.3 Disjoint cusps

We are left with the remaining case in which C_R and C_N are disjoint, hence C_R is self tangent.

We have a full-sized rigid horoball H_r in the rigid cusp diagram. Let H_n be a nonrigid horoball of largest Euclidean radius. Note $r(H_n) < 1/2$. H_r and H_n are not tangent, since the cusps are assumed to be disjoint, so the corollary to Lemma 3.2.3 implies that the center of H_n is a distance at least one away from the center of H_r. As in (i), we consider the least volume cusp diagram depending on the center of H_r.

3.4.3.1 H_r is not centered at any singularity

Then the center of H_r must stay a distance at least 1 away from the order 6 singularity, at least $1/\sqrt{3}$ away from the order 3 singularity, and at least $1/2$ away from the order 2 singularity, so that the translates of H_r by these rotations do not overlap with H_r. When $d < \sqrt{7}$, the disks just defined cover the quadrilateral in which the center of H_r must lie. Therefore $d \geq \sqrt{7}$ and vol(O) $> v_0$.

3.4.3.2 H_r is centered at the order 2 singularity

Since H_n must be a distance at least 1 away from the center of H_r, we must have $d/2 > 1$, i.e. $d > 2$. Consider the order two elliptic isometry g which exchanges H_r at $(d/2, 0)$ with H_∞. Then g's axis is either parallel to or perpendicular to the x-axis. If not, g's axis meets the interior of the face of $V(C_R)$ bounded by two vertical half planes and the intersection of $\mathcal{P}(H_r)$ and $\mathcal{P}(\rho_3(H_r))$. But g cannot act as a reflective symmetry of this triangle.

If g's axis is parallel or perpendicular to the x-axis, then g sends a full-sized horoball a distance $d/2$ away from H_r to a horoball of radius $2/d^2$ which is a distance $2/d$ away from H_r. See figure 16. This horoball is a distance $d/2 - 2/d$ away from a full-sized horoball, so for them to not overlap we must have (as in section 3.4.1.4) $d \geq \sqrt{8}$.

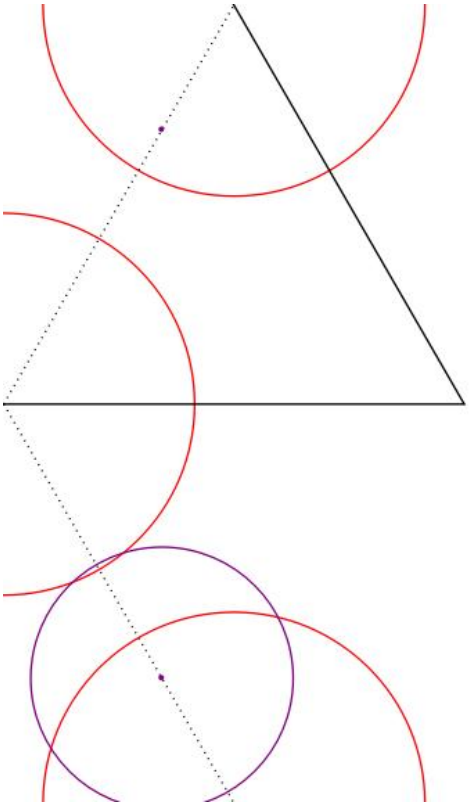

Figure 16: The purple horoball is the image under g of a full-sized red horoball

3.4.3.3 H_r is centered at the order 3 singularity

For this case only, change coordinates so that H_r is centered at $(0,0)$, there is a π rotation ρ_2 about the point $(d/4, \sqrt{3}d/12)$, a $\pi/3$ rotation ρ_6 about the point $(d/2, -\sqrt{3}d/6)$.

We have $d > \sqrt{3}$. Consider the order 2 elliptic exchanging H_r with H_∞, g_θ, where θ is the angle the line of reflection makes with the x-axis.

There is an upper bound on θ arising from the fact that the axis of g_θ cannot intersect $\rho_2(H_r)$. Let C denote the intersection of the horosphere $\partial\rho_2(H_r)$ with the vertical plane above the line making an angle of θ with the x-axis. C is a circle of radius $\sqrt{1/4 - d^2/3\sin^2(\pi/6-\theta)}$ with center a distance $\sqrt{1/4 + d^2/3\cos^2(\pi/6-\theta)}$ away from the origin (the center of g_θ's axis). These circles do not intersect provided

$$\sqrt{\frac{1}{4} + \frac{d^2}{3}\cos^2(\pi/6-\theta)} < 1 + \sqrt{\frac{1}{4} - \frac{d^2}{3}\sin^2(\pi/6-\theta)}$$

Setting these quantities equal to one another, we may solve for

$$\theta_u(d) := \frac{\pi}{6} - \arccos\sqrt{\frac{d^2+6}{12}}$$

and we have that $\theta \leq \theta_u(d)$.

On the other hand, there is a lower bound on θ arising from the fact that $H := g_\theta(\rho_2(H_r))$ cannot overlap with its translates by ρ_6. Let $a(d,\theta)$ denote the distance from the center of H to $(d/2, -\sqrt{3}d/6)$. One can verify that $\theta_1(d) < \pi/12$ for all $\sqrt{3} < d \leq 2$, so the center of H lies below the x-axis and makes an angle of $\pi/6 - 2\theta$ with it. H has radius $3/2d^2$ and its center is a distance $\sqrt{3}/d$ away from the origin. Hence the law of cosines implies

$$a^2(d,\theta) = \frac{d^2}{3} + \frac{3}{d^2} - 2\cos 2\theta$$

In order that H not overlap with $\rho_6(H)$, we must have $r(H) \leq a(d,\theta)/2$, which implies

$$\frac{9}{d^4} \leq \frac{d^2}{3} + \frac{3}{d^2} - 2\cos 2\theta$$

and solving for θ, we have

$$\theta \geq \theta_l(d) := \frac{1}{2}\arccos\left(\frac{d^2}{3} + \frac{3}{d^2} - \frac{9}{d^4}\right)$$

But as the plot in Figure 17 below verifies, for $\sqrt{3} < d \leq 2$, we have $\theta_l(d) > \theta_u(d)$. So $d > 2$ which implies $\mathrm{vol}(O) > 5v_0/6$.

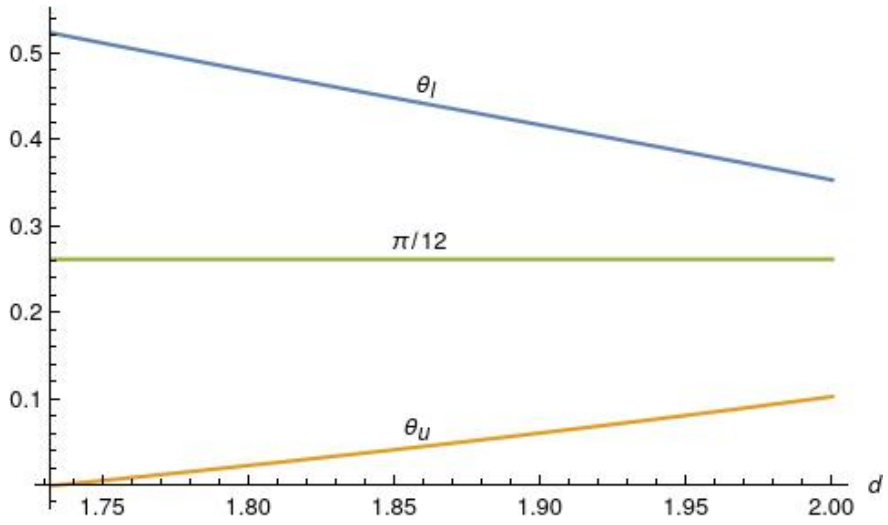

Figure 17: For $\sqrt{3} < d \leq 2$, $\theta_u(d) < \theta_l(d)$ is a contradiction

3.4.3.4 H_r is centered at the order 6 singularity

A priori we have $d > \sqrt{3}$, in order for the center of H_n to be a distance at least one away from H_r.

It is not clear what we can leverage to make d be larger, since in principle the radius of H_n can be arbitrarily small. There is a tradeoff. If $r(H_n)$ is large, then it forces d to be larger. If $r(H_n)$ is small, then there is more "empty space" between this horoball and H_∞. We make this notion precise by defining the *Voronoi cell truncated at height* h of C_R by

$$V_h(C_R) = V(C_R) \cap \{(z,t) \mid t \geq h\} \text{ for } 0 < h \leq 1$$

We may simply refer to this as the *truncated Voronoi cell*.

A few observations are immediate:

- $\operatorname{vol} V_1(C_R) = \operatorname{vol} C_R$
- $\operatorname{vol} V_h(C_R) = \operatorname{vol} V(C_R)$ for sufficiently small h
- $\operatorname{vol} V_h(C_R) \leq \operatorname{vol} V(C_R)$ for $0 < h \leq 1$

Let $\mathcal{B}$ denote the entirety of the horoballs in $\mathbb{H}^3$ which project to either cusp. Recall from section 2.3 that $V(C_R)$ may be characterized by taking the intersection of exteriors of visible planes which separate horoballs of $\mathcal{B}$ centered in the plane from H_∞ (and taking a fundamental domain for $\Gamma(C_R)$ acting on this region).

We can obtain $V_h(C_R)$ by making the above construction with planes visible above height h, and intersecting with the horoball $\{(z,t) \mid t \geq h\}$.

We define a *model* of the truncated Voronoi cell by making the above construction with only a subset of the planes visible above height h. This model will be *accurate*, meaning $\operatorname{model} V_h(C_R) = V_h(C_R)$ as sets, for all h greater than or equal to some $h_{\min} > 0$. When there is $H \in \mathcal{B} - \{H_\infty\}$ visible above height h not included in our model, then $\operatorname{model} V_h(C_R) \neq V_h(C_R)$, and the model ceases to be accurate.

Our model for the truncated Voronoi cell $\operatorname{model} V_h(C_R)$ includes $\mathcal{P}(H_r)$. We

(1) Compute $\operatorname{vol}(\operatorname{model} V_h(C_R))$ for all $h_{\min} \leq h \leq 1$ for some $h_{\min} > 0$.

(2) Prove that the only bisecting planes that are visible above height $h_{\min}$ are the ones included in our model. In this way we prove that the model is accurate, and hence in step (1) we are actually describing $\operatorname{vol}(V_h(C_R))$.

In figure 18, we are looking down on the model with our eye at ∞.

When

$$0 < \sqrt{1-h^2} \leq \frac{d}{2} \iff \sqrt{1-d^2/4} \leq h < 1$$

we see a portion of a spherical chimney and a flat chimney. Hence

$$\operatorname{vol}(\operatorname{model} V_h(C_R)) = \frac{1}{6}\operatorname{vol}(\Pi_s(1,h)) + \operatorname{vol}(\Pi_f(A,h))$$

where $A = \text{quadrilateral} \setminus$ one sixth of a circle of radius $\sqrt{1-h^2}$.

When

$$\frac{d}{2} < \sqrt{1-h^2} < \frac{d}{\sqrt{3}} \iff 0 < h \leq \sqrt{1-d^2/4}$$

we see the picture on the right. The model now decomposes into a portion of a spherical chimney, two congruent orthoschemes, and a flat chimney. We obtain

$$\operatorname{vol}(\operatorname{model} V_h(C_R)) = \frac{\pi/6 - 2\alpha}{2\pi}\operatorname{vol}(\Pi_s(1,h)) + 2\operatorname{vol}(S_{\alpha,\pi/2-\alpha,\gamma}) + \operatorname{vol}(\Pi_f(A,h))$$

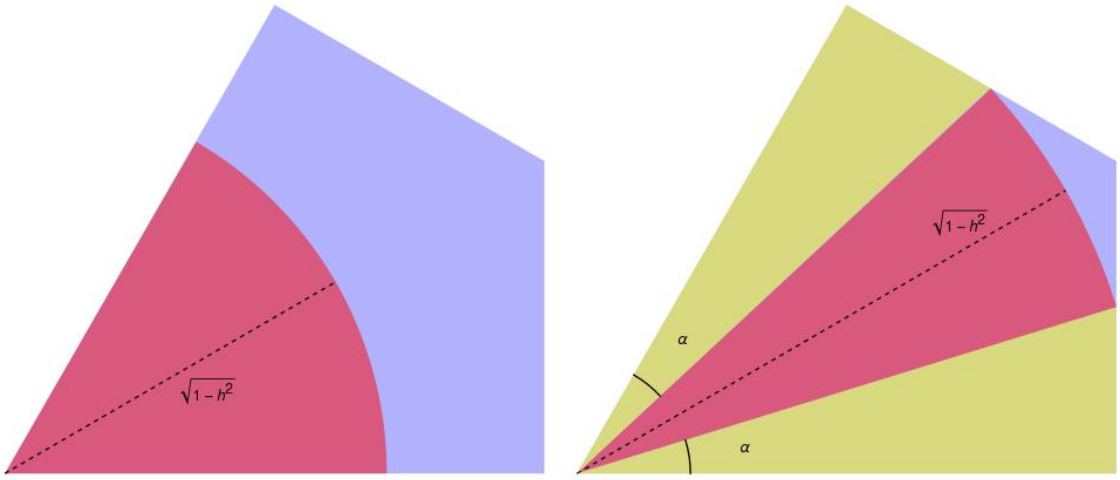

Figure 18: View of model $V_h(C_R)$ with our eye at ∞

where $\alpha = \arccos \frac{d}{2\sqrt{1-h^2}}$, $\gamma = \arccos \frac{d}{2}$ and A is the quadrilateral minus the area already accounted for, namely two congruent triangles and a sector of a circle.

One can observe that when $d = \sqrt{3}$, in the limit as $h \to 0$ the model consists of two orthoschemes $S_{\pi/6,\pi/3,\pi/6}$. We utilize the computer algebra system Mathematica to compute $\text{vol}(\text{model}\, V_h(C_R))$ numerically according to these formulas.

In order to verify that $\text{model}\, V_h(C_R) = V_h(C_R)$ for a range of h-values, we need to compute an upper bound on the radius of horoballs whose bisecting planes are not included in our model.

Let H_z denote a horoball covering the nonrigid cusp with largest Euclidean radius less than $1/2$. In order that $g_\theta(H_z)$ does not have larger radius than H_z, we must have $|z| \geq 1$. Also $z \neq (d/2, \sqrt{3}d/6)$, since a nonrigid cusp cannot have an order 3 axis running into it.

Likewise, let H_w denote a horoball covering the rigid cusp with largest Euclidean radius less than $1/2$. If $|w| < 1$, then $g_\theta(H_w)$ must be a full-sized ball. Assuming $\sqrt{3} < d \leq 2$ and a disk of no tangency of radius 1 on ∂H_∞, the only full-sized balls are at order six singularities, i.e. H_w is a $1/d$-ball. For $0 < \theta < \pi/6$, $\mathcal{P}(H_w)$ is visible at height $\sqrt{4-d^2}/2$. Keeping this in mind, we now assume that H_w is a horoball covering C_R with largest Euclidean radius less than $1/2$ and is not a $1/d$-ball. Therefore $|w| \geq 1$. Now the only difference between w

and z is that w can possibly be the order 3 singularity at $(d/2, \sqrt{3}d/6)$.

Lemma 3.4.2. *For $\sqrt{3} < d \leq 2$ define*

$$r_1(d) = \begin{cases} \frac{d-\sqrt{3}\sqrt{4-d^2}}{4} & \text{if } \sqrt{3} < d \leq \sqrt{2+\sqrt{3}} \\ \frac{\sqrt{3+d^2-\sqrt{12d^2-3}}}{2} & \text{if } \sqrt{2+\sqrt{3}} < d \leq 2 \end{cases}$$

Let H stand for H_z or H_w when $w \neq (d/2, \sqrt{3}d/6)$ in the notation above. Then $r(H) \leq r_1(d)$.

Proof. Let z denote the center of H. Let a and b denote the distances between z and the order 3 and nearest order 2 singularities respectively. In order that $\rho_3(H)$ does not overlap with H, we must have $r(H) \leq \sqrt{3}a/2$. Likewise, if $\rho_2(H)$ does not overlap with H, we have $r(H) \leq b$. Then

$$r(H) \leq \min\left\{\frac{\sqrt{3}a}{2}, b\right\}$$

Geometrically it is clear that a is maximized when $z = (d/2, \sqrt{1-d^2/4})$, and that for d close to $\sqrt{3}$ we have $\sqrt{3}\alpha/2 < \beta$. Setting these two quantities equal yields

$$\frac{\sqrt{3}}{2}\left(\frac{\sqrt{3}d}{6} - \sqrt{1-d^2/4}\right) = \sqrt{1-d^2/4}$$

which has the solution $d = \sqrt{2+\sqrt{3}}$.

Therefore, for $d \leq \sqrt{2+\sqrt{3}}$, we have

$$r(H) \leq \frac{\sqrt{3}}{2}\left(\frac{\sqrt{3}d}{6} - \frac{\sqrt{4-d^2}}{2}\right) = \frac{d-\sqrt{3}\sqrt{4-d^2}}{4}$$

When $d > \sqrt{2+\sqrt{3}}$, consider the locus of points

$$\{\zeta \in \mathbb{C} \mid \frac{\sqrt{3}a}{2} = b\}$$

This locus is a line, and as a function on this line, b is continuous and convex. It will be maximized at either $(d/2, d/(4+2\sqrt{3}))$ or the point where the line meets the circle $|\zeta| = 1$.

With the assistance of Mathematica we compute the value of b at the intersection of the line and the circle $|\zeta| = 1$ to be

$$\frac{\sqrt{3+d^2-\sqrt{12d^2-3}}}{2}$$

and verify that for $\sqrt{3} < d < 2$ this quantity is at least as large as $d/(4+2\sqrt{3})$, the value of b at the point $(d/2, d/(4+2\sqrt{3}))$. □

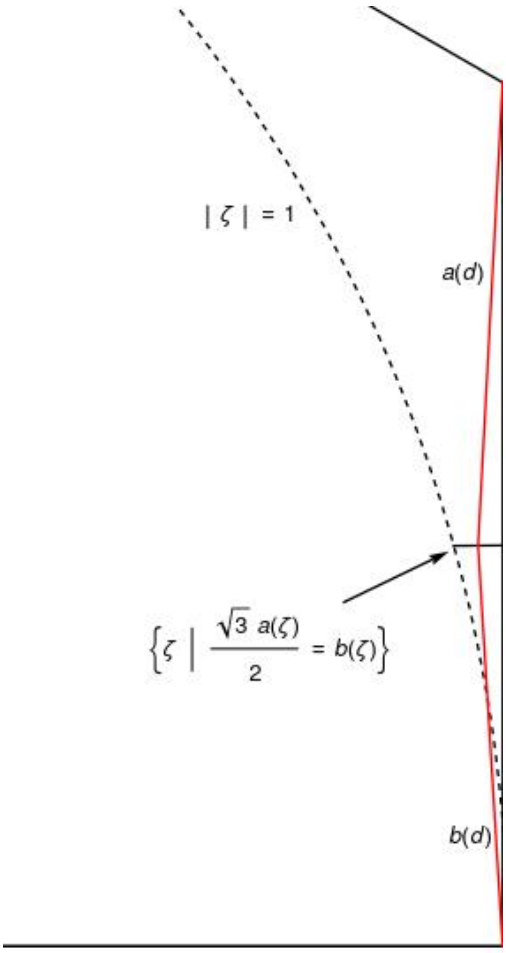

Figure 19: The setting of Lemma 3.4.2

Lemma 3.4.3. *For* $\sqrt{3} < d \leq 2$ *and* $0 \leq \theta \leq \pi/12$ *define*

$$a(d,\theta) = \sqrt{\frac{3}{d^2} + \frac{d^2}{4} - \sqrt{3}\cos(\pi/6 - 2\theta)}$$
$$b(d,\theta) = \sqrt{\frac{3}{d^2} + \frac{d^2}{3} - 2\cos(2\theta)}$$

and define $\theta(d)$ *implicitly by* $a(d,\theta(d)) = \frac{\sqrt{3}}{2d} b(d,\theta(d))$.

Let H be the horoball centered at the order 3 singularity. Except in the special case when $d = \sqrt{2\sqrt{3}}$ and $\theta = \pi/12$, we have $r(H) \leq r_2(d)$, where

$$r_2(d) = \frac{d}{2\sqrt{3}} b(d, \theta(d))$$

Proof. Recall that $0 \leq \theta < \pi/6$ is the angle g_θ's axis makes with the x-axis. If $0 \leq \theta \leq \pi/12$, we will compare $g_\theta(H)$ with $\rho_2(H)$ centered at $(d/2, -\sqrt{3}d/6)$ or with the order 2 singularity at $(d/2, 0)$. If $\pi/12 < \theta < \pi/6$, the distance between $g_\theta(H)$ and H is equal to the distance between $g_{\pi/6-\theta}(H)$ and $\rho_2(H)$, so we may assume that $0 \leq \theta \leq \pi/12$ in the subsequent calculations.

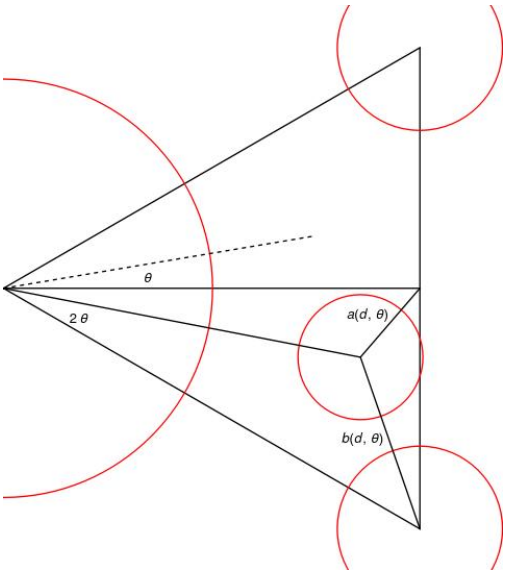

Figure 20: The setting of Lemma 3.4.3

We see that the center of $g_\theta(H)$ is a distance $\sqrt{3}/d$ away from the origin, lies on or below the x-axis at an angle of $\pi/6 - 2\theta$. Let $a(d, \theta)$ and $b(d, \theta)$ denote the distance from the center of $g_\theta(H)$ to $(d/2, 0)$ and $(d/2, -\sqrt{3}d/6)$ respectively. From the law of cosines we have

$$a^2(d, \theta) = \frac{3}{d^2} + \frac{d^2}{4} - \sqrt{3}\cos(\pi/6 - 2\theta)$$
$$b^2(d, \theta) = \frac{3}{d^2} + \frac{d^2}{3} - 2\cos 2\theta$$

Observe that $b(d, \theta)$ is increasing and $a(d, \theta)$ is decreasing for fixed d and increasing θ.

From Lemma 3.2.3, we have $r(g_\theta(H)) = \frac{3}{d^2} r(H)$. In order that $g_\theta(H)$ does not overlap with $\rho_2(H)$, we must have

$$2\sqrt{r(g_\theta(H)) \cdot r(H)} \leq b(d,\theta) \Leftrightarrow r(H) \leq \frac{d}{2\sqrt{3}} b(d,\theta)$$

In order that $g_\theta(H)$ does not overlap with its translate by ρ_2, we must have

$$r(g_\theta(H)) \leq a(d,\theta) \Leftrightarrow r(H) \leq \frac{d^2}{3} a(d,\theta)$$

Therefore

$$r(H) \leq \min\left\{ \frac{d^2}{3} a(d,\theta), \frac{d}{2\sqrt{3}} b(d,\theta) \right\}$$

Let $\theta(d)$ be defined implicitly by the relation

$$a(d,\theta) = \frac{\sqrt{3}}{2d} b(d,\theta)$$

which follows from setting the two quantities in the upper bound for $r(H)$ equal to one another. For $\theta < \theta(d)$ we have $a(d,\theta) > \frac{\sqrt{3}}{2d} b(d,\theta)$.

Therefore

$$r(H) \leq \frac{d}{2\sqrt{3}} b(d,\theta(d))$$

proving the claim. □

The special case for which the above radius bound does not apply occurs when $g_\theta(H)$ is centered at the order 2 singularity. In order for $g_\theta(H)$ to lie on the x-axis we must have $\theta = \pi/12$ and in order that $g_\theta(H)$ is a distance $d/2$ away from the origin, we have

$$\frac{d}{2} = \frac{\sqrt{3}}{d} \iff d = \sqrt{2\sqrt{3}}$$

Ignoring this case for the moment, we may conclude that if H is the largest non-rigid horoball or the largest rigid horoball which is neither full-sized nor a $1/d$-ball, then

$$r(H) \leq r_*(d) := \max\{r_1(d), r_2(d)\}$$

Let

$$h_*(d) = \max\left\{ \sqrt{2r_1(d)}, \sqrt{2r_2(d)}, \sqrt{4-d^2}/2 \right\},$$

where $\sqrt{4-d^2}/2$ is the visible height of the bisecting planes contributed by a $1/d$-ball. [1]

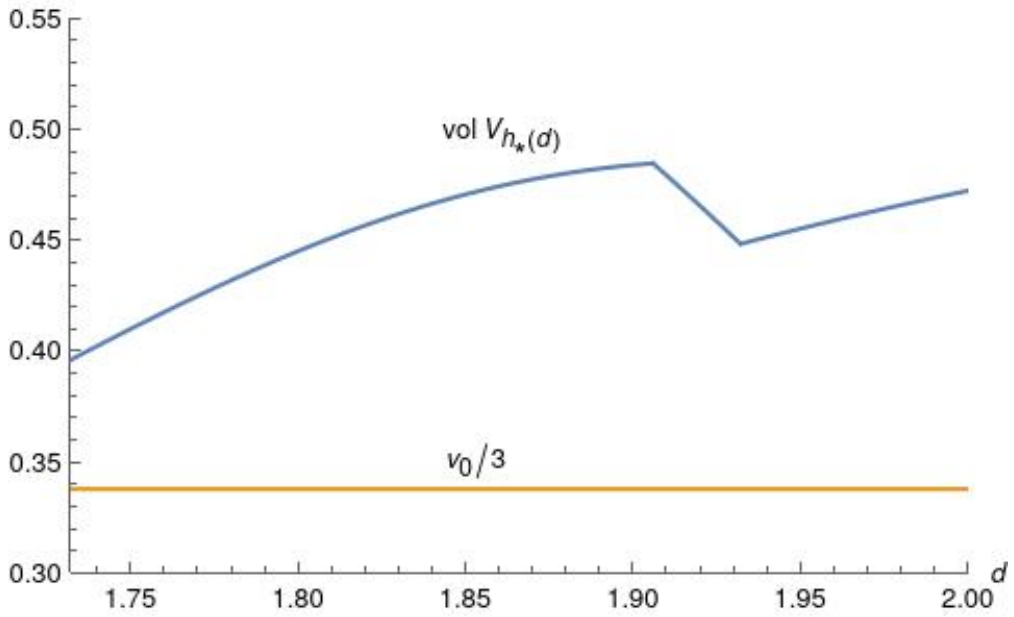

Figure 21: Plotting $\operatorname{vol} V_{h_*(d)}$ vs. $v_0/3$

Thus our model of the Voronoi cell is accurate for all $h_*(d) \leq h \leq 1$.

In figure 21, we plot $\operatorname{vol} \operatorname{model} V_{h_*(d)}(C_R) = \operatorname{vol} V_{h_*(d)}(C_R)$ for $\sqrt{3} < d \leq 2$ against $v_0/3$. We remark that for $\sqrt{3} < d <\approx 1.90574$, $\sqrt{2r_2(d)}$ exceeds both $\sqrt{2r_1(d)}$ and $\sqrt{4-d^2}/2$. For larger values of d, $\sqrt{2r_1(d)}$ dominates. The second non-smooth point on the graph is due to the fact $r_1(d)$ is not differentiable at $d = \sqrt{2+\sqrt{3}}$.

Since we proved the models are accurate (other than in the exceptional case mentioned above), we may conclude that $\operatorname{vol} V(C_R) > \operatorname{vol} V_{h_*(d)}(C_R) > v_0/3$ for $\sqrt{3} < d \leq 2$. Since $V_{h_*(d)}(C_R) \cap V(C_N) = \emptyset$, we may separately apply Meyerhoff's bound to the nonrigid cusp and obtain

$$\operatorname{vol}(O) \geq \frac{2v_0}{\sqrt{3}} \cdot \frac{\sqrt{3}}{4} + \operatorname{vol} V(C_R) > \frac{v_0}{2} + \frac{v_0}{3} = \frac{5v_0}{6}$$

We return to consider the exceptional case, namely when $d = \sqrt{2\sqrt{3}}, \theta = \pi/12$, H_w is centered at the order 3 singularity, and $g_{\pi/12}(H_w)$ is centered at the order 2 singularity. The radius of $g_{\pi/12}(H_w)$ is equal to $\sqrt{3}r(H_w)/2 < r(H_w)$. If $r(H_w) \leq r_2(\sqrt{2\sqrt{3}})$, then our model

[1]In fact, when $\theta = 0$, the $1/d$-balls do not contribute a visible plane, but we may think of this as a worst case estimate.

is still valid and there is nothing to prove.

Suppose $r(H_w) > 0.2 > r_2(\sqrt{2\sqrt{3}}) \approx 0.188$. We claim this contradicts the fact that $\mathcal{P}(H_z)$ contributes a face to the Voronoi cell. Let $(\omega, t) \in \mathbb{H}^3$ denote the point of intersection of the planes $\mathcal{P}(H_r), \mathcal{P}(H_w)$, and $\mathcal{P}(g_{\pi/12}(H_w))$. In order that $\mathcal{P}(H_z)$ is visible at least above height t, we must have

$$(\sqrt{2r(H_z)})^2 \geq t^2 + \delta^2 \text{ where } \delta = |\omega - z|$$

As a function of z, δ is minimized for some z on the circle $|z| = 1$. The distance from a point to a circle is attained at the radial projection of the point onto the circle. The radial projection of ω onto $|z| = 1$ is outside of the fundamental domain F_∞, so the minimal value of δ is attained at $z = (d/2, \sqrt{4 - d^2}/2)$.

Using Mathematica, we compute the minimal value for $1/2(t^2 + \delta^2)$ and show that if $r(H_w) > 0.2$, this exceeds $r_1(\sqrt{2\sqrt{3}})$, which yields the contradictory inequality $r(H_z) > r_1(\sqrt{2\sqrt{3}})$. Then $r(H_w) \leq 0.2$. Then we compute

$$\operatorname{vol} V_{\sqrt{0.4}}(C_R) > v_0/3 \text{ which implies that } \operatorname{vol}(O) > 5v_0/6$$

This concludes the proof that an orbifold with one rigid $(6, 3, 2)$ cusp and one nonrigid cusp is either $O_{(6,3,2)}$ or has volume greater than $5v_0/6$. Let us remark that we actually have $\operatorname{vol}(O) > v_1$ in all except the final two cases. The methods used to obtain $\operatorname{vol}(O) > 5v_0/6$ in the final case may be extended to obtain $\operatorname{vol}(O) > v_1$. First, one can verify that $V_{h_*(d)}(C_R) > v_1 - v_0/2$ except for d very close to $\sqrt{3}$. The case of d very close to $\sqrt{3}$ may be dispensed with as in the exceptional case above, namely, if the horoball centered at the order 3 singularity is too large then the nonrigid horoballs will not contribute to the Voronoi cell $V(C_R)$. The main challenge to is to compute a radius bound on non full-sized horoballs for $2 < d < \sqrt{5}$. We omit these details, as they add no more clarity to an already long and technical argument.

3.5 Proof of Theorem 3.3

Theorem 3.3. *Let O be a complete, orientable, finite-volume hyperbolic 3-orbifold with one nonrigid cusp and one rigid cusp of type $(4,4,2)$. Then either $O = O_{(4,4,2)}$ or $\mathrm{vol}(O) > v_1$, where $v_1 \approx 0.91596544\ldots$ is the volume of an ideal tetrahedron with dihedral angles $\pi/4, \pi/4$, and $\pi/2$.*

Introduce coordinates on the plane so there are order 4 singularities at the origin and (d,d) and equivalent order 2 singularities at $(d,0)$ and $(0,d)$. Then $\mathrm{vol}(C_R) = d^2/2$.

3.5.1 Cusps are simultaneously maximized

There are full-sized balls H_r and H_n in the rigid cusp diagram. The minimal volume diagram has H_r centered at an order 4 singularity and H_n centered at an order 2 singularity. Then $d \geq 1$, so $\mathrm{vol}(C_R) \geq 1/2$. Meyerhoff's bound yields

$$\mathrm{vol}(O) \geq \frac{2v_0}{\sqrt{3}}\left(\frac{\sqrt{3}}{4} + \frac{1}{2}\right) = \left(\frac{\sqrt{3}+2}{2\sqrt{3}}\right) v_0 > v_0$$

since $\sqrt{3}+2 > \sqrt{3}+\sqrt{3} = 2\sqrt{3}$.

3.5.2 Rigid cusp is not self tangent

There is a full-sized ball H_n in the rigid cusp diagram. Since H_n cannot be centered at an order 4 singularity, the minimal volume diagram has H_n centered at the order 2 singularity. Thus $d \geq 1/\sqrt{2}$.

First suppose that $d = 1/\sqrt{2}$, and let H be a (rigid cusp) horoball centered at an order 4 singularity. Then we claim that $r(H) = 1/4$ and H is tangent to H_n.

Let ρ_4 denote the elliptic isometry which acts as $\pi/2$ rotation around a vertical order 4 axis. Since $d = 1/\sqrt{2}$, H_n is tangent to $\rho_4(H_n)$, and therefore there is an order 2 elliptic isometry g whose axis passes through the point of tangency between these two balls. Notice the axis terminates at order 4 singularities. The action of g can be described geometrically as inversion in the hemisphere of radius $1/2$ centered directly below the point of tangency

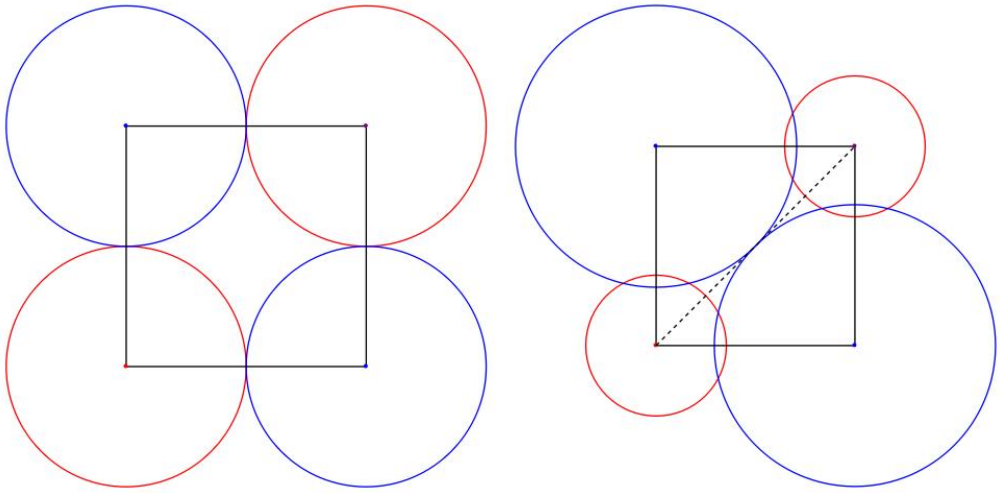

Figure 22: Least volume rigid cusp diagrams when (a) cusps are simultaneously maximized (b) rigid cusp is not self tangent

between H_n and $\rho_4(H_n)$, followed by reflection in the vertical half plane which contains the order 4 singularities.

Proposition 3.5.1. *When $d = 1/\sqrt{2}$, H is tangent to H_n, equivalently, $r(H) = 1/4$.*

Proof. Suppose that $r(H) < 1/4$. Then H is not tangent to H_n, and it must be tangent to some (nonrigid) horoball H' of radius r'. If $r' < r$, then there is a disk of no tangency on H (hence also on H_∞) of Euclidean radius greater than 1. This contradicts $d = 1/\sqrt{2}$, since there are points of tangency on H_∞ with distance between them equal to 1. So we may assume that $r' \geq r$.

Let ρ_4 denote the elliptic isometry which acts as $\pi/2$ rotation around the order 4 singularity at (d, d) (the same argument below works if instead we consider the order 4 singularity at the origin). Since $d = 1/\sqrt{2}$, H_n is tangent to $\rho_4(H_n)$, and therefore there is an order 2 elliptic isometry g whose axis passes through the point of tangency between these two balls. Notice the axis terminates at order 4 singularities. The action of g can be described geometrically as inversion in the hemisphere of radius $1/2$ centered directly below the point of tangency between H_n and $\rho_4(H_n)$, followed by reflection in the vertical half plane which

contains the order 4 singularities.

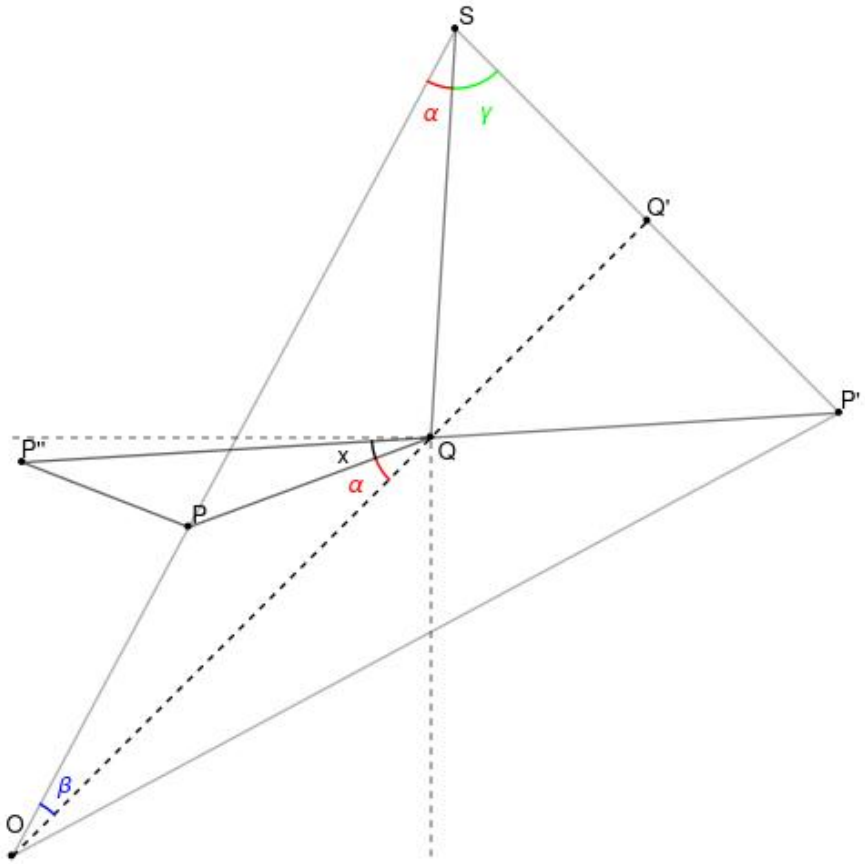

Figure 23: Computing the distance between H' and $\rho_4^2(g(H'))$.

In figure 23, O is the center of the hemisphere of inversion, Q is the order 4 singularity at (d, d), and P is the center of H'. S is the inverse of P, $P' = g(P)$ is the reflection of S, and $P'' = \rho_4^2(P')$. Let $\alpha = \angle OQP, \beta = \angle QOP, e = |OP|, c = |PQ|$, and $c' = |SQ|$. Observe that $|SQ| = |P'Q| = |P''Q|$.

We want to compute the distance $|PP''|$.

The triangles POQ and QOS are similar, since

$$\begin{aligned} S \text{ is the inverse of } P \text{ in the circle centered at } O \text{ of radius } |OQ| &\iff |OP||OS| = |OQ|^2 \\ &\iff \frac{|OP|}{|OQ|} = \frac{|OQ|}{|OS|} \end{aligned}$$

and $\angle POQ = \angle QOS = \beta$.

Then $\angle OSQ = \angle OQP = \alpha$. If $\gamma = \angle Q'SQ$ then by considering the right triangle $OQ'S$ we have $\gamma = \pi/2 - (\alpha + \beta)$. If $x = \angle PQP''$, then equality of the vertical angles $\angle OQP'' = \angle P'QQ'$ implies $x + \alpha = \alpha + \beta$, i.e. $x = \beta$. Similarity of POQ and QOS yields

$$\frac{c'}{c} = \frac{|OS|}{|OQ|} = \frac{\frac{1}{4e}}{\frac{1}{2}} \iff c' = \frac{1}{2e}c$$

Now the law of cosines gives

$$\begin{aligned} |PP''|^2 &= c^2 + (c')^2 - 2cc'\cos\beta \\ &= c^2\left(1 + \frac{1}{4e^2} - \frac{1}{e}\cos\beta\right) \end{aligned}$$

Recall that the horoballs centered at P and P'' have radii r' and $\frac{r'}{4e^2}$ respectively. In order that these horoballs do not overlap, we must have

$$\begin{aligned} 2\sqrt{r' \cdot \frac{r'}{4e^2}} \leq c\sqrt{1 - \frac{1}{e}\cos\beta + \frac{1}{4e^2}} &\iff \\ \frac{r'}{c} \leq \sqrt{e^2 - e\cos\beta + \frac{1}{4}} & \end{aligned}$$

Since H' is tangent to H, we have $r' = \frac{c^2}{4r}$. Moreover, the assumption $r' \geq r$ is equivalent to $c \geq 2r$, so

$$\frac{r'}{c} = \frac{c}{4r} \geq \frac{2r}{4r} = \frac{1}{2}$$

and we must have

$$\frac{1}{2} \leq \sqrt{e^2 - e\cos\beta + \frac{1}{4}} \iff \cos\beta \leq e$$

For fixed $\beta \in [0, \pi/2]$ the maximum value of e, denoted e_0 occurs when P is on the segment joining Q to the center of H_n.

Then the law of sines yields

$$\frac{e_0}{\sin\pi/4} = \frac{\sqrt{2}(1/2 - e_0\cos\beta)}{\sin\beta} \iff e_0 = \frac{1}{2(\sin\beta + \cos\beta)}.$$

Observe

$$e_0 - \cos\beta = \frac{1 - 2\cos^2\beta - 2\cos\beta\sin\beta}{2(\sin\beta + \cos\beta)} = -\frac{\cos(2\beta) + \sin(2\beta)}{2(\cos\beta + \sin\beta)}$$

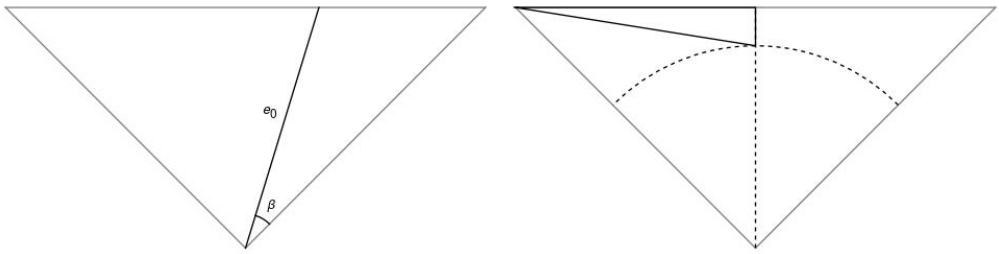

Figure 24: (a) the maximum value of e (b) if $\beta \geq \pi/4$, the maximum distance from P to the center of H_n.

The denominator is positive for $0 \leq \beta \leq \pi/2$ and the numerator is positive for $0 \leq \beta \leq 3\pi/8$, so if $\beta \leq 3\pi/8$ we have

$$e \leq e_0 < \cos\beta$$

contradicting our previous requirement.

But in fact if $\beta \geq \pi/4$, H' is already too close to H_n. For in this case, $c \geq \frac{1}{2\sqrt{2}} = 2^{-3/2}$ and $r' \geq \frac{c}{2} \geq 2^{-5/2}$. Since $g(H')$ cannot have radius larger than $1/2$ we must have

$$\frac{1}{2} \geq \frac{r'}{4e^2} \iff e^2 \geq \frac{r'}{2} \geq 2^{-7/2} \iff e \geq 2^{-7/4}$$

Then the distance from P to the center of H_n is at most

$$\sqrt{(2^{-3/2})^2 + (2^{-3/2} - 2^{-7/4})^2} \approx .358$$

In order for H' to not overlap with H_n, this distance be greater than or equal to

$$2\sqrt{\frac{1}{2} \cdot r'} = \sqrt{2r'} \geq \sqrt{2^{-3/2}} = 2^{-3/4} > 1/2$$

but

$$1/2 < \text{distance between centers of } H_n \text{ and } H' \leq .358$$

is a contradiction. The only way this contradiction is avoided is if $H' = H_n$, and the conclusion of the proposition follows. □

The above proposition implies that when $d = 1/\sqrt{2}$, we have the cusp diagrams for $O_{(4,4,2)}$ computed earlier, so Theorem 3.4 implies that $O = O_{(4,4,2)}$.

One can also observe that the order 2 elliptic g mentioned above, when combined with the isometries stabilizing ∞, generates a group with fundamental domain a $(\pi/4, \pi/4, \pi/2)$ ideal tetrahedron - i.e. O has volume at least v_1.

Now suppose that $d > \frac{1}{\sqrt{2}}$. Then H_n is no longer tangent to $\rho_4(H_n)$, and the isometry g is not necessarily an element of the group. A priori, it seems we cannot force the rigid cusp to have more volume, so instead we use Proposition 3.2.1 to get a better lower bound on $\mathrm{vol}(C_N)$.

We inquire what is the maximum distance between the center of H_n and the center of H, a horoball tangent to H_n.

Lemma 3.5.1. *Let H be any horoball tangent to H_n, and let e be the distance between their centers. If H covers the rigid cusp, then $e \leq d$, and if H covers the nonrigid cusp then*

$$e \leq a(d) := \sqrt{1 + d - \sqrt{1 + 2d - d^2}}$$

Proof. The first claim is clear, since H can be centered at an order 4 singularity, a distance d away from the center of H_n. If H covers C_N, then H cannot be centered at an order 4 singularity. The maximum distance will be attained when the center of H lies on the equidistant line between the order 2 singularities (otherwise, H is closer to one of H_n or $\rho_4(H_n)$ than the other).

Let a denote the distance between the centers of H and H_n and b denote the distance between the center of H and the nearest order 4 singularity. Since H is tangent to H_n, its radius $r = \frac{a^2}{2}$ is determined. Geometrically, it is clear that the minimum value for b corresponds to the maximum value for a, so we seek a lower bound on b.

In order that H does not overlap its translates by the $\pi/2$-rotation, we must have

$$r \leq \frac{b}{\sqrt{2}} \iff a^2 \leq \sqrt{2}b$$

The law of cosines implies that

$$\sqrt{2}b \geq a^2 = d^2 + b^2 - \sqrt{2}db$$

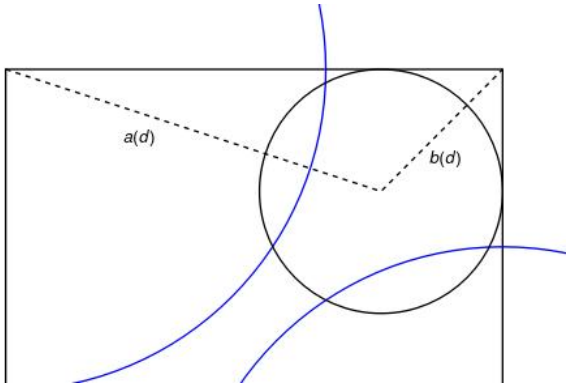

Figure 25: The maximum distance between H and H_n

so

$$b^2 - (\sqrt{2}(d+1))b + d^2 \leq 0$$

In order for this inequality to be true, the value of b must be between the two roots of the polynomial on the left hand side. This implies that

$$b \geq \frac{d+1-\sqrt{1+2d-d^2}}{\sqrt{2}}$$

This lower bound on b corresponds to the following upper bound on a

$$a \leq \sqrt{\sqrt{2}b} \leq \sqrt{1+d-\sqrt{1+2d-d^2}}$$

□

Now we apply Proposition 3.2.1 to obtain

$$\text{vol}(O) \geq \frac{2v_0}{\sqrt{3}}\left(v_n(1/d, 1/a(d)) + \frac{d^2}{2}\right)$$

We conclude from figure 26 that $\text{vol}(O) > v_0$ for $1/\sqrt{2} < d \leq \sqrt[4]{3}/\sqrt{2}$. Notice if $d \geq \sqrt[4]{3}/\sqrt{2}$, the apriori bound of $\text{vol}(C_N) \geq \sqrt{3}/4$ is sufficient to guarantee $\text{vol}(O) \geq v_0$ by Meyerhoff's bound.

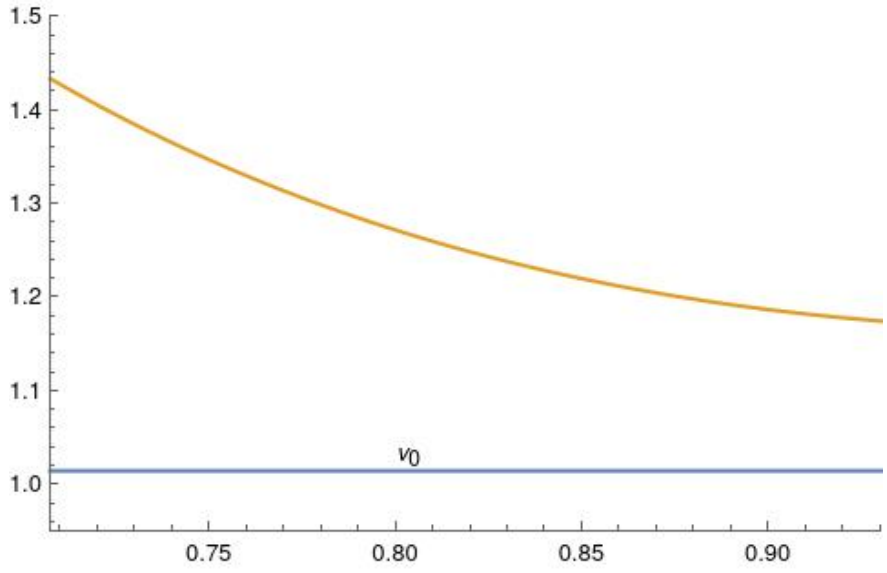

Figure 26: Plot of v_0 versus the lower bound on vol(O)

3.5.3 Disjoint cusps

There is a full-sized ball H_r in the rigid cusp diagram. If H_r is not centered at any singularity, then $d \geq 1$, so $\text{vol}(C_R) \geq 1/2$.

If H_r is centered at the order 2 singularity, then the center of the largest horoball covering C_N must be a distance at least one away from the order 2 singularities. This implies $d > 1$, so $\text{vol}(C_R) > 1/2$.

The least volume case occurs when H_r is centered at an order 4 singularity. In principle, the horoball at the other order 4 singularity need not be full-sized. A priori, this gives $d \geq 1/2$, but if one considers that the horoball H_z of largest Euclidean radius which covers C_N must be a distance at least 1 away from H_r, we have $d > 1/\sqrt{2}$.

We handle this case by the same methods applied in the $(6, 3, 2)$ case of disjoint cusps, by estimating the volume of $V(C_R)$. Our model includes the plane $\mathcal{P}(H_r)$. See the Figure 3.5.3 for the decompositions of $V_h(C_R)$ into spherical chimneys, orthoschemes, and flat chimneys depending on the value of h.

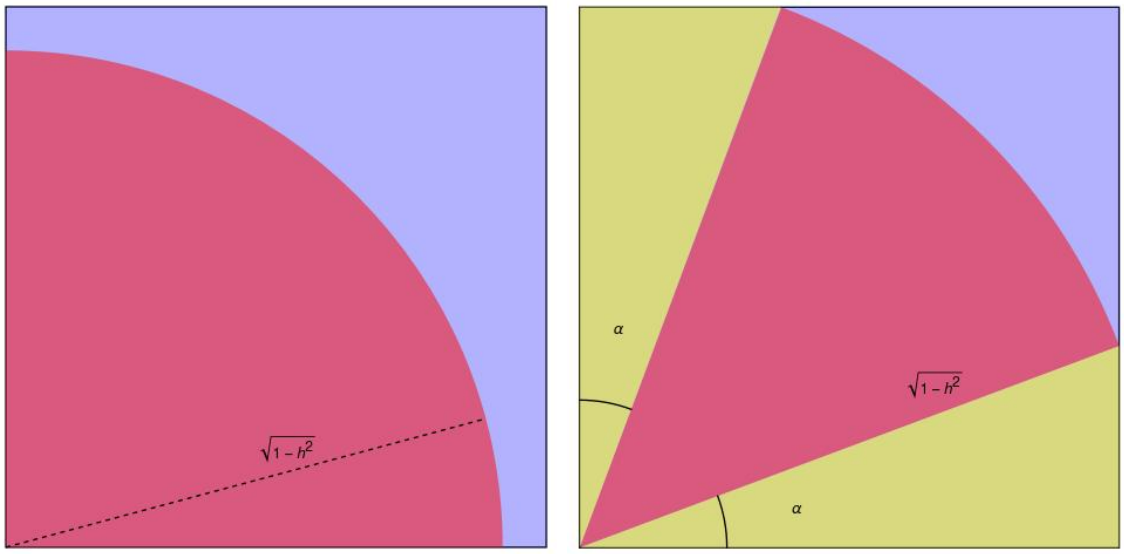

The resulting volume formula is

$$\operatorname{vol}\operatorname{model} V_h(C_R) = \begin{cases} \frac{1}{4}\operatorname{vol}\Pi_s(1,h) + \operatorname{vol}\Pi_f(A,h) & \text{if } \sqrt{1-d^2} \le h < 1 \\ \frac{\pi/2-2\alpha}{2\pi}\operatorname{vol}\Pi_s(1,h) + 2\operatorname{vol} S_{\alpha,\pi/2-\alpha,\gamma} + \operatorname{vol}\Pi_f(A,h) & \text{if } 0 < h \le \sqrt{1-d^2} \end{cases}$$

where

$$\alpha = \arccos\frac{d}{\sqrt{1-h^2}} \text{ and } \gamma = \arccos d$$

Next, we bound the radius of horoballs not included in our model.

There is an order 2 elliptic isometry $g_\theta \in \Gamma$ whose axis passes through the point of tangency of H_r and H_∞, where θ denotes the angle that the projection of g_θ's axis makes with the x-axis.

The point of tangency between H_r and H_∞ is a lift of a finite vertex in the singular locus of O. There is a third axis through this vertex of order m, where $m \in \{2,3\}$. Since the order 2 and order 4 axes are perpendicular, we must have $m = 2$ due to spherical trigonometry. In a $(2,3,4)$ spherical triangle group, the angle between the order 2 and order 4 axes must be $\pi/4$, as can be seen using the spherical law of cosines (compare Theorems 2.5.3 and 2.5.4 of [33]). So there is another order 2 elliptic g' whose axis goes throught the point of tangency and makes an angle of $\pi/4$ with the axis of g_θ. Without loss of generality, we may assume $0 \le \theta < \pi/4$, for otherwise we exchange the roles of g_θ and g'.

Let H_z and H_w be horoballs covering C_N and C_R respectively of largest Euclidean radius among all such horoballs which are not full-sized. Since the center of H_z must satsify $|z| \geq 1$, we must have $d > \frac{1}{\sqrt{2}}$. If $d \geq \frac{1}{\sqrt[4]{2}}$, then Meyerhoff's bound yields

$$\frac{2v_0}{\sqrt{3}}\left(\frac{\sqrt{3}}{4}+\frac{1}{2}\right) = \left(\frac{\sqrt{6}+2}{2\sqrt{6}}\right)v_0 \approx .921819\ldots > v_1$$

So we shall consider $1/\sqrt{2} < d < 1/\sqrt[4]{2}$.

If $|w| < 1$, then $g_\theta(H_w)$ must be a full-sized horoball. As we shall see, the horoball at (d,d) cannot be full-sized, so H_w is the image under g_θ of a full-sized horoball centered at one of the points $(\pm 2d, 0), (0, \pm 2d)$. In analogy with the $1/d$-balls in the $(6,3,2)$ case, we say H_w is a $1/2d$-ball, as this is its distance from H_r. For $0 < \theta < \pi/4$, $\mathcal{P}(H_w)$ is visible at height $\sqrt{1-h^2}$. Keeping this in mind, we now assume $|w| \geq 1$.

Lemma 3.5.2. *For $1/\sqrt{2} < d < 1/\sqrt[4]{2}$, define*

$$r_1(d) = \frac{d - \sqrt{1-d^2}}{\sqrt{2}}$$

Let H stand for H_z or H_w when $w \neq (d,d)$ and in the notation above. Then $r(H) \leq r_1(d)$.

Proof. Let z denote the center of H and let a be the distance from z to (d,d). Then $0 < a \leq d - \sqrt{1-d^2}$, noting that H is not centered at (d,d). In order that H does not overlap with $\rho_4(H)$, we must have

$$r(H) \leq \frac{\sqrt{2}a}{2} \leq \frac{1}{\sqrt{2}}(d - \sqrt{1-d^2})$$

□

Now we bound $r(H_w)$ when $w = (d,d)$.

Lemma 3.5.3. *Let H be centered at the order 4 singularity at (d,d). For $1/\sqrt{2} < d < 1/\sqrt[4]{2}$, there is a function $r_2(d)$ for which $r(H) \leq r_2(d)$.*

Proof. We will compare $g_\theta(H)$ to $\rho_2(g_\theta(H))$ centered at $(d, -d)$, to its translate by ρ_2, and to the full-sized horoball centered at $(2d, 0)$. When $\pi/8 < \theta < \pi/4$, the distance between the centers of $g_\theta(H)$ and H is equal to the distance between the centers of $g_{\pi/4-\theta}(H)$ and $\rho_2(H)$, so without loss of generality we assume $0 \leq \theta \leq \pi/8$.

Let $a(d, \theta)$ be the distance from the center of $g_\theta(H)$ to $(d, 0)$, let $b(d, \theta)$ be the distance between the centers of $g_\theta(H)$ and $\rho_2(H))$ centered at $(d, -d)$, and let $c(d, \theta)$ be the distance between the centers of $g_\theta(H)$ and $\rho_2(H_r)$ centered at $(2d, 0)$. Applying the law of cosines yields

$$a^2(d, \theta) = d^2 + \frac{1}{2d^2} - \sqrt{2}\cos(\pi/4 - 2\theta)$$
$$b^2(d, \theta) = 2d^2 + \frac{1}{2d^2} - 2\cos(2\theta)$$
$$c^2(d, \theta) = 4d^2 + \frac{1}{2d^2} - \sqrt{8}\cos(\pi/4 - 2\theta)$$

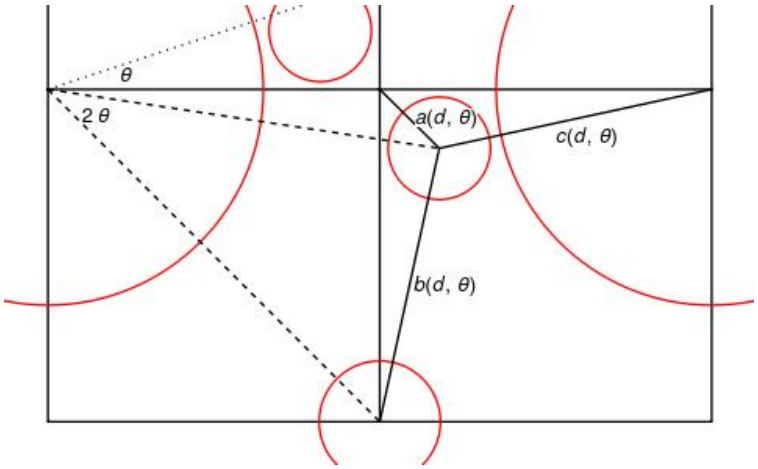

Figure 27: The setting of Lemma 3.5.3

Comparing $g_\theta(H)$ to $\rho_2(g_\theta(H)), \rho_2(H)$, and $\rho_2(H_r)$ respectively yields the following inequalities which must be satisfied.

$$r(g_\theta(H)) \leq a(d, \theta)$$
$$2\sqrt{r(g_\theta(H)) \cdot r(H)} \leq b(d, \theta)$$
$$2\sqrt{r(g_\theta(H)) \cdot 1/2} \leq c(d, \theta)$$

Recalling from Lemma 3.2.3 that $r(g_\theta(H)) = r(H)/2d^2$, we obtain from these inequalities the upper bound

$$r(H) \leq \min\left\{2d^2a(d,\theta), \frac{d}{\sqrt{2}}b(d,\theta), (d\cdot c(d,\theta))^2\right\}$$

Define $\theta_1(d)$ and $\theta_2(d)$ implicitly by the relations

$$2d^2a(d,\theta_1(d)) = \frac{d}{\sqrt{2}}b(d,\theta_1(d))$$
$$(dc(d,\theta_2(d)))^2 = \frac{d}{\sqrt{2}}b(d,\theta_2(d))$$

and set $\theta(d) = \min\{\theta_1(d), \theta_2(d)\}$.

Then for $\theta < \theta(d)$, we have

$$\frac{d}{\sqrt{2}}b(d,\theta) \leq \min\left\{2d^2a(d,\theta), (d\cdot c(d,\theta))^2\right\}$$

Since b increases with fixed d and increasing θ, we define

$$r_2(d) = \frac{d}{\sqrt{2}}b(d,\theta(d))$$

and we have $r(H) \leq r_2(d)$. □

Remark: There are no special cases in the above lemma as there were in the corresponding lemma of the $(6,3,2)$ case, since $g_\theta(H)$ is centered at an order 4 singularity only if $d = 1/\sqrt{2}$ and $g_\theta(H)$ is centered at the order 2 singularity only if $d = 1/\sqrt[4]{2}$.

Now define

$$h_*(d) = \max\left\{\sqrt{2r_1(d)}, \sqrt{2r_2(d)}, \sqrt{1-d^2}\right\}$$

and the lemmas above prove that model $V_h(C_R)$ is accurate for all $h_*(d) \leq h \leq 1$.

In figure 28, we plot $\operatorname{vol} V_{h_*(d)}(C_R) + v_0/2$ against v_1 for $1/\sqrt{2} < d < 1/\sqrt[4]{2}$ and observe that

$$\operatorname{vol}(O) \geq \operatorname{vol} V_{h_*(d)}(C_R) + v_0/2 > v_1$$

for $.73 < d < 1/\sqrt[4]{2}$.

We rule out the case $1/\sqrt{2} < d \leq .74$ in the following

Lemma 3.5.4. *If $1/\sqrt{2} < d \leq .74$, the nonrigid cusp makes no contribution to $V(C_R)$.*

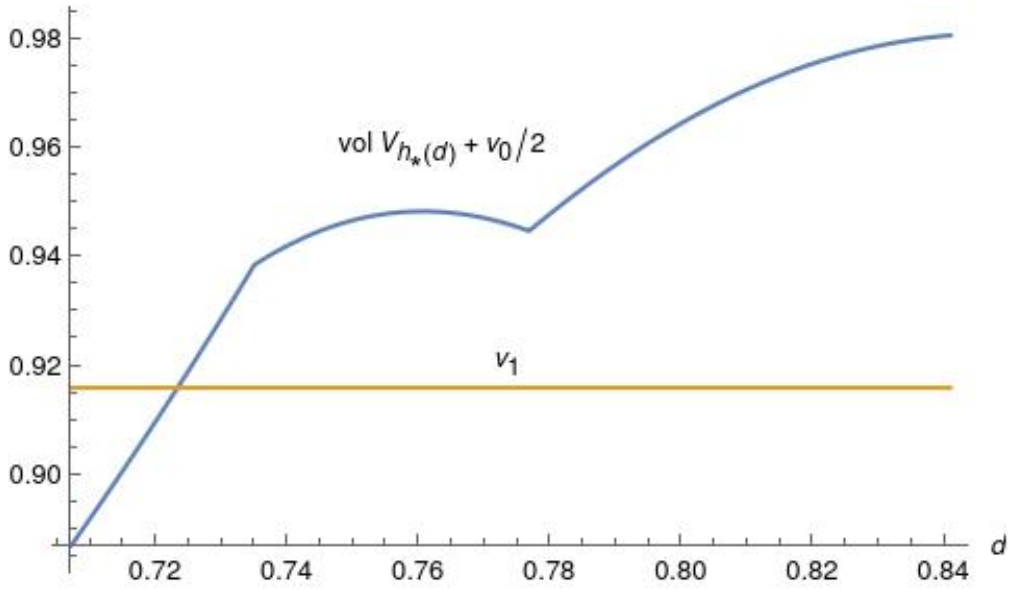

Figure 28: The lower bound for vol(O) vs. v_1

Proof. Let H_z denote the nonrigid horoball of largest Euclidean radius, centered at z. Recall $|z| \geq 1$ and $r(H_z) \leq r_1(d)$.

Let H denote the image of the full-sized horoball centered at $(2d, 0)$ under g_θ. Then H is a horoball of radius $1/8d^2$. Its center is a distance $1/2d$ away from the origin and makes an angle of 2θ with the x-axis. Since $d > 1/\sqrt{2}$, H is not centered at the order 2 singularity at $(d, 0)$. In order that H does not intersect this axis, we must have

$$\left(\frac{1}{8d^2}\right)^2 \leq \frac{1}{4d^2} + d^2 - \cos 2\theta,$$

equivalently

$$\cos 2\theta \leq d^2 + \frac{1}{4d^2} - \frac{1}{64d^4}$$

which implies that

$$\theta \geq \frac{1}{2} \arccos\left(d^2 + \frac{1}{4d^2} - \frac{1}{64d^4}\right)$$

Define $\theta_{\min}(d)$ to be the right hand side of the above inequality.

The smallest visible height on $\mathcal{P}(H)$ within the fundamental domain for $\Gamma_\infty(C_R)$ is above the order 4 singularity at (d, d). Let $t(d, \theta)$ denote this height, and $a(d, \theta)$ denote the distance from the center of H to (d, d). Then

$$a^2(d, \theta) = 2d^2 + \frac{1}{4d^2} - \sqrt{2}\cos(\pi/4 - 2\theta)$$

and

$$a^2(d, \theta) + t^2(d, \theta) = \frac{1}{4d^2}$$

For fixed d, $t(d, \theta)$ increases as θ increases. Hence

$$t(d, \theta) \geq t(d, \theta_{\min}) = \sqrt{\frac{1}{4d^2} - a^2(d, \theta_{\min})} = \sqrt{\sqrt{2}\cos(\pi/4 - 2\theta_{\min}) - 2d^2}$$

So on the one hand, the visible height of $\mathcal{P}(H_z)$ is bounded below by $t(d, \theta)$, and on the other hand the visible height is bounded above by $\sqrt{2r_1(d)}$. As we see in figure 29, $t(d, \theta_{\min})$ exceeds $\sqrt{2r_1(d)}$ for all $1/\sqrt{2} < d < .74$.

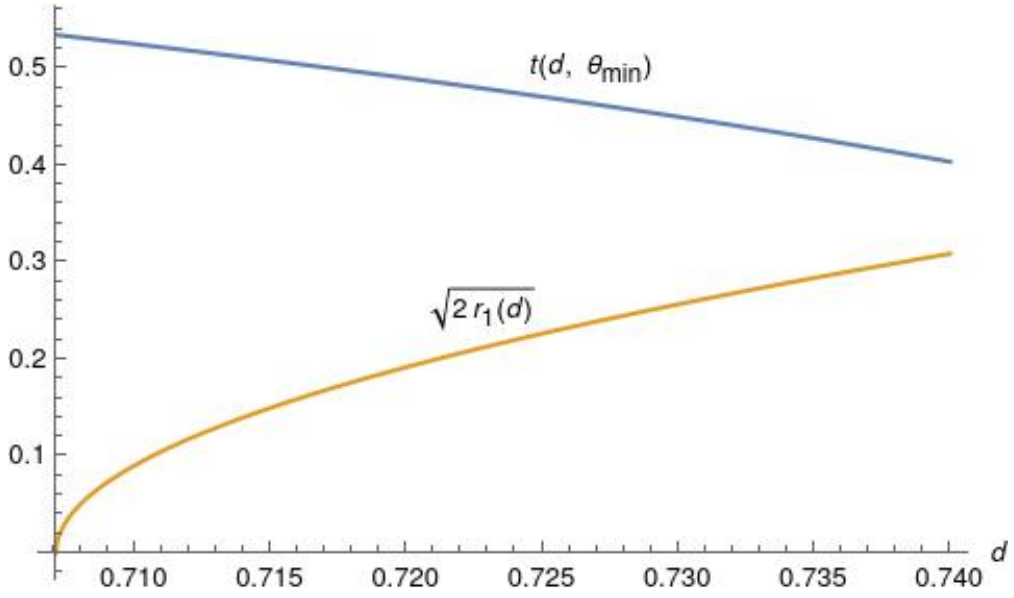

Figure 29: $t(d, \theta_{\min}) \leq$ visible height of $\mathcal{P}(H) \leq \sqrt{2r_1(d)}$ is not satisfied for $1/\sqrt{2} < d < .74$

□

This concludes the proof of Theorem 3.3

4.0 Orbifolds commensurable with the figure eight knot complement

In this chapter, we describe a joint work [16] with J. DeBlois, H. A. Ekanayake, M. Fincher, A. Gharagozlou, and P. Mondal on constructing a census of small volume orbifolds commensurable with the figure eight knot complement. We first give a broad overview of the project, and then describe our main contributions in greater detail.

Throughout this section, we assume all orbifolds to be oriented and all maps (isometries, covers) to be orientation preserving.

Definition 4.0.1. Orbifolds Q_1 and Q_2 are *commensurable* if there is a covering orbifold Q so $Q \to Q_1$ and $Q \to Q_2$ both are finite sheeted covers.

Let M be the figure eight knot complement. Then M is a hyperbolic 3-manifold of volume $2v_0$ (compare example 4.3.3). M covers the minimal volume orbifold $Q = \mathbb{H}^3/PGL_2(O_3)$ of volume $v_0/12$. Here O_3 denotes the ring of integers in the number field $\mathbb{Q}(\sqrt{-3})$.

Definition 4.0.2. We define the category $\mathcal{C}_3$ whose objects are the isometry classes of orbifolds commensurable with M. Given orbifolds O_1, O_2 there is an arrow from O_1 to O_2 for each covering map $O_1 \to O_2$.

The goal of this project is to describe the subcategory $\mathcal{C}_3^{\leq 2v_0}$ of $\mathcal{C}_3$ whose objects have volume at most $2v_0$.

4.1 Outline of the program

A number of components are required to complete the picture of $\mathcal{C}_3^{\leq 2v_0}$. The first is $\mathcal{C}_{\text{main}}$, a subcategory of $\mathcal{C}_3^{\leq 2v_0}$ consisting of covers of Q. As will be described in section 4.2, Q may be obtained from face pairings on a certain tetrahedron T in $\mathbb{H}^3$, and covers of Q are given by triangulations built from copies of T. We can determine when one element of $\mathcal{C}_{\text{main}}$ covers another, thus we have a description of this subcategory.

An orbifold in $\mathcal{C}_3$ is *minimal* if it covers no other orientable orbifold. $Q \in \mathcal{C}_{\text{main}}$ is minimal,

but $\mathcal{C}_3$ contains other minimal orbifolds which do not lie in $\mathcal{C}_{\text{main}}$. These minimal orbifolds correspond to maximal discrete groups in the commensurability class determined by the maximal order $\mathcal{O} = M_2(O_3)$ in the quaternion algebra $A = M_2(\mathbb{Q}(\sqrt{-3}))$ over the number field $\mathbb{Q}(\sqrt{-3})$. Section 6.1 of [16] gives exposition, referring to [26], on how to determine these maximal groups. As this author was not personally involved in this aspect of the project, we will be content to cite the results. The reader who is interested in how to obtain them is encouraged to refer to section 6 of [16] and [26] for more background.

Theorem 4.1 (Proposition 6.3 of [16]). *For distinct primes $\pi_1, \ldots, \pi_n \in O_3$ and $\pi = \pi_1 \ldots \pi_n$,*

$$\widetilde{\Gamma}_\pi = \left\{ \begin{bmatrix} x & \pi y \\ z & w \end{bmatrix} \in PGL_2(O_3) \mid x, y, z, w \in O_3 \right\}$$

has index $\prod_{i=1}^{n}(N(\mathcal{P}_i)+1)$ in $PGL_2(O_3)$, where for each i, $N(\mathcal{P}_i)$ is the norm of the prime ideal generated by π_i.

For each $1 \leq i < n$, there are $k_i, l_i \in O_3$ such that

$$k_i \prod_{j=1}^{i} \pi_j + l_i \prod_{j=i+1}^{n} \pi_j = 1.$$

Define

$$M_\pi = \begin{bmatrix} 0 & \pi \\ 1 & 0 \end{bmatrix} \text{ and } N_i = \begin{bmatrix} \prod_{j=1}^{i} \pi_j & \pi \\ l_i & -k_i \prod_{j=1}^{i} \pi_j \end{bmatrix}$$

Then

$$\Gamma_\pi = \langle \widetilde{\Gamma}_\pi, M_\pi, N_1, \ldots, N_{n-1} \rangle$$

is a maximal discrete group. Γ_π is the normalizer in $PGL_2(\mathbb{C})$ of $\widetilde{\Gamma}_\pi$ and $[\Gamma_\pi : \widetilde{\Gamma}_\pi] = 2^n$.

Every maximal discrete group commensurable with but not equal to $PGL_2(O_3)$ is of the form Γ_π for some $\pi \in O_3$.

As we shall see, $\text{vol}(Q) = v_0/12$, so the above theorem implies that for a product of distinct primes $\pi = \pi_1 \ldots \pi_n$,

$$\text{vol}(Q_\pi) = \frac{1}{2^n} \left(\prod_{i=1}^{n} (N(\mathcal{P}_i)+1) \right) \frac{v_0}{12}$$

This reduces the problem of classifying minimal orbifolds of small volume to classifying prime ideals in O_3 of small norm. We give more details in section 4.4.

Any $P \in \mathcal{C}_3 - \mathcal{C}_{\text{main}}$ will lie in the lattice of covers of some minimal Q_π. For π a product of distinct primes in O_3, let $Q_\pi = \mathbb{H}^3/\Gamma_\pi$, and $\widetilde{Q}_\pi = \mathbb{H}^3/\widetilde{\Gamma}_\pi$. For a cover $P \to Q_\pi$, represented by a subgroup $\Gamma \leq \Gamma_\pi$, define its *canonical cover* as $\widetilde{P} = \mathbb{H}^3/(\Gamma \cap PGL_2(O_3))$. Then (see Corollary 8.9 of [16]) $\widetilde{P}$ covers $\widetilde{Q}_\pi$ and the cover $\widetilde{P} \to P$ is normal with deck transformation group contained in $(\mathbb{Z}/2\mathbb{Z})^n$. Moreover, covers $P \to Q_\pi$ and $P' \to Q_\pi$ are isomorphic if and only if $\widetilde{P} \to \widetilde{Q}_\pi$ and $\widetilde{P'} \to \widetilde{Q}_\pi$ are isomorphic and the group of deck transformations of $\widetilde{P} \to P$ contains that of $\widetilde{P}' \to P'$.

In practice, to describe covers of Q_π up to a given volume bound, we enumerate covers $\widetilde{P}$ of $\widetilde{Q}_\pi$. By the work of Mark Fincher, we can compute the full group G (not just those that preserve the triangulation) of self-isometries of $\widetilde{P}$ and describe a cover $P \to Q_\pi$ as $\widetilde{P}/H$ for some subgroup $H \leq G$. See Fincher's thesis [18] and sections 7 and 8 of [16] for more details.

This concludes the general outline of the program for describing the category $\mathcal{C}_3^{\leq 2v_0}$. In the remainder of the chapter we will

(i) Describe a recursive algorithm to construct covers of the minimal orbifold $\mathbb{H}^3/PGL_2(O_3)$.

(ii) Describe algorithms to compute geometric and topological information about elements of $\mathcal{C}_{\text{main}}$. In particular, for such an orbifold we can determine how many cusps it has and the type of each one, its singular locus, and whether it has a triangulation preserving cover of another element of $\mathcal{C}_{\text{main}}$

(iii) Use Proposition 6.3 of [16] to list the Q_π with volume $\leq v_0$ and describe how to find its canonical cover $\widetilde{Q}_\pi \in \mathcal{C}_{\text{main}}$.

4.2 Constructing covers of $\mathbb{H}^3/PGL_2(O_3)$

There is a tesselation $\mathcal{T}_3$ of $\mathbb{H}^3$ by regular ideal tetrahedra. The orientation preserving symmetry group of this tesselation is $PGL_2(O_3)$. A fundamental domain for the action of $PGL_2(O_3)$ on $\mathbb{H}^3$ is described as follows: For $z = 1/2 + \sqrt{3}i/6$, let T_0 be the convex hull in

upper half space of ∞ and the points on the unit hemisphere above $0, 1/2$, and $z \in \mathbb{C}$. Let σ denote reflection in the vertical plane above the real axis and let $T = T_0 \cup \sigma(T_0)$. T is a tetrahedron with one ideal vertex at ∞ and finite vertices on the unit hemisphere above $0, z$, and $\overline{z}$. We label the vertices of T as follows:

$$\begin{aligned} v &\leftrightarrow \infty \\ e &\leftrightarrow \text{ vertex above } 0 \\ f_0 &\leftrightarrow \text{ vertex above } z \\ f_1 &\leftrightarrow \text{ vertex above } \overline{z} \end{aligned}$$

We follow the convention that faces are labeled with the same label as the vertex they do not contain. For example, face f_0 is contained in the vertical half plane above the line through 0 and $\overline{z}$. See Figure 30

Reflections in the faces of T_0 generate the full symmetry group $PGL_2(O_3)$ of $\mathcal{T}_3$ (see [23] for more details). Let σ_v denote reflection in the face labeled v, likewise for σ_{f_1}, σ_e. By taking products of reflections in faces of T_0 which meet at an edge, we obtain rotations about the edges of T_0 which pair the faces of T. In particular, $\rho_f = \sigma_{f_1}\sigma$ is the order 6 rotation about the axis connecting e to v, $\rho_e = \sigma_e\sigma$ is the order 2 rotation about the axis connecting v to the midpoint of the segment connecting f_0 to f_1, and $\rho_v = \sigma_v\sigma$ is the order 2 rotation about the axis connecting e to the midpoint of the segment connecting f_0 to f_1.

Note that ρ_f identifies face f_1 with face f_0, while ρ_v and ρ_e self-identify faces v and e respectively. Moreover, these are the unique isometries which identify the aforementioned faces.

The following fact allows us to enumerate elements of $\mathcal{C}_{\text{main}}$.

Proposition 4.2.1 (Fact 2.8 of [16])**.** *An orbifold O is a degree m covering $O \to Q = \mathbb{H}^3/PGL_2(O_3)$ if and only if O is triangulated by m isometric copies of T.*

In [19], the authors construct a census of cusped hyperbolic 3-manifolds which are obtained by face pairings on some collection of regular ideal tetrahedra. They first define a *combinatorial tetrahedral tessellation* to be an ideal triangulation where all edges have order 6. This follows since the sum of dihedral angles around an edge in a manifold must be 2π,

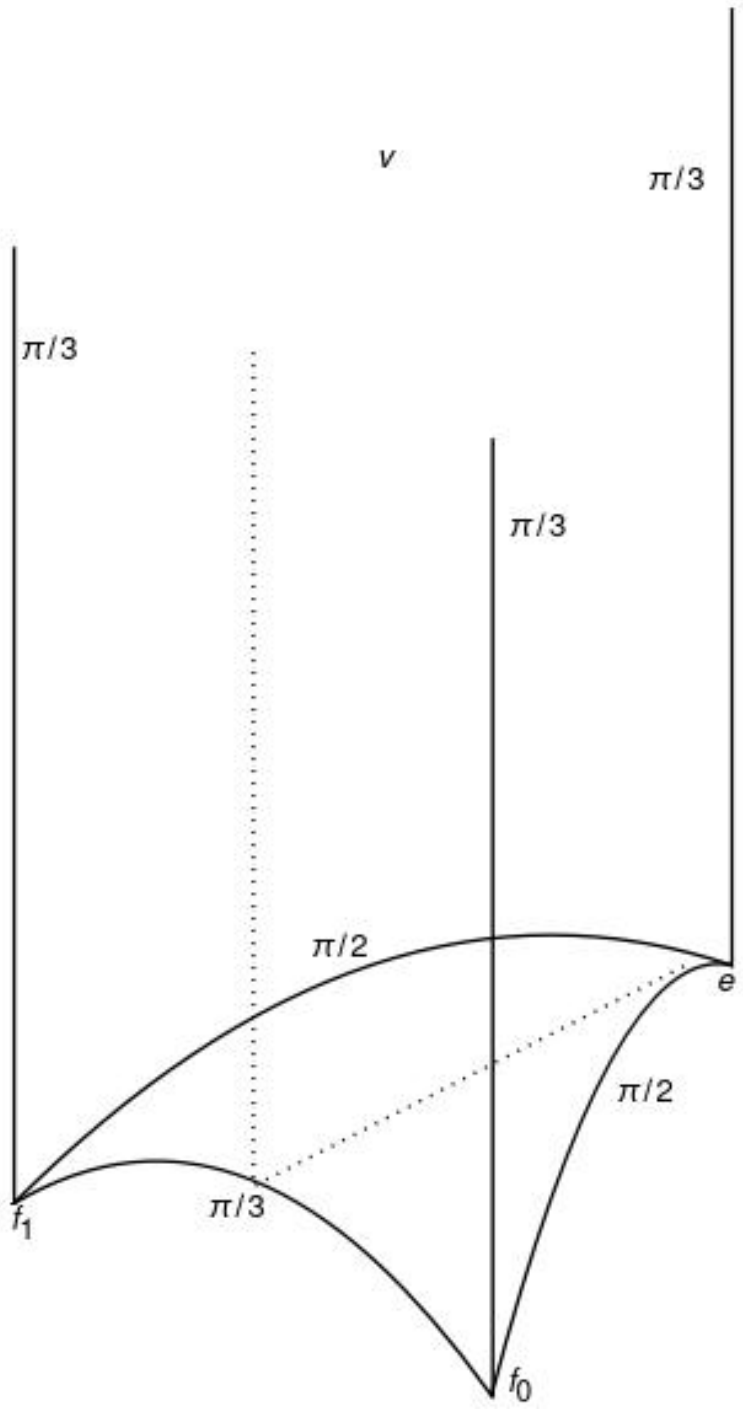

Figure 30: The tetrahedron T

and in a regular ideal tetrahedron every dihedral angle is $\pi/3$. A combinatorial tetrahedral tesselation determines a tetrahedral manifold. The authors describe an algorithm which enumerates all combinatorial tetrahedral tessellations with at most n tetrahedra. They then introduce the *isometry signature* to determine when two combinatorially distinct tessellations yield isometric tetrahedral manifolds.

We briefly and informally describe their algorithm to enumerate (orientable) combinatorial tetrahedral tessellations. One may think of the procedure as recursively constructing a tree. The root of the tree is a single tetrahedron with none of its faces identified. Each node of the tree is a collection of tetrahedra with some subset of their faces identified in pairs. A leaf of the tree is a collection of tetrahedra with all faces identified in pairs.

Given a partial triangulation $\mathcal{T}$ at a node, the node's children will be triangulations $\mathcal{T}'$ obtained from $\mathcal{T}$ in the following way

- $\mathcal{T}'$ is obtained from $\mathcal{T}$ by gluing a new tetrahedron to an open face of $\mathcal{T}$,
- or $\mathcal{T}'$ is obtained from $\mathcal{T}$ by choosing a pair of open faces in $\mathcal{T}$ and identifying them by some odd permutation of their vertices.

In particular, a node should have one child for each possible way of carrying out the above modification of its partial triangulation.

The algorithm searches the tree and records those triangulations at its leaves which are combinatorial tetrahedral tessellations, namely those triangulations where each edge meets six tetrahedra. In practice, the tree is not first constructed and then searched. The algorithm constructs the tree recursively while keeping a lookout for combinatorial tetrahedral tessellations.

The size of the tree grows exponentially with the maximum number of tetrahedra, but the performance of the algorithm may be improved substantially by pruning the tree. One can see that there will be different nodes of the tree whose triangulations are combinatorially isomorphic. The authors avoid duplicate computation in this scenario by keeping a list of combinatorial invariants of the partial triangulations which have already been visited during the search. They use Burton's *isomorphism signature* [8] as the complete invariant of the combinatorial isomorphism type of a triangulation. If the recursion arrives at a

new triangulation whose isomorphism signature has already been encountered, that node's subtree is not searched. The tree may also be pruned when we can guarantee that a node's subtree does not contain a combinatorial tetrahedral tessellation. For example, an edge may have valence greater than six or the triangulation may have non-manifold topology.

Now we explain how to adapt this algorithm to our setting, give a pseudocode description of it in Algorithms 1 and 2, and briefly remark on some implementation details.

Definition 4.2.1. By a *triangulation* $\mathcal{T}$, we mean the data of n-tetrahedra $T_0, \ldots, T_{n-1}$, each of which is isometric to T, and maps which identify some subset of pairs of faces. We say a triangulation is *closed* if all of its faces are identified in pairs, otherwise we refer to it as a *partial triangulation*.

Our situation is much more rigid than that of the authors of [19] - their regular ideal tetrahedra are much more symmetric than our copies of T. In particular, given two tetrahedra T_i, T_j, the face pairing between them is uniquely determined by specifying an open face of T_i. Face f_0 of T_i can only be glued to face f_1 of T_j, face v of T_i may only be glued to face v of T_j, etc.

On the other hand, our situation is more flexible in that we don't require each edge to have valence six. For our triangulation to represent an orbifold, we only require that the sum of dihedral angles around each edge be an integer submultiple of 2π. We say such a triangulation is *valid*

What is the appropriate combinatorial invariant which determines our triangulations (up to a relabeling of the tetrahedra)? The isomorphism signature is not sufficient as its purpose is to encode the combinatorial isomorphism type of an abstract simplicial complex. The authors of [19] are able to use it with no modification since their tetrahedra are regular, but in our tetrahedra the sets of faces $\{f_0, f_1\}, \{v\}, \{e\}$ are geometrically distinct and different edges have different dihedral angles. For this reason, we develop our own invariant called the triangulation's *destination sequence*. This is related to, but distinct from Burton's notion with the same name.

Definition 4.2.2. For a closed triangulation $\mathcal{T}$ of n tetrahedra $T_0, \ldots, T_{n-1}$, the destination sequence determined by the pair $(\mathcal{T}, T_0)$ is an array s of length $4n$ whose entries

$(s_0, s_1, \ldots, s_{4n-1})$ are determined as follows:

Label the faces of T with integers as $v = 0, f_0 = 1, f_2 = 2$, and $e = 3$. Write $k = 4i + j$ where $i \in \{0, \ldots, n-1\}$ and $j \in \{0, 1, 2, 3\}$. Then s_k is the index of the tetrahedron that intersects T_i along face j, where this tetrahedron is given the next free index if it has not yet been encountered.

From the n different choices of initial tetrahedron T_0, we obtain n different sequences. Among these, we define the *destination sequence* of $\mathcal{T}$ to be the lexicographically minimal one.

Example 4.2.1. For the triangulation of $Q = \mathbb{H}^3/PGL_2(O_3)$ with one copy of T its destination sequence is

$$(0000)$$

Example 4.2.2. It is an instructive example to try to construct all triangulations with two copies of T. Call them T_a and T_b. Let $T_a(v)$ denote face v of T_a, and likewise. Then

$$T_a(v) \text{ can be glued to itself or } T_b(v)$$
$$T_a(e) \text{ can be glued to itself or } T_b(e)$$
$$T_a(f_0) \text{ can be glued to } T_a(f_1) \text{ or } T_b(f_1)$$

Once these three choices are made, the remaining identification is determined - hence there are eight possible face pairings. One of these results in a disconnected cover of Q, which we are not interested in. Of the remaining seven cases, six of them have an edge whose dihedral angle sum is $4\pi/3$. The only set of face pairings which results in a valid triangulation is

$$\{T_a(v) \leftrightarrow T_b(v), T_a(f_0) \leftrightarrow T_b(f_1), T_a(f_1) \leftrightarrow T_b(f_0), T_a(e) \leftrightarrow T_b(e)\}$$

Regardless of whether T_a or T_b is labeled T_0, we obtain the destination sequence

$$(1111, 0000)$$

Example 4.2.3. To see an example where the destination sequences differ depending on which tetrahedron is labeled T_0, consider the valid triangulation with three tetrahedra T_a, T_b, T_c and face pairings

$$\begin{array}{lll} T_a(v) \leftrightarrow T_a(v) & T_a(f_0) \leftrightarrow T_a(f_1) & T_a(e) \leftrightarrow T_b(e) \\ T_b(v) \leftrightarrow T_c(v) & T_b(f_0) \leftrightarrow T_c(f_1) & T_b(e) \leftrightarrow T_a(e) \\ T_c(v) \leftrightarrow T_b(v) & T_c(f_0) \leftrightarrow T_b(f_1) & T_c(e) \leftrightarrow T_c(e) \end{array}$$

The corresponding destination sequences are

$$\begin{array}{ll} \text{When } T_a = T_0 & (0001, 2220, 1112) \\ \text{When } T_b = T_0 & (1112, 0001, 2220) \\ \text{When } T_c = T_0 & (1110, 0002, 2221) \end{array}$$

The lexicographically minimal sequence arises from $T_a = T_0$. This is the destination sequence of the orbifold determined by this valid triangulation.

The algorithms of this section were implemented in `C++`[1], interfacing with *Regina's* [10] rich support for triangulations. We implemented a wrapper class `O3Tetrahedron` which represents a copy of T. It implements basic features of Regina's `Tetrahedron` class, such as a method to perform face pairing on two copies of T; see `O3Tetrahedron.h` for more details. The user of the class need not worry about the various bookkeeping details underlying its implementation. For example, Regina does not allow a face to be glued to itself, but our tetrahedra have such face pairings. We won't explain here how such details are handled, as the interested reader is free to examine the code. Likewise, a wrapper class `O3Triangulation` represents a triangulation composed of copies of an `O3Tetrahedron` identified under face pairings.

Using the resources of Pitt's Center for Research Computing (CRC), we were able to enumerate all triangulations of orbifolds in $\mathcal{C}_{\text{main}}$ containing at most 36 tetrahedra in roughly 3 and a half days of computing time. To complete the enumeration of $\mathcal{C}_{\text{main}}^{\leq 2v_0}$, using ideas and code of Goerner from [22] we modified the enumeration algorithm to utilize multiple threads[2].

[1]The code is available at https://github.com/tgaona22/O3Enumeration

[2]See `threadpool.h` and `concurrent_enumerate.cpp`

```
result ← {}
already_seen ← {}
Function recurse(Triangulation T):
    if checkClosedEdges(T) returns true then
        if destSeq(T) ∈ already_seen then
            return
        else
            add destSeq(T) to already_seen
        if T has no open faces then
            add destSeq(T) to result
            return
        Choose a tetrahedron t ∈ T
        if size(T) < max_tets then
            for f ∈ {v, f_0, f_1, e} do
                if f is open in t then
                    recurse(T with new tetrahedron glued to face f of t)
        for f ∈ {v, f_0, f_1, e} do
            if f is open in t then
                for t̃ ∈ {t_0, ..., t_{size(T)−1}} do
                    f̃ ← the face which pairs with f
                    if f̃ is open in t̃ then
                        recurse(T with face f of t glued to face f̃ of t̃)
recurse(Triangulation with one unglued tetrahedron)
return result
```

Algorithm 1: Enumerating triangulations

Data: a triangulation T

Result: returns false if there is an invalid edge in T

Function `checkClosedEdges` *(Triangulation* T*)*:

```
for each edge e in T do
    if e has no open adjacent faces then
        if the dihedral angle around e is not an integer submultiple of 2π then
            return false;
        end
    else if the dihedral angle around e exceeds 2π then
        return false;
end
return true;
```

Algorithm 2: a method to test whether a triangulation has edges which cannot be made valid by further face pairings

We summarize our data in Tables 1 and 2 in the appendix. The notation for orbifolds is O_k^n, where n is the number of tetrahedra and the index k is the position of O_k^n's destination sequence in the lexicographically sorted list of all destination sequences of triangulations with n-tetrahedra.

4.3 Cusps and singular loci of elements of $\mathcal{C}_{\text{main}}$

In this section, we describe algorithms for computing topological and geometric data from the triangulations enumerated by the methods of the previous section. For this section, when we say orbifold we mean a triangulation of an element of $\mathcal{C}_{\text{main}}^{\leq 2v_0}$

4.3.1 Cusps

First we show how to construct two dimensional triangulations of cross sections of an orbifold's cusps. Since T has an ideal vertex, our orbifolds all have at least one cusp. We illustrate the method via an example.

Example 4.3.1. We will construct triangulations of the cross sections of O_0^6's cusps. Its destination sequence is

$$(0001, 2330, 1442, 4113, 3225, 5554)$$

In T, the link of the ideal vertex is an equilateral Euclidean triangle. Each tetrahedron T_i in the triangulation contributes an equilateral triangle t_i to one of the cusp cross sections. The edges of t_i are labeled f_0, f_1, and e corresponding to the face of T_i which contains it. The first step is to group triangles which belong to the same cusp cross section. Consider T_0. Across faces f_0, f_1, and e it meets itself and T_1 respectively. T_1 meets T_3 across faces f_1 and f_0. Finally T_3 meets itself across face e. By similar considerations beginning with T_2, we see that O_0^6 has two cusps, and the triangles which belong to each cross section are

$$\{t_0, t_1, t_3\} \text{ and } \{t_2, t_4, t_5\}$$

Focus on the cusp cross section containing the triangles t_0, t_1 and t_3. The edge pairings on this collection of triangles are induced by the face pairings of O_0^6. See Figure 31, where edges with an equal number of hash marks are identified.

Finally, we determine the cone points of the Euclidean 2-orbifold which is the quotient of $\{t_0, t_1, t_3\}$ modulo the edge pairings. One cone point with angle π is created since edge e of t_3 is identified to itself under a π-rotation about its midpoint. By "walking around" the four different vertex classes of the triangulation, we compute their angles. The white vertex has angle 2π, hence is not a cone point. The red and green vertices have cone angles $\pi/3$ and $2\pi/3$ respectively. Therefore this is the cross section of a $(2, 3, 6)$ cusp.

Similar considerations show that the remaining cusp is of the same type. See Figure 32 for a triangulation of its cross section.

The pseudocode for this algorithm is given in Algorithm 3. This is implemented as a method of the `O3Triangulation` class.

Data: a triangulation $\mathcal{T}$

Result: a collection of triangulations of cross sections of $\mathcal{T}$'s cusps

cusps $\leftarrow \{\}$ `/* Group triangles by cusp cross section */`

while $\mathcal{T}$ *has tetrahedra not yet visited* **do**

  cusp $\leftarrow$ { unvisited tetrahedron of $\mathcal{T}$};

  while cusp *has unexamined tetrahedron* T **do**

    for $f \in \{f_0, f_1, e\}$ **do**

      add tetrahedron glued to face f of T to cusp;

    end

  end

  add cusp to cusps;

end

for *each* cusp *in* cusps **do**

  Create a triangle t_i for each tetrahedron $T_i \in$ cusp;

  Glue edge f of t_i to t_j if face f of T_i is glued to T_j;

  for *each vertex* $v \in$ cusp **do**

    v.cone_angle $\leftarrow 0$;

    for *each lift* $\widetilde{v}$ *of* v *in* $\sqcup t_i$ **do**

      v.cone_angle $\leftarrow v$.cone_angle+ angle around $\widetilde{v}$ in t_i;

    end

  end

end

return cusps;

Algorithm 3: triangulating cusp cross sections

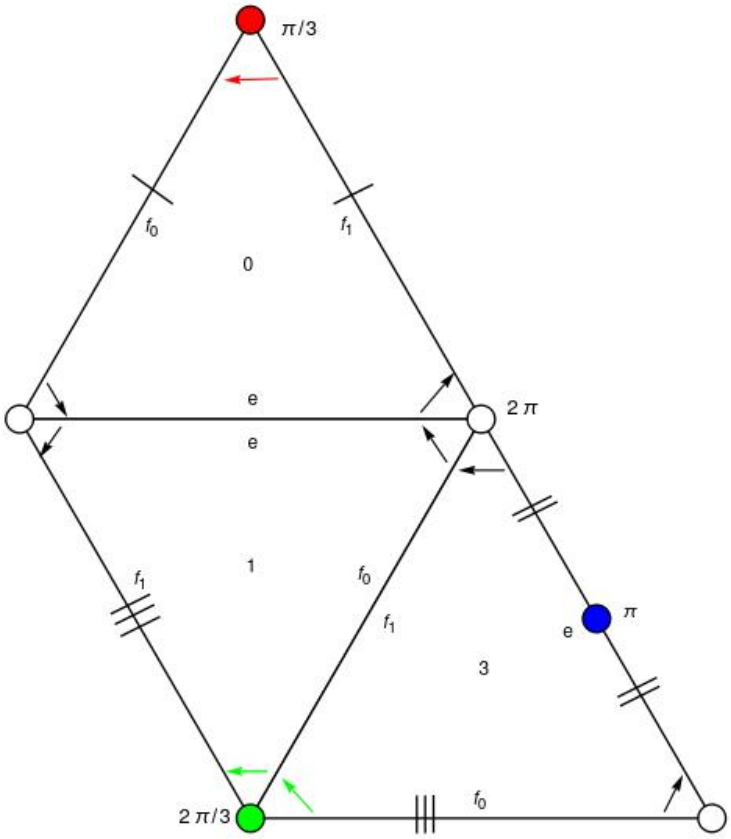

Figure 31: Cusp cross section determined by $\{t_0, t_1, t_3\}$

4.3.2 Singular Locus

Next we show to construct the singular locus of a triangulation $\mathcal{T}$ of $O \in \mathcal{C}_{\text{main}}$. Our starting point is the following fact.

Definition 4.3.1. For T, we define its *1-skeleton* to be the union of the vertices and edges of T along with the edges connecting the midpoint of the segment $f_0 f_1$ to v and e respectively.

Fact 4.3.1. *The singular locus of $O \in \mathcal{C}_{main}$ lifts to a subset of the* 1*-skeleton of its triangulation $\mathcal{T}$.*

Proof. A point in the interior of a tetrahedron has a neighborhood isometric to a ball which factors through the projection to O. A point in the 2-skeleton but not in the 1-skeleton of $\mathcal{T}$

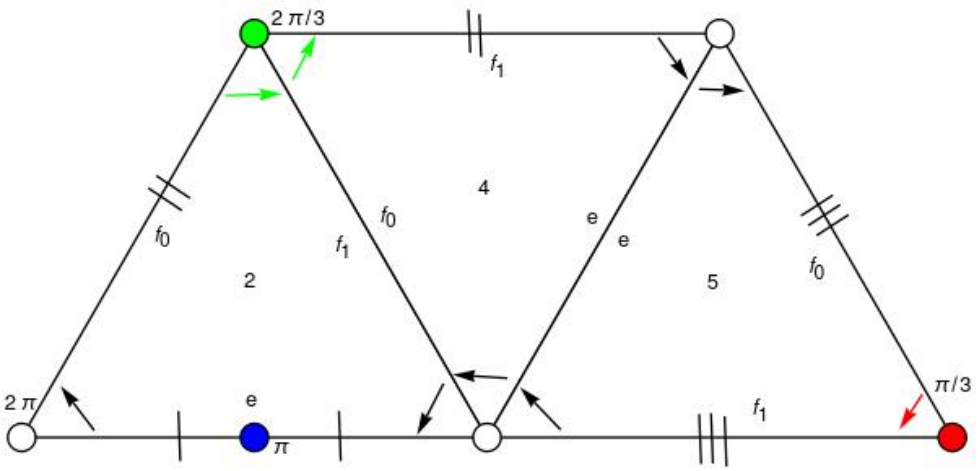

Figure 32: Cusp cross section determined by $\{t_2, t_4, t_5\}$

has a neighborhood which lifts via the quotient map to two half balls glued together along their meridional disks to form a ball. □

Again, we work a simple example by hand before giving the general algorithm.

Example 4.3.2. Recall O_0^2 has destination sequence

$$(1111, 0000)$$

First we examine the gluing data to draw the 1-skeleton of the triangulation of O_0^2. In Figure 33 (a), we label each edge with its dihedral angle. Any edge with dihedral angle 2π is not contained in the singular locus, hence is removed in figure (b). Also, in Figure 33 (b) we label each edge by its order, namely k if its dihedral angle is $2\pi/k$.

Notice that the vertex labeled IV connected two edges of dihedral angle π. After removing those edges, notice that vertex IV is just a point on an order 3 axis in the singular locus. Thus we delete vertex IV and join vertices III and V by an edge with label 3. See Figure 34. Notice that vertex I represents a (3,3,3) rigid cusp, while the other vertices are trivalent with labelings (p, q, r) satisfying $1/p+1/q+1/r > 1$, consistent with Theorem 2.1. The cusp itself is not part of the singular locus, and need not have edges of the singular locus running into it. But when it does, we include it in the singular locus diagram.

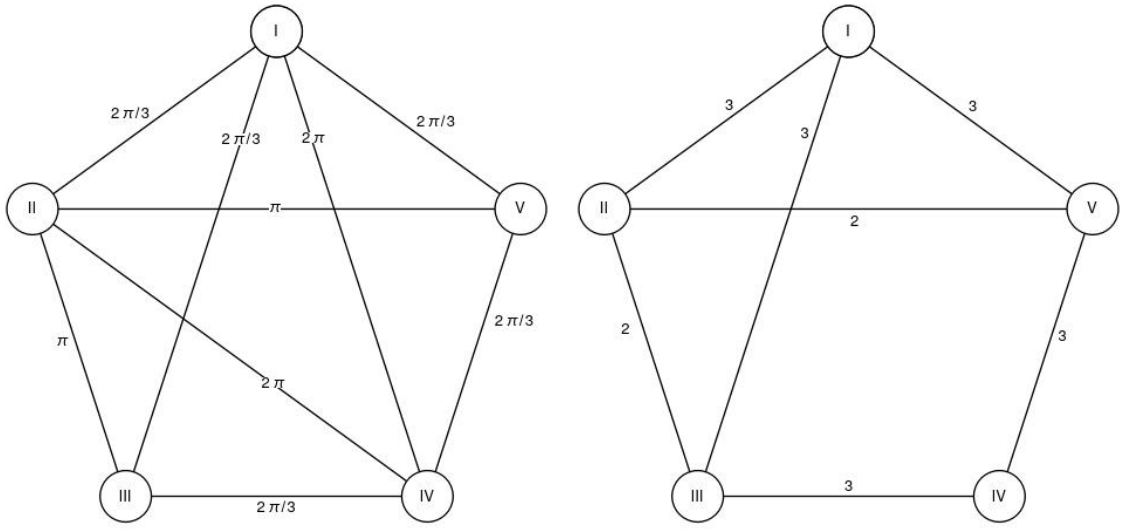

Figure 33: (a) 1-skeleton of the triangulation (b) after removing non-singular edges

Example 4.3.3. The singular locus of an orbifold need not have any vertices. In chapter 1 of [31], Purcell describes an algorithm due to Menasco which takes the diagram of a link and produces a decomposition of its complement into ideal polyhedra identified via face pairings. The results of applying this algorithm to the figure eight knot are illustrated in Figure 35.[3]

The face pairings are the unique ones implied by the coloring and direction of the arrows. For example, the face in the background of the tetrahedron at left is identified to the face in the right foreground of the other tetrahedron by a rotation in the back edge followed by a one-third rotation about the middle of the right foreground face. One obtains a hyperbolic structure on the figure eight knot complement by realizing these tetrahedra as regular ideal tetrahedra in $\mathbb{H}^3$. The face pairings prescribed by Figure 35 can be realized as isometries of $\mathbb{H}^3$.

If in addition, we quotient by the order two rotation about the blue axis, we obtain an orbifold of volume v_0. Its singular locus is a closed geodesic labeled two. Notice that the order two axis is disjoint from and preserves the cusp, so this orbifold still has a torus cusp.

[3]This example is originally due to Thurston and can be found in the first few pages of his notes. This author confesses that he still doesn't understand Thurston's pictures there.

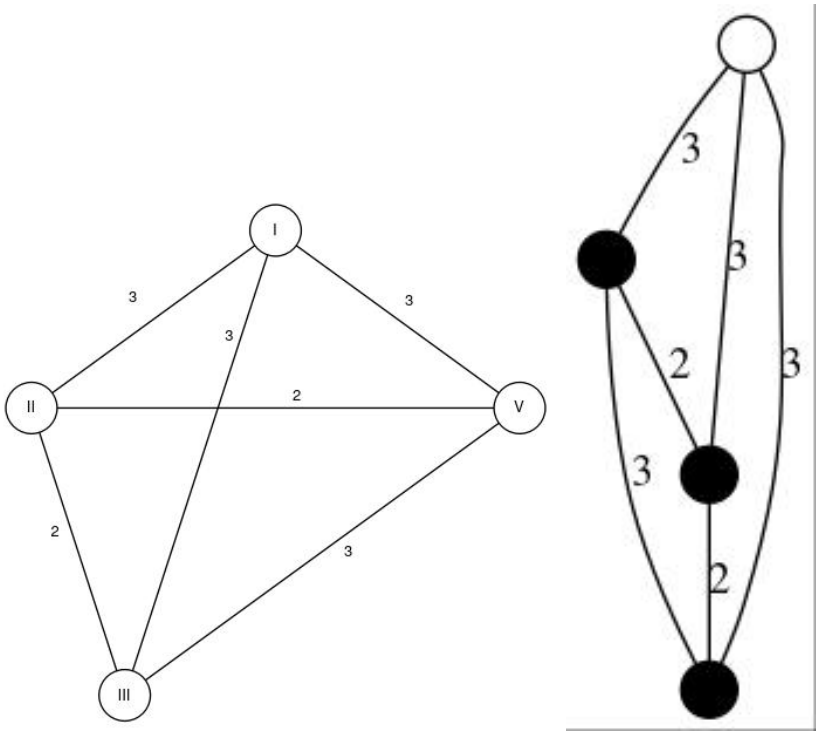

Figure 34: (a) the singular locus (b) output of the algorithm

Presumably a similar construction can be applied to the figure eight's "sister".

This is realized in our census. The manifolds O_{19}^{24} and O_{20}^{24} each have one torus cusp and empty singular locus; these are the figure eight complement and its "sister". They both double cover O_{10}^{12}, an orbifold with one torus cusp and singular locus a single closed geodesic of order 2.

Example 4.3.4. Figure 36 shows the singular locus algorithm's output for O_0^{10}, an orbifold of volume $5v_0/6$ with one $(2,2,2,2)$ cusp and one $(6,3,2)$ cusp. By Theorem 3.2, O_0^{10} is isometric to $O_{(6,3,2)}$. Compare figures 36 and 5.

The pseudocode for computing the singular locus is presented in Algorithm 4. It is implemented as a method in `O3Triangulation`. In practice, we compute an adjacency matrix representation of the graph and pass this output to the program Graphviz [21] to generate pictures such as Figure 36.

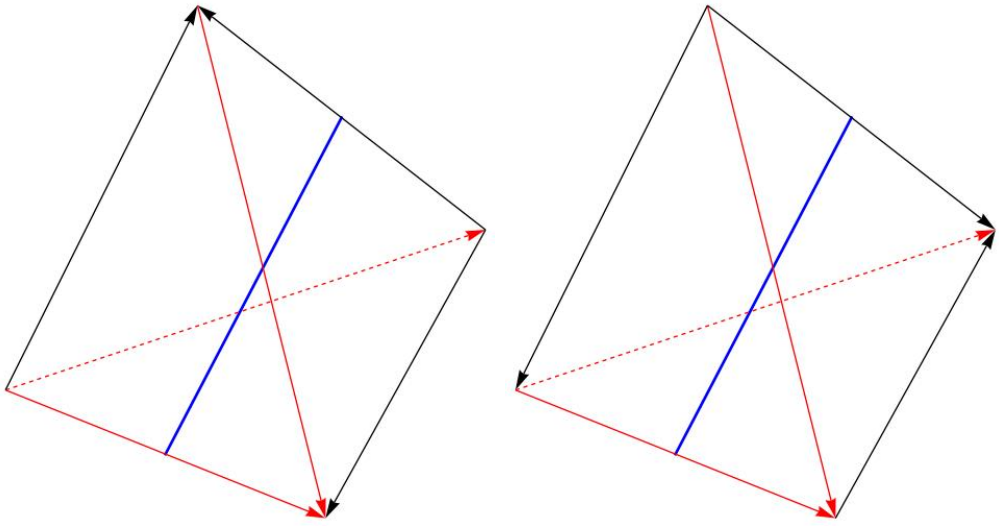

Figure 35: Tetrahedral decomposition of the figure eight knot complement

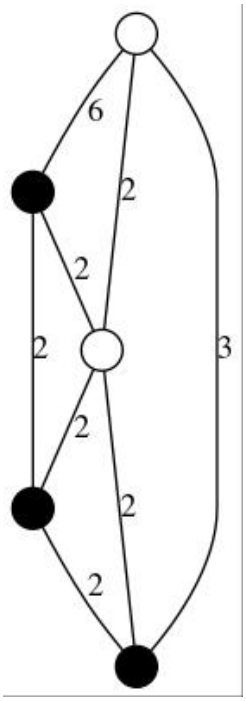

Figure 36: Singular locus of O_0^{10}

Data: a triangulation $\mathcal{T}$

Result: a graph representing the singular locus of $\mathcal{T}$

locus $\leftarrow$ 1-skeleton of $\mathcal{T}$;

Compute dihedral angle around each edge in locus;

Delete edges with angle 2π;

for *each vertex v of valence 2* **do**

  if *v's edges terminate in vertices $v_0 \neq v_1$* **then**

    Delete v;

    Join v_0 to v_1 by an edge of the same label as those that came from v;

  end

end

return locus;

Algorithm 4: computing the singular locus

4.4 Enumerating Q_π and $\widetilde{Q}_\pi$ with small volume

Here we use Theorem 4.1 to enumerate the minimal orbifolds in $\mathcal{C}_3$ other than $\mathbb{H}^3/PGL_2(O_3)$. We also describe how to find their canonical covers $\widetilde{Q}_\pi \in \mathcal{C}_{\text{main}}$. For a number field $\mathbb{K}$, its ring of integers $O_\mathbb{K}$ is the set of elements in $\mathbb{K}$ which satisfy a monic polynomial with coefficients in $\mathbb{Z}$. For the quadratic extension $\mathbb{Q}(\sqrt{-3})$ of $\mathbb{Q}$, the ring of integers is explicitly identified as

$$O_3 = O_{\mathbb{Q}(\sqrt{-3})} = \{a + b\zeta \mid a, b \in \mathbb{Z}\}$$

where $\zeta = \frac{1+\sqrt{-3}}{2}$.

We take the following facts about ideals in O_3 for granted. Recall that the product of ideals $I_1, \ldots, I_k$ is the additive subgroup of O_3 generated by $\{a_1 \ldots a_k \mid a_i \in I_i\}$.

Fact 4.4.1. *Let I be a nonzero ideal in O_3.*

(1) O_3/I is a finite ring.

(2) If I is prime, then I is maximal.

(3) I may be written as a product of prime ideals, uniquely up to ordering.

The first two facts imply that for a nonzero prime ideal $P \subset O_3$, O_3/P is a finite field. For any nonzero ideal $I \subset O_3$, define its *norm* $n(P)$ to be the cardinality of O_3/I. The Chinese Remainder Theorem implies that the norm on ideals is multiplicative. This combined with the third fact shows that it is enough for us to determine the norms of prime ideals in O_3.

Let P be a prime ideal in O_3. Then $P \cap \mathbb{Z}$ is a prime ideal in $\mathbb{Z}$, hence is equal to $p\mathbb{Z}$ for some prime number $p \in \mathbb{Z}$.

Lemma 4.4.1. *Let $p \in \mathbb{Z}$ be prime. Then $n(pO_3) = p^2$ and either*

- *$pO_3 = P^2$ for some prime ideal $P \subset O_3$*
- *$pO_3 = P_1P_2$ for prime ideals $P_1, P_2 \subset O_3$*
- *pO_3 is itself prime*

We say respectively that p ramifies, splits, or is inert

Proof. The map $O_3 \to \mathbb{Z}^2$ defined by

$$a + b\zeta \mapsto (a, b)$$

is an additive group isomorphism. It sends the ideal pO_3 to $p\mathbb{Z} \times p\mathbb{Z}$. Hence

$$O_3/pO_3 \approxeq (\mathbb{Z} \times \mathbb{Z})/(p\mathbb{Z} \times p\mathbb{Z}) \approxeq (\mathbb{Z}/p\mathbb{Z})^2$$

Therefore $n(pO_3) = p^2$. Write $pO_3 = P_1 \dots P_m$ where P_i is a prime ideal in O_3. Since the norm is multiplicative

$$p^2 = n(P_1) \dots n(P_m)$$

and the possibilities are constrained by the limited factorizations of p^2. When $pO_3 = P^2$ or $pO_3 = P_1P_2$, then $n(P) = n(P_i) = p$. □

We take for granted that the class number of $\mathbb{Q}(\sqrt{-3})$ is 1, which implies that O_3 is a principal ideal domain. Hence any prime ideal in O_3 has the form πO_3 for some prime element πO_3. The above lemma implies that $n(\pi O_3)$ is either p or p^2 for some $p \in \mathbb{Z}$. The integer primes of norm less than 48 may be classified as ramified, split, or inert by computing the Legendre symbol $(\frac{-3}{p})$ as in Lemma 0.3.10 of [26]. The only ramified prime is $3 = -(\sqrt{-3})^2$.

The inert primes are 2 and 5 (the primes 11, 17, 23, 41, and 47 are also inert but have norm greater than 48). The remaining primes split as can be seen below.

$$\begin{aligned}
7 &= (2-\sqrt{-3})(2+\sqrt{-3}) \\
13 &= (1-2\sqrt{-3})(1+2\sqrt{-3}) \\
19 &= (4-\sqrt{-3})(4+\sqrt{-3}) \\
31 &= (2+3\sqrt{-3})(2-3\sqrt{-3}) \\
37 &= (5+2\sqrt{-3})(5-2\sqrt{-3}) \\
43 &= (4+3\sqrt{-3})(4-3\sqrt{-3})
\end{aligned}$$

Recall that for $\pi = \pi_1 \dots \pi_n$ a product of distinct primes $\pi_i \in O_3$,

$$\mathrm{vol}(Q_\pi) = \frac{1}{2^n} \prod_{i=1}^{n} (n(\pi_i O_3) + 1) \frac{v_0}{12}$$

Then we obtain the list of Q_π with volume at most $2v_0$ as in Theorem 6.1 of [16]. To identify the canonical covers $\widetilde{Q}_\pi \in \mathcal{C}_{\mathrm{main}}$, we rely on the following fact (see section 6.2 of [16]).

Proposition 4.4.1 (Proposition 6.5 of [16]). *For $\pi = \pi_1 \dots \pi_n$ a product of distinct primes in O_3, Q_π has one $(2,3,6)$ cusp and $\widetilde{Q}_\pi$ has 2^n cusps of the same type.*

Using Algorithm 3 we compute the cusp data of each element in $\mathcal{C}_{\mathrm{main}}$. This is enough to determine $\widetilde{Q}_\pi$ for $\pi = \sqrt{-3}, 2, 2\sqrt{-3}$. For example, when $\pi = 2\sqrt{-3}$, the degree of $\widetilde{Q}_\pi \to Q_\pi$ is $2^2 = 4$. So $\mathrm{vol}(\widetilde{Q}_\pi) = 20\frac{v_0}{12}$, and of the 14 elements of $\mathcal{C}_{\mathrm{main}}$ with 20 tetrahedra, only O_5^{20} has four $(2,3,6)$ cusps. Therefore $\widetilde{Q}_\pi = O_5^{20}$

For each complex conjugate pair of primes or prime products, the cusp data narrows the possibilities for $\widetilde{Q}_\pi$ down to a pair of orientation-reversing isometric elements of $\mathcal{C}_{\mathrm{main}}$. For example, when $\pi = 2 + \sqrt{-3}$, $\mathrm{vol}(\widetilde{Q}_\pi) = 8\frac{v_0}{12}$ and of the three elements of $\mathcal{C}_{\mathrm{main}}$ with 8 tetrahedra, both O_0^8 and O_1^8 have two $(2,3,6)$ cusps. One of these is $\widetilde{Q}_\pi$ and the other is $\widetilde{Q}_{\overline{\pi}}$. To distinguish between the two, we rely on the explicit description of $\widetilde{\Gamma}_\pi$ given in Theorem 4.1, namely

$$\widetilde{\Gamma}_\pi = \left\{ \begin{bmatrix} x & \pi y \\ z & w \end{bmatrix} \in PGL_2(O_3) \mid x, y, z, w \in O_3 \right\}$$

Recall from section 4.2 that $PGL_2(O_3)$ is generated by ρ_f, ρ_e, and ρ_v. My advisor implemented algorithm which takes the destination sequence of $O = \mathbb{H}^3/\Gamma \in \mathcal{C}_{\text{main}}$ and produces a generating set for each subgroup in the conjugacy class of Γ. Each generator is a word in ρ_f, ρ_e and ρ_v. If $O = \widetilde{Q}_\pi$, then one of these subgroups is $\widetilde{\Gamma_\pi}$. Algorithm 5 takes as input $O = \mathbb{H}^3/\Gamma \in \mathcal{C}_{\text{main}}$ and π a product of distinct primes in O_3 and decides if $O = \widetilde{Q}_\pi$.

We implement this in Mathematica [24] where all calculations are done symbolically. After evaluating each word as a matrix, we test if its upper right entry is divisible by π in O_3. Suppose that $x = \pi y$, where $y = a + b\zeta \in O_3$. Then $y = \frac{\overline{\pi}}{|\pi|^2}x$ and we may solve for a and b via

$$a = \frac{y + \overline{y} - b}{2}, b = \frac{y - \overline{y}}{\sqrt{-3}}$$

Conversely, we do not assume that x is divisible by π, but if we define y, a, and b as above, then x is divisible by π if and only if $y = a + b\zeta$ and $a, b \in \mathbb{Z}$. Using this algorithm, we identify the$\widetilde{Q}_\pi, \widetilde{Q}_{\overline{\pi}}$ with volume $\leq 2v_0$ which correspond to the elements of the orientation-reversing isometric pair in $\mathcal{C}_{\text{main}}$ determined by the cusp data. The results of this section are summarized in Table 3 (compare Corollary 6.2 of [16]). The last four rows of Q_π have $\text{vol}(\widetilde{Q}_\pi) > 2v_0$.

Data: $O = \mathbb{H}^3/\Gamma \in \mathcal{C}_{\text{main}}$ and π a product of distinct primes in O_3

Result: returns true iff Γ is conjugate to $\widetilde{\Gamma}_\pi$

subgroupGens $\leftarrow$ a list of generators for each subgroup in the conjugacy class of Γ;

Function `test` *(Matrix m, π)***:**

$x \leftarrow$ upper right entry of m;

$y \leftarrow \frac{\overline{\pi}}{|\pi|^2} x$;

$b \leftarrow \frac{y-\overline{y}}{\sqrt{-3}}$;

$a \leftarrow \frac{y+\overline{y}-b}{2}$;

return $a, b \in \mathbb{Z}\&\&y == a + b\zeta$;

for *each subgroup H in the conjugacy class of* Γ **do**

failed $\leftarrow$ false;

for *each generator w of H* **do**

$m \leftarrow w$ evaluated as a matrix;

if `test` *(m, π) returns false* **then**

failed $\leftarrow$ true;

break;

end

end

if failed *is false* **then**

return true;

end

end

return false;

Algorithm 5: Determining $\widetilde{Q}_\pi$

Appendix Data about $\mathcal{C}_{\mathbf{main}}$

Table 1: Number $s(n)$ of elements of $\mathcal{C}_{\text{main}}$ triangulated by n tetrahedra

n	$s(n)$	n	$s(n)$	n	$s(n)$
1	1	17	0	33	2
2	1	18	5	34	0
3	1	19	0	35	3
4	1	20	14	36	38
5	1	21	2	37	1
6	4	22	2	38	2
7	0	23	0	39	2
8	3	24	21	40	31
9	1	25	0	41	0
10	2	26	1	42	30
11	0	27	4	43	3
12	12	28	11	44	19
13	0	29	1	45	8
14	4	30	25	46	2
15	2	31	1	47	2
16	2	32	10	48	61

Table 2: Destination sequences and cusp types for elements of $\mathcal{C}_{\text{main}}$ triangulated by at most 10 tetrahedra

O_k^n	destination sequence	cusp(s)
O_0^1	0000	$(2,3,6)$
O_0^2	$1111, 0000$	$(3,3,3)$
O_0^3	$0001, 2220, 1112$	$(2,3,6)$
O_0^4	$0110, 1002, 3221, 2333$	$(2,3,6) \times 2$
O_0^5	$0123, 2202, 1011, 4330, 3444$	$(2,3,6) \times 2$
O_0^6	$0001, 2330, 1442, 4113, 3225, 5554$	$(2,3,6) \times 2$
O_1^6	$0123, 2201, 1014, 5540, 4352, 3435$	$(2,2,2,2)$
O_2^6	$1112, 0003, 4440, 5551, 2225, 3334$	$(3,3,3)$
O_3^6	$1112, 0003, 4550, 5441, 2335, 3224$	$(3,3,3)$
O_0^8	$0121, 2300, 1042, 4514, 3253, 5436, 7665, 6777$	$(2,3,6) \times 2$
O_1^8	$0122, 2301, 1040, 4514, 3253, 5436, 7665, 6777$	$(2,3,6) \times 2$
O_2^8	$1221, 0330, 3004, 2115, 6552, 7443, 4777, 5666$	$(3,3,3) \times 2$
O_0^9	$0001, 2340, 1562, 6614, 5153, 4427, 3238, 8885, 7778$	$(2,3,6)$
O_0^{10}	$0001, 2340, 1562, 6414, 5133, 4627, 3258, 8895, 7976, 9789$	$(2,3,6), (2,2,2,2)$
O_1^{10}	$1121, 0300, 3045, 2617, 6266, 8772, 4434, 9553, 5999, 7888$	$(3,3,3) \times 2$

Table 3: Minimal elements of $\mathcal{C}_3 - \mathcal{C}_{\text{main}}$

π	$\text{vol}(Q_\pi)$	$\widetilde{Q_\pi}$
$\sqrt{-3}$	$2\frac{v_0}{12}$	O_0^4
2	$\frac{5}{2}\frac{v_0}{12}$	O_0^5
$2 \pm \sqrt{-3}$	$4\frac{v_0}{12}$	$+ : O_0^8, - : O_1^8$
$1 \pm 2\sqrt{-3}$	$7\frac{v_0}{12}$	$+ : O_0^{14}, - : O_1^{14}$
$4 \pm \sqrt{-3}$	$10\frac{v_0}{12}$	$+ : O_8^{20}, - : O_7^{20}$
5	$13\frac{v_0}{12}$	O_0^{26}
$2 \pm 3\sqrt{-3}$	$16\frac{v_0}{12}$	$+ : O_4^{32}, - : O_5^{32}$
$5 \pm 2\sqrt{-3}$	$19\frac{v_0}{12}$	$+ : O_1^{38}, - : O_0^{38}$
$4 \pm 3\sqrt{-3}$	$22\frac{v_0}{12}$	$+ : O_{15}^{44}, - : O_{16}^{44}$
$2\sqrt{-3}$	$5\frac{v_0}{12}$	O_5^{20}
$\sqrt{-3}(2 \pm \sqrt{-3})$	$8\frac{v_0}{12}$	$+ : O_3^{32}, - : O_2^{32}$
$2(2 \pm \sqrt{-3})$	$10\frac{v_0}{12}$	$+ : O_{15}^{40}, - : O_{14}^{40}$
$\sqrt{-3}(1 \pm 2\sqrt{-3})$	$14\frac{v_0}{12}$	
$2(1 \pm 2\sqrt{-3})$	$\frac{35}{2}\frac{v_0}{12}$	
$\sqrt{-3}(4 \pm \sqrt{-3})$	$20\frac{v_0}{12}$	
$2\sqrt{-3}(2 \pm \sqrt{-3})$	$20\frac{v_0}{12}$	

Bibliography

[1] Colin C. Adams. The noncompact hyperbolic 3-manifold of minimal volume. *Proc. Amer. Math. Soc.*, 100(4):601–606, 1987.

[2] Colin C. Adams. Limit volumes of hyperbolic three-orbifolds. *J. Differential Geom.*, 34(1):115–141, 1991.

[3] Colin C. Adams. Noncompact hyperbolic 3-orbifolds of small volume. In *Topology '90 (Columbus, OH, 1990)*, volume 1 of *Ohio State Univ. Math. Res. Inst. Publ.*, pages 1–15. de Gruyter, Berlin, 1992.

[4] Colin C. Adams. Volumes of hyperbolic 3-orbifolds with multiple cusps. *Indiana Univ. Math. J.*, 41(1):149–172, 1992.

[5] Alan F. Beardon. *The geometry of discrete groups*, volume 91 of *Graduate Texts in Mathematics*. Springer-Verlag, New York, 1983.

[6] A. Borel. Commensurability classes and volumes of hyperbolic 3-manifolds. *Ann. Scuola Norm. Sup. Pisa Cl. Sci. (4)*, 8(1):1–33, 1981.

[7] K. Böröczky. Packing of spheres in spaces of constant curvature. *Acta Math. Acad. Sci. Hungar.*, 32(3-4):243–261, 1978.

[8] Benjamin A. Burton. The Pachner graph and the simplification of 3-sphere triangulations. In *Computational geometry (SCG'11)*, pages 153–162. ACM, New York, 2011.

[9] Benjamin A. Burton. The cusped hyperbolic census is complete, 2014.

[10] Benjamin A. Burton, Ryan Budney, William Pettersson, et al. Regina: Software for low-dimensional topology. `http://regina-normal.github.io/`, 1999–2021.

[11] James W. Cannon, William J. Floyd, Richard Kenyon, and Walter R. Parry. Hyperbolic geometry. In *Flavors of geometry*, volume 31 of *Math. Sci. Res. Inst. Publ.*, pages 59–115. Cambridge Univ. Press, Cambridge, 1997.

[12] Chun Cao and G. Robert Meyerhoff. The orientable cusped hyperbolic 3-manifolds of minimum volume. *Invent. Math.*, 146(3):451–478, 2001.

[13] J. H. Conway. The orbifold notation for surface groups. In *Groups, combinatorics & geometry (Durham, 1990)*, volume 165 of *London Math. Soc. Lecture Note Ser.*, pages 438–447. Cambridge Univ. Press, Cambridge, 1992.

[14] Daryl Cooper, Craig D. Hodgson, and Steven P. Kerckhoff. *Three-dimensional orbifolds and cone-manifolds*, volume 5 of *MSJ Memoirs*. Mathematical Society of Japan, Tokyo, 2000. With a postface by Sadayoshi Kojima.

[15] H. S. M. Coxeter. *Introduction to geometry*. John Wiley & Sons, Inc., New York-London, 1961.

[16] J. DeBlois, H. A. Ekanayake, M. Fincher, T. Gaona, A. Gharagozlou, and P. Mondal. Orbifolds commensurable with the figure eight knot complement. 2022.

[17] William D. Dunbar and G. Robert Meyerhoff. Volumes of hyperbolic 3-orbifolds. *Indiana Univ. Math. J.*, 43(2):611–637, 1994.

[18] Mark Fincher. Computations with hyperbolic 3-orbifolds. Ph.D thesis.

[19] Evgeny Fominykh, Stavros Garoufalidis, Matthias Goerner, Vladimir Tarkaev, and Andrei Vesnin. A census of tetrahedral hyperbolic manifolds. *Exp. Math.*, 25(4):466–481, 2016.

[20] Theodore W. Gamelin. *Complex analysis*. Undergraduate Texts in Mathematics. Springer-Verlag, New York, 2001.

[21] Emden R. Gansner, Gordon Woodhull, et al. Graphviz. `http://graphviz.org/`. open source graph visualization software.

[22] Matthias Goerner. A census of hyperbolic platonic manifolds and augmented knotted trivalent graphs. *New York J. Math.*, 23:527–553, 2017.

[23] Allen Hatcher. Hyperbolic structures of arithmetic type on some link complements. *J. London Math. Soc. (2)*, 27(2):345–355, 1983.

[24] Wolfram Research, Inc. Mathematica, Version 13.0. Champaign, IL, 2021.

[25] John M. Lee. *Introduction to Riemannian manifolds*, volume 176 of *Graduate Texts in Mathematics*. Springer, Cham, 2018. Second edition of [MR1468735].

[26] Colin Maclachlan and Alan W. Reid. *The arithmetic of hyperbolic 3-manifolds*, volume 219 of *Graduate Texts in Mathematics*. Springer-Verlag, New York, 2003.

[27] A. Marden. *Outer circles*. Cambridge University Press, Cambridge, 2007. An introduction to hyperbolic 3-manifolds.

[28] Bruno Martelli. *An Introduction to Geometric Topology*. independently published, 2022.

[29] Robert Meyerhoff. The cusped hyperbolic 3-orbifold of minimum volume. *Bull. Amer. Math. Soc. (N.S.)*, 13(2):154–156, 1985.

[30] Robert Meyerhoff. Sphere-packing and volume in hyperbolic 3-space. *Comment. Math. Helv.*, 61(2):271–278, 1986.

[31] Jessica S. Purcell. *Hyperbolic knot theory*, volume 209 of *Graduate Studies in Mathematics*. American Mathematical Society, Providence, RI, [2020] ©2020.

[32] Arlan Ramsay and Robert D. Richtmyer. *Introduction to hyperbolic geometry*. Universitext. Springer-Verlag, New York, 1995.

[33] John G. Ratcliffe. *Foundations of hyperbolic manifolds*, volume 149 of *Graduate Texts in Mathematics*. Springer-Verlag, New York, 1994.

[34] William P. Thurston. *The geometry and topology of 3-manifolds*. mimeographed lecture notes, 1979.